

REFINEMENTS OF THE SEAL SUBROUTINES  
AND FAN AIR FLOW MAPS FOR THE  
XR-3 LOADS AND MOTION PROGRAM

Robert Alexander Finley

DUDLEY KNOX LIBRARY  
NAVAL POSTGRADUATE SCHOOL  
MONTEREY, CALIFORNIA 93940

# NAVAL POSTGRADUATE SCHOOL

## Monterey, California



# THESIS

REFINEMENTS OF THE SEAL SUBROUTINES  
AND FAN AIR FLOW MAPS FOR THE  
XR-3 LOADS AND MOTION PROGRAM

by

Robert Alexander Finley

December 1974

Thesis Advisor:

A. Gerba Jr.

Approved for public release; distribution unlimited.

164910



REPORT DOCUMENTATION PAGE		READ INSTRUCTIONS BEFORE COMPLETING FORM
1. REPORT NUMBER	2. GOVT ACCESSION NO.	3. RECIPIENT'S CATALOG NUMBER
4. TITLE (and Subtitle) Refinements of the Seal Subroutines and Fan Air Flow Maps for the XR-3 Loads and Motion Program		5. TYPE OF REPORT & PERIOD COVERED Master's Thesis; December 1974
7. AUTHOR(s) Robert A. Finley		6. PERFORMING ORG. REPORT NUMBER
9. PERFORMING ORGANIZATION NAME AND ADDRESS Naval Postgraduate School Monterey, California 93940		8. CONTRACT OR GRANT NUMBER(s)
11. CONTROLLING OFFICE NAME AND ADDRESS Naval Postgraduate School Monterey, California 93940		10. PROGRAM ELEMENT, PROJECT, TASK AREA & WORK UNIT NUMBERS
14. MONITORING AGENCY NAME & ADDRESS (if different from Controlling Office) Naval Postgraduate School Monterey, California 93940		12. REPORT DATE December 1974
		13. NUMBER OF PAGES 146
		15. SECURITY CLASS. (of this report) Unclassified
		15a. DECLASSIFICATION/DOWNGRADING SCHEDULE
16. DISTRIBUTION STATEMENT (of this Report) Approved for public release; distribution unlimited.		
17. DISTRIBUTION STATEMENT (of the abstract entered in Block 20, if different from Report)		
18. SUPPLEMENTARY NOTES		
19. KEY WORDS (Continue on reverse side if necessary and identify by block number) XR-3 XR-3 Loads and Motion Computer Program Fan Air Flow Maps XR-2 Bow and Stern Seal Subroutines		
20. ABSTRACT (Continue on reverse side if necessary and identify by block number) Refinements to the bow and stern seal subroutines of the XR-3 Loads and Motion computer program are made. New lift fan performance maps are developed and presented. Comparison studies of simulated performance of the original XR-3 model with the old and new fan maps are made under varying sea conditions. Measured roll and pitch transient behavior of the XR-3 test craft in calm water is compared with the		



UNCLASSIFIED

SECURITY CLASSIFICATION OF THIS PAGE(When Data Entered)

(20. ABSTRACT Continued)

simulated response of both the original and the new model. In addition, simulated performances of the original and new models in irregular ahead seas are compared.

UNCLASSIFIED

SECURITY CLASSIFICATION OF THIS PAGE(When Data Entered)





Refinements of the Seal Subroutines  
and Fan Air Flow Maps for the  
XR-3 Loads and Motion Program

by

Robert Alexander Finley  
Lieutenant Commander, United States Navy  
B.S., United States Naval Academy, 1965

Submitted in partial fulfillment of the  
requirements for the degree of

MASTER OF SCIENCE IN ELECTRICAL ENGINEERING

from the

NAVAL POSTGRADUATE SCHOOL  
December 1974



## ABSTRACT

Refinements to the bow and stern seal subroutines of the XR-3 Loads and Motion computer program are made. New lift fan performance maps are developed and presented. Comparison studies of simulated performance of the original XR-3 model with the old and new fan maps are made under varying sea conditions. Measured roll and pitch transient behavior of the XR-3 test craft in calm water is compared with the simulated response of both the original and the new model. In addition, simulated performances of the original and new models in irregular ahead seas are compared.



## TABLE OF CONTENTS

I.	INTRODUCTION -----	11
	A. BACKGROUND -----	11
	B. OBJECTIVES -----	13
II.	FAN PERFORMANCE MAP ANALYSIS AND COMPARISON ----	14
	A. INTRODUCTION -----	14
	B. FAN MAP ANALYSIS AND DERIVATION -----	16
	C. SIMULATED PERFORMANCE COMPARISONS BETWEEN ORIGINAL AND NEW FAN MAPS -----	24
III.	SEAL MODEL REFINEMENTS -----	37
	A. INTRODUCTION AND BASIC MODELING TECHNIQUE --	37
	B. BOW SEAL MODELING -----	49
	C. STERN SEAL MODELING -----	59
IV.	DATA ANALYSIS OF ACTUAL CRAFT TRANSIENT MOTION AND COMPUTER SIMULATION -----	67
	A. INTRODUCTION -----	67
	B. RUN DATA ANALYSIS -----	74
	C. SIMULATION STUDIES OF THE TWO MODELS -----	76
V.	CONCLUSIONS AND RECOMMENDATIONS -----	109
APPENDIX A.	Listing of BOWSEAL SUBROUTINE BOWSL -----	115
APPENDIX B.	Listing of Stern Seal Subroutine STNSL ----	120
APPENDIX C.	Listing of FAN subroutine FAN -----	124
APPENDIX D.	Listing of Initial Conditions Subroutine INCON -----	127
BIBLIOGRAPHY	-----	144
INITIAL DISTRIBUTION LIST	-----	145



## LIST OF TABLES

I.	Sea State Wave Components -----	27
II.	Simulated XR-3 Performance with Different Fan Maps -----	28
III.	Calm Water Forced Oscillations Response -----	77





## LIST OF FIGURES

1.	Performance and Fan Map Curves for the Joy Axivane Fan (Model AVR 87-55D2058) -----	18
2.	Manufacturers' Specifications for the Joy Axivane Fan -----	19
3.	Bow Seal and Plenum Chamber Fan Maps, Adjusted for Ducting Losses -----	22
4.	Stern Seal Fan Map Adjusted to Account for Ducting Loss -----	23
5.	Computer Simulation, Plenum Pressure versus Time, Speed 20 knots, Original Fan Maps, Sea State 1 -----	29
6.	Computer Simulation, Pitch Angle versus Time, Speed 20 knots, Original Fan Maps, Sea State 1 -----	30
7.	Computer Simulation, C.G. Draft versus Time, Speed 20 knots, Original Fan Maps, Sea State 1 -----	31
8.	Computer Simulation, C.G. Accèleration versus Time, Speed 20 knots, Original Fan Maps, Sea State 1 -----	32
9.	Computer Simulation, Plenum Pressure versus Time, Speed 20 knots, New Fan Maps, Sea State 1 -----	33
10.	Computer Simulation, Pitch Angle versus Time, Speed 20 knots, New Fan Maps, Sea State 1 -----	34
11.	Computer Simulation, C.G. Draft versus Time, Speed 20 knots, New Fan Maps, Sea State 1 -----	35
12.	Computer Simulation, C.G. Acceleration versus Time, Speed 20 knots, New Fan Maps, Sea State 1 -----	36
13.	Cross Sectional View of Pneumatic Seal as Installed in the XR-3 -----	40
14.	Bow and Stern Seal Deflection Model (not to scale) -----	45



15.	Seal Trailing Edge Height Above Keel versus Seal Wetted Length -----	47
16.	Roll Motion versus Time, 20.429 knots -----	68
17.	Pitch versus Time, 20.429 knots -----	69
18.	Pitch Motion versus Time, 20.429 knots -----	70
19.	Roll Transient versus Time, 11.79 knots -----	78
20.	Computer Simulation, Roll Angle versus Time, 11.79 knots, Original XR-3 -----	79
21.	Computer Simulation, Roll Angle versus Time, 11.79 knots, New XR-3 -----	80
22.	Pitch versus Time, 15.93 knots -----	81
23.	Pitch Transient versus Time, 15.93 knots -----	82
24.	Roll Transient versus Time, 15.93 knots -----	83
25.	Computer Simulation, Pitch Angle versus Time, 15.93 knots, Original XR-3 -----	84
26.	Computer Simulation Roll Angle versus Time, 15.93 knots, Original XR-3 -----	85
27.	Computer Simulation, Pitch Angle versus Time, 15.93 knots, New XR-3 -----	86
28.	Computer Simulation, Roll Angle versus Time, 15.93 knots, New XR-3 -----	87
29.	Roll Transient versus Time, 19.45 knots -----	88
30.	Pitch versus Time, 19.45 knots -----	89
31.	Pitch Transient versus Time, 19.45 knots -----	90
32.	Computer Simulation, Roll Angle versus Time, 19.45 knots, Original XR-3 -----	91
33.	Computer Simulation, Pitch Angle versus Time, 19.45 knots, Original XR-3 -----	92
34.	Computer Simulation, Roll Angle versus Time, 19.45 knots, New XR-3 -----	93
35.	Computer Simulation, Pitch Angle versus Time, 19.45 knots, New XR-3 -----	94



36.	Computer Simulation, 3 Degree Pitch Step Response, 19.45 knots, Original XR-3, Pitch versus Time -----	96
37.	Computer Simulation, 3 Degree Pitch Step Response, 19.45 knots, Original XR-3, Plenum Pressure versus Time -----	97
38.	Computer Simulation, 3 Degree Pitch Step Response, 19.45 knots, Original XR-3, Draft at C.G. versus Time -----	98
39.	Computer Simulation, 3 Degree Pitch Step Response, 19.45 knots, New XR-3, Pitch versus Time -----	99
40.	Computer Simulation, 3 Degree Pitch Step Response, 19.45 knots, New XR-3, Plenum Pressure versus Time -----	100
41.	Computer Simulation, 3 Degree Pitch Step Response, 19.45 knots, New XR-3, Draft at C.G. versus Time -----	101
42.	Computer Simulation, Plenum Pressure versus Time, 19.45 knots, New XR-3, Sea State 2 -----	103
43.	Computer Simulation, Plenum Pressure versus Time, 19.45 knots, Original XR-3, Sea State 2 --	104
44.	Computer Simulation, Draft at C.G. versus Time, 19.45 knots, New XR-3, Sea State 2 -----	105
45.	Computer Simulation, Draft at C.G. versus Time, 19.45 knots, Original XR-3, Sea State 2 -----	106
46.	Computer Simulation, Pitch Angle versus Time, 19.45 knots, New XR-3, Sea State 2 -----	107
47.	Computer Simulation, Pitch Angle versus Time, 19.45 knots, Original XR-3, Sea State 2 -----	108
48.	Bottom View of the XR-3 Showing Planing Areas at the Rear -----	111



### ACKNOWLEDGEMENT

The author wishes to express his sincere appreciation to Associate Professor Alex Gerba Jr. without whose guidance and encouragement this period of study would not have been completed.

In addition the author wishes to thank Associate Professor Donald M. Layton and his technical assistant Mr. Michael O'Dell who spent many hours of their time collecting data used in this study.

And lastly the author would like to give a special measure of thanks to a close friend, Lcdr. G. T. Forbes, USN, who was of great assistance throughout this project.





## I. INTRODUCTION

### A. BACKGROUND

The speed limitation of the conventional displacement vessel has been recognized for many years. In an effort to effect a quantum increase in surface vessel speed the United States Navy has been developing various craft whose principal means of support is other than hydrostatic lift.

One type of craft currently receiving much attention is the surface effect ship or craft. In this category are the air cushion vehicles and captured air bubble craft (CAB). The general nature of these craft and their construction is well presented by Robert L. Trillo in Ref. 1. In these craft either all or a major portion of its support is derived from a pressure differential between the atmosphere and a plenum chamber which is open at the bottom. The speed advantages gained by this type of vessel are derived from two principal characteristics. It does not waste energy displacing a large volume of water and the frictional forces between the hull and water are greatly reduced by the craft riding on a cushion of air with only a minimum of the craft structure actually in contact with the water.

Vessels of this type are generally separated into two categories - "Air Cushion Vehicles" whose weight is entirely supported by the pressure differential in the plenum chamber and "Captured Air Bubble Craft" whose weight is partially



supported by sidewalls which extend into the water. It is the second type of vessel in which the United States Navy has become primarily interested for ocean going applications.

The term Captured Air Bubble (CAB) is possibly a misnomer since in this type of craft the air does leak out and has to be continually replenished by supply fans. The leakage though is relatively slow when it is compared to the air cushion vehicle which has continuous air gap around the periphery of the craft and hence the fans that replenish the air in the plenum chamber have to be larger and more powerful than those of a CAB of similar size.

This thesis is concerned with one aspect of the development of the Captured Air Bubble vehicle and that is the simulation of such craft utilizing a digital computer, specifically the Loads and Motion Program developed by Oceanics, Inc.

The basic rigid body analysis and spatial relationships of the Loads and Motion program are well documented in Ref. 2. Also covered are the principal dynamic and static approximations used in developing the equations of motion for the craft in its six degrees of freedom.

A copy of this program was delivered to the Naval Postgraduate School in October of 1972 which had been specifically tailored for the Bell (100B) 100 ton craft. Leo and Boncal in Ref. 3 succeeded in converting this program to represent the XR-3 test craft.



## B. OBJECTIVE

The purpose of this thesis was to take a second more detailed look into all of the aspects of seal modeling and the fan performance map with the idea of possibly making improvements in these representations before testing the computer model of the XR-3 under dynamic conditions.



## II. FAN PERFORMANCE MAP ANALYSIS AND COMPARISON

### A. INTRODUCTION

As the surface effect ship is predominately dependent on the plenum lifting force for its performance, the characteristics of the lifting fans are important if valid studies of the craft in question are to be made.

Leo and Boncal reported in Ref. 3 that the steady state operating conditions of the XR-3 were obtained by increasing the leakage area of the craft until the proper equilibrium pressure was maintained in the main plenum. This area was twenty-six square feet. As the cross-sectional area of the plenum is less than twenty square feet this leakage area was out of proportion to properly represent the leakage area of the XR-3.

While operating above hump speed the XR-3 test craft has been observed to have a gap underneath the sternseal of from four to five inches. Slight leakage does occur at the bowseal as reported by Ref. 3 but the total leakage area is estimated to be not over four square feet.

To appreciate the effect this leakage area has on computed craft performance an understanding is required of the method by which the pressure is calculated in the plenum.

When the program is executed an estimation of the initial operating conditions must be supplied by the user. Besides velocity and thrust, initial conditions for plenum pressure, displacement and pitch angle must be supplied. From the





displacement, pitch angle and velocity for calm water conditions, a plenum volume is computed. Using the leakage areas supplied, exit flow rates are computed for the bow and stern seals. The fan subroutine is then called using the pressure in the plenum, bow and stern seals as primary arguments. Using these pressures supply flow rates are established for the fans that supply air to the plenum, and both seals. As the seals discharge into the main plenum the sum of these fan flow rates establish the total influx rate. The net flow being the difference between the influx and efflux rates establishes the new plenum pressure for the next calculation interval based upon the adiabatic perfect gas law. This new pressure creates a new plenum lifting force which is then balanced by the defining differential equations of motion resulting in a new operating condition of craft attitude and displacement.

In studying craft motion in calm water the leakage area is of little or no consequence since no additional leakage areas are normally developed beneath the sidewalls or seals, and the rate of change of plenum volume is relatively slow. On the other hand, when the program is executed in simulated sea states where gap areas are generated beneath the seals and sidewalls and plenum volume does change quite rapidly the leakage areas and fan maps become of prime importance.

It must be emphasized though that it is not the leakage area itself that affects craft performance. It is rather the relative size of the fixed leakage area with respect to



the variable leakage areas generated around the periphery of the craft by wave motion and craft attitude and position which is important.

#### B. FAN MAP ANALYSIS AND DERIVATION

Isolation of the factors which caused the large discrepancy between observed steady state gap area and calculated area required an examination of both the efflux and influx equations for possible errors.

The equation used to establish leakage flow rates under the seals and the sidewalls are the same. This equation is given below

$$\dot{Q} = C_f A_L (2\Delta p / \rho)^{1/2}$$

It is the general flow equation for a sharp edged orifice in turbulent flow conditions. As the orifice coefficient,  $C_f$ , is the only variable in the equation that could be dependent on craft geometry and its range was limited between unity and six tenths; the efflux equations were eliminated as the source of the error. The only area left for possible error was the fan maps themselves.

The fan maps in question are arrays which give fan flow rates in cubic feet per second as a function of plenum or seal pressure. They are entered as data in "INCON" as characteristics of the specific craft being modeled.



It was found that the fan maps constructed by Leo and Boncal to represent the fans installed in the XR-3 were based upon incorrect information. Actual fan performance data for the fans currently installed is presented<sup>1</sup> in Figure 1, and physical characteristics in Figure 2.

The fan performance map given by the manufacturer, Joy Manufacturing Company, is based upon flow that is not impeded by air ducts. It is therefore optimistic for any system that contains long ducts as these ducts will modify considerably the fan performance by creating ducting losses.

The best way to obtain the actual fan performance maps in a duct system would be to actually measure the flow rates as the pressure in the receiving reservoir (in this case the plenum) is varied. As this method was impractical in the case of the XR-3 another method of estimating the modified fan performance had to be devised.

The method outlined below was utilized and although it probably does not give exact results the fan maps thus achieved should adequately represent the actual fan performance of the XR-3.

---

<sup>1</sup>The fan data was provided by Associate Professor of Aerology D.M. Layton who is in charge of the actual XR-3 test program at the Naval Postgraduate School. He has verified that the fans installed are Joy Model AVR87-55D2058 for which the data given in Figures 1 and 2 are correct.





MANUFACTURING COMPANY  
 CLEVELAND, OHIO  
 SEP 21, 1962 DL/ER

FAN MODEL: AVR87-55D2058  
 UNIT NO: 500702-47-01 (DIRECT DRIVE)  
 AIR DELIVERY: 0.075 CFM  
 FAN TESTED FLOWING INTO 8.75" DIA. DUCT

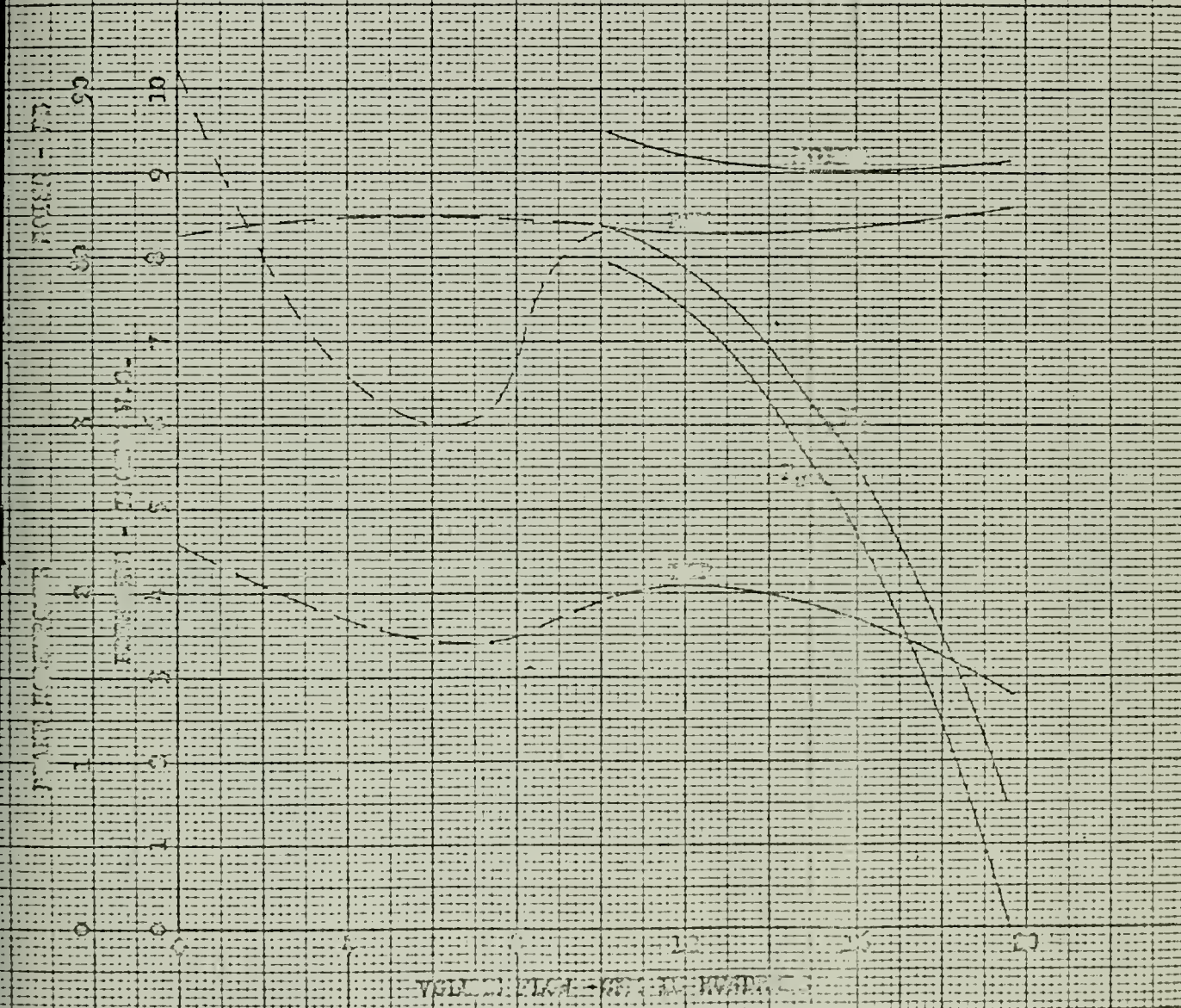


FIGURE 1

PERFORMANCE AND FAN MAP CURVES FOR THE JOY AXIVANE FAN  
 (MODEL AVR 87-55D2058)







19



The first step used in arriving at the new fan maps was to establish a realistic leakage area. Once this leakage area was established a steady state efflux rate was established. Because in steady state operating conditions the influx and efflux rates must be equal the flow rate supplied by the lift fans in total was established. It was at this point that a second assumption was made. This assumption was that there were greater losses in the ducting supplying air to the bow seal and main plenum chamber than there were in the ducting supplying the rear seal. This assumption was based upon the fact that the ducting to the bowseal and main plenum had to carry the air forward approximately sixteen feet to their discharge orifices whereas the stern seal ducting was only a few feet long with only one curve in it to impede flow.

As a result the fraction of total flow assigned to the stern seal was greater on an individual fan basis than was the air supplied by the bow seal or main plenum fans. Another assumption was that the same map could adequately represent both the bow seal supply fans and those supplying the main chamber. This last assumption was based on similar duct lengths and construction.

Now knowing the individual fan flow rates and the actual plenum pressure a pressure drop in the duct for steady state conditions was established. This pressure drop was the difference between the known plenum operating pressure (24.84 lbs/ft<sup>2</sup>) and the indicated fan discharge pressure



for that flow rate. This pressure drop was then scaled for different flow rates based upon the fact that pressure losses vary with the square of the flow rates. In this manner new fan maps were computed for the bow seal and main plenum, and the stern sea. These maps are presented in Figures 3 and 4.

The last step was to go back to the leakage area and make the slight adjustments needed to give the required plenum steady state pressure of  $24.84 \text{ lbs/ft}^2$ . The final leakage areas established were  $.08 \text{ ft}^2$  for the bow seal and  $3.79 \text{ ft}^2$  for the stern seal.

In the original fan subroutine the horsepower generated by the fans is computed based upon the influx rate and the pressure differential between the atmosphere and the plenum. As the actual work done per unit time by the fans this figure can be misinterpreted as the actual power needed by the fans to generate printed work rate. This would only hold true if the fans operated with one hundred percent efficiency and there were no ducting losses. In actuality fans of this nature which supply relatively large volumes of air at low pressure rarely operate at over seventy percent efficiency and can achieve that only over an extremely narrow operating range. These physical characteristics of fans were well presented by R.D. Moyer in 1946 in Ref. 4.

For the fans that are used in the XR-3 the Joy Manufacturing Company has provided the fan's horsepower requirements



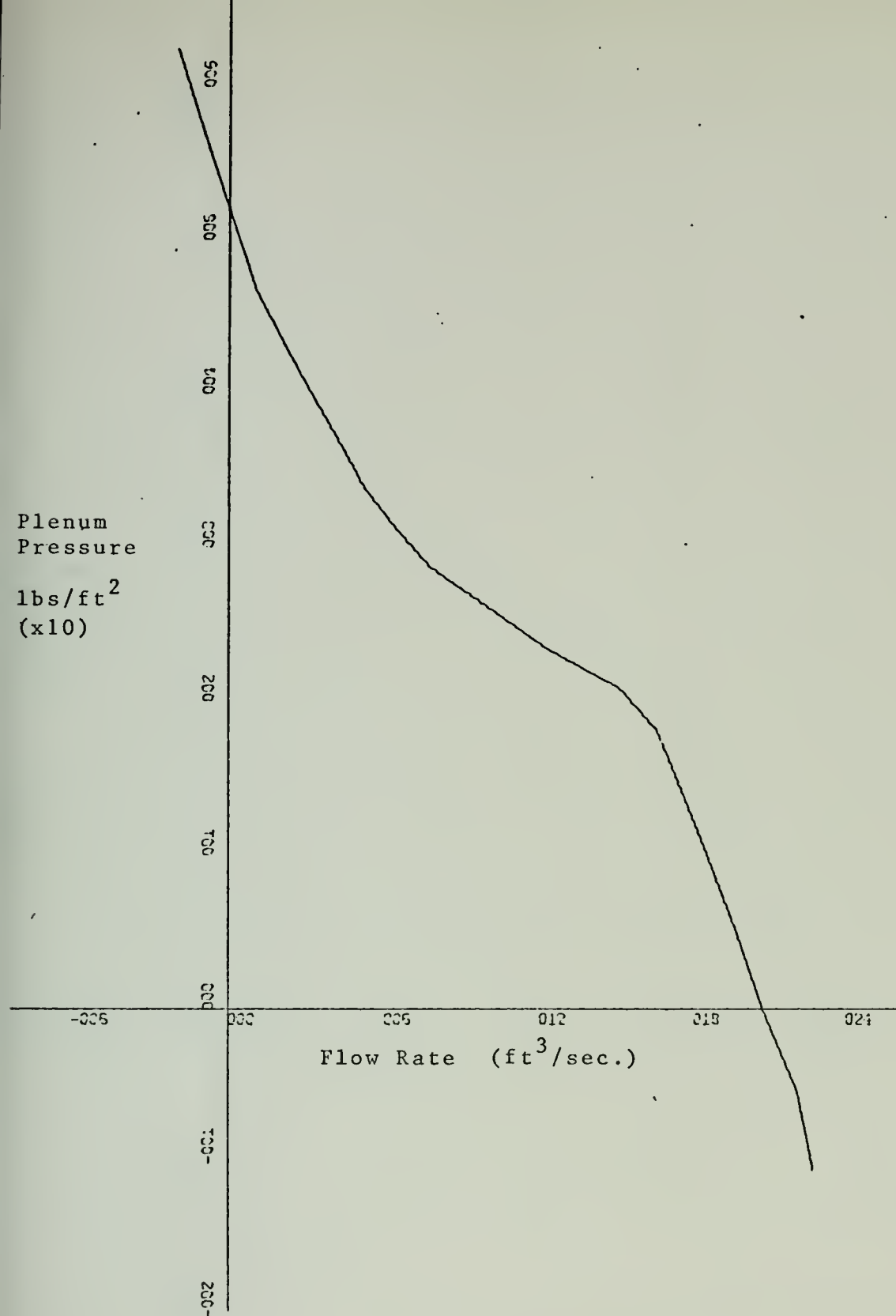


FIGURE 3

BOW SEAL AND PLENUM CHAMBER FAN MAPS, ADJUSTED FOR DUCTING LOSSES





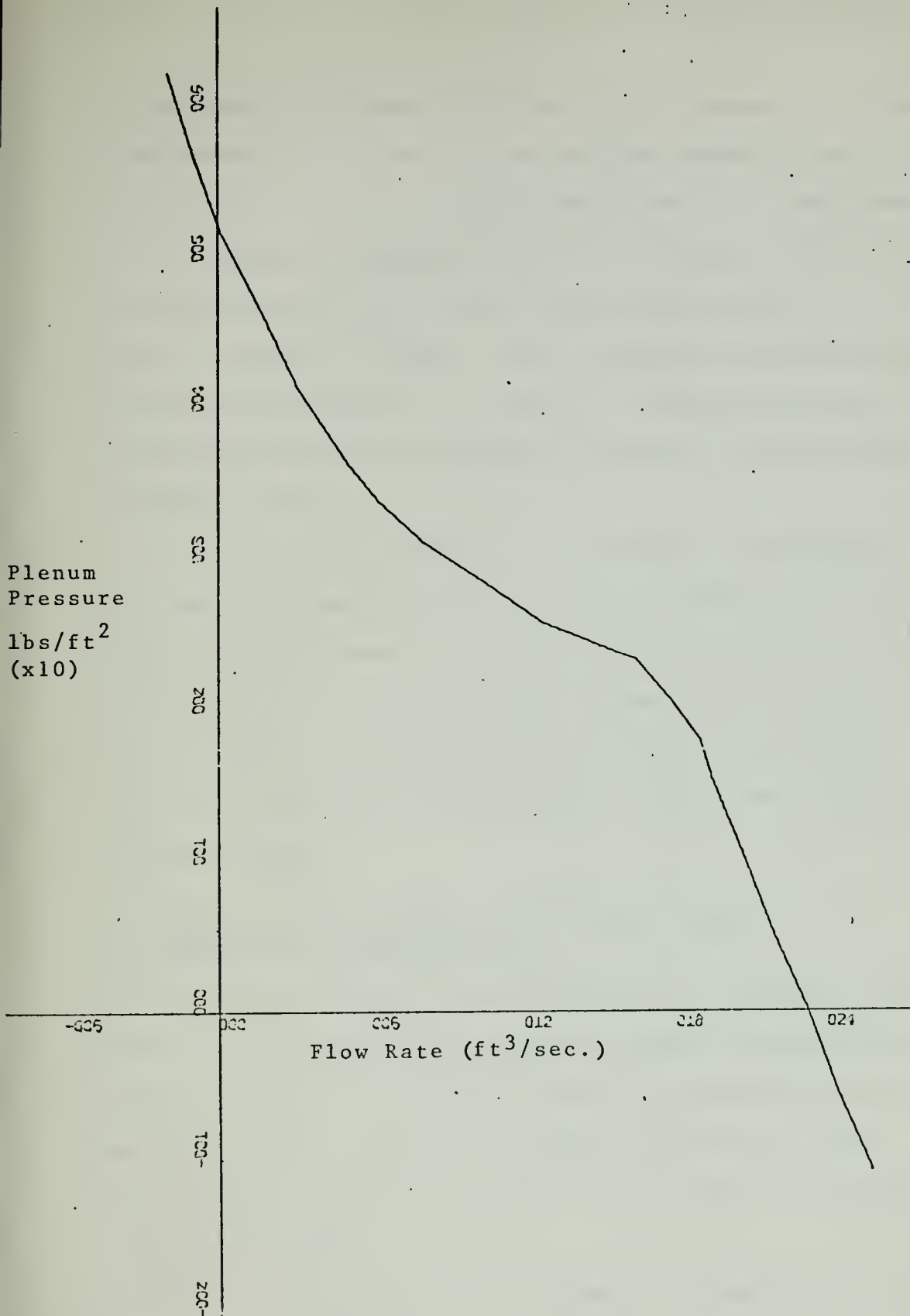


FIGURE 4  
STERN SEAL FAN MAP, ADJUSTED TO ACCOUNT FOR DUCTING LOSS



on the same performance graph as the fan maps. This power requirement is plotted for the entire operating range of the fans and is fairly consistent at about 2 horsepower. This horsepower requirement does not change under the new fan maps since the fan map discharge pressures at the fan exhaust remains the same. This horsepower map was entered in the fan subroutine as a table of look up and actual power requirements were computed from it using flow rate as the entering argument.

In the COLFIL subroutine (the routine that prints out all data and draws all graphs) the fan power label was changed to "fan power (ideal)" to avoid possible confusion. In the fan subroutine the print option was modified to give the actual power required as well as the ideal power. Also the fan efficiency is computed and is given as an output of this subroutine.

#### C. SIMULATED PERFORMANCE COMPARISONS BETWEEN ORIGINAL AND NEW FAN MAPS

As stated earlier it was believed that changing the leakage areas and the fan maps would have a significant effect only when the computer model was run under conditions where the plenum volume underwent comparatively rapid fluctuations and/or the leakage areas around the periphery of the hull varied.

These assumptions were confirmed by simulated runs under varying sea conditions. In all these comparison tests the two XR-3 models used were identical except that the original



fan maps were replaced by the newly developed ones in one model. Both simulated craft were run using the original seals as developed in Ref. 3. Craft weight was 5813 lbs, center of gravity 9.57 feet from the stern, speed was held constant at 20 knots. All runs were made into ahead seas. The sea conditions chosen were irregular sea state 1, irregular sea state 2, regular seas 1 and regular seas 2. The latter two were so named because the amplitudes and frequencies chosen for these regular seas runs were the major component of irregular sea state 1 and irregular sea state 2 respectively. The actual amplitudes and frequencies for these runs are tabulated on page 27.

In the simulation runs into regular seas 1 dramatic differences were noted in the fluctuation of plenum pressure and heave accelerations. With the original fan maps, variations in plenum pressure were limited to about  $2.2 \text{ lbs/ft}^2$  whereas with the new maps the variations were over  $6.9 \text{ lbs/ft}^2$ . This represents an increase in fluctuations of over 315 percent. Because the plenum normally provides over seventy percent of the supporting force for the craft similarly large variations were noted in heave acceleration both at the bow and at the center of gravity. Pitch motion, though, did not change much being less than .1 degree in both cases.

Results for the runs in other sea conditions are tabulated on page 28. The differences noted for the runs in irregular sea state 2 and regular seas 2 were not as great.



This has been attributed to the craft's ability to conform its attitude to the wave slope in the case of the longer wave lengths associated with greater sea states. This ability to conform then reduces the high frequency volumetric changes in the plenum chamber, thereby reducing pressure fluctuations. Figures 5 through 12 are the results of running both models in the simulated sea state one. By visually comparing the corresponding variances of the two models it is readily apparent that the fan maps do significantly change the performance characteristics of the model. By examining the table on page 28 it is also apparent that one must be careful in predicting behavior as the variation in measured variables does not vary directly with the sea conditions. The new fan maps have in effect defined a similar but different craft.





TABLE I. SEA STATE WAVE COMPONENTS

Run 1 Regular Seas 1 Heading 180

<u>Wave Components</u>	<u>Amplitude (ft)</u>	<u>Frequency (rad/sec)</u>
1	.0598	4.1526

Run 2 Regular Seas 2 Heading 180

<u>Wave Components</u>	<u>Amplitude (ft)</u>	<u>Frequency (rad/sec)</u>
1	.2721	1.8447

Run 3 Irregular Sea State 1 Heading 180

<u>Wave Components</u>	<u>Amplitude (ft)</u>	<u>Frequency (rad/sec)</u>
1	.0029	2.553
2	.0324	3.256
3	.0599	4.1526
4	.0558	5.2961
5	.0401	6.7545
6	.0262	8.6145
7	.0165	10.9867
8	.0102	14.0122

Run 4 Irregular Sea State 2 Heading 180

<u>Wave Components</u>	<u>Amplitude (ft)</u>	<u>Frequency (rad/sec)</u>
1	.0168	1.1786
2	.1464	1.4745
3	.2721	1.8447
4	.2668	2.3077
5	.2052	2.8871
6	.1410	3.6118
7	.0928	4.5185
8	.0600	5.6528



TABLE II   SIMULATED XR-3 PERFORMANCE WITH DIFFERENT  
FAN MAPS

Comparison of XR-3 Loads and Motion Computer Program performance with original for maps with XR-3 with new fan maps are given below:

RUN	QUANTITY	XR-3 (original)	XR-3 (new)
1. Regular Seas 1	Plenum Pressure	24.8±1.09 PSF	24.8±3.45 PSF
	Pitch Angle	3±.05 deg.	2.7±.05 deg.
	Draft	6.25±.05 in.	5.9±.1 in.
	C.G. Acceleration	±.04 g	±.15 g
2. Irregular Sea State 1	Plenum Pressure	24.8±2.0 PSF	24.8±15 PSF
	Pitch Angle	3.2±.1 deg.	2.5±.2 deg.
	Draft	6.5±.05 in.	5.75±.1 in.
	C.G. Acceleration	±.07 g	±.4 g
3. Regular Seas 2	Plenum Pressure	23.75±5.75 PSF	24.8±7 PSF
	Pitch Angle	5.1±4.75 deg.	4.2±3.8 deg.
	Draft	7.25±2.3 in.	6.0±2.9 in.
	C.G. Acceleration	±.23 g	±.27 g
4. Irregular Sea State 2	Plenum Pressure	5 to 33 PSF	-5 to 40 PSF
	Pitch Angle	.8±2.2 deg.	.8±2.5 deg.
	Draft	8±6 in.	10±7 in.
	C.G. Acceleration	±.46 g	±.7 g



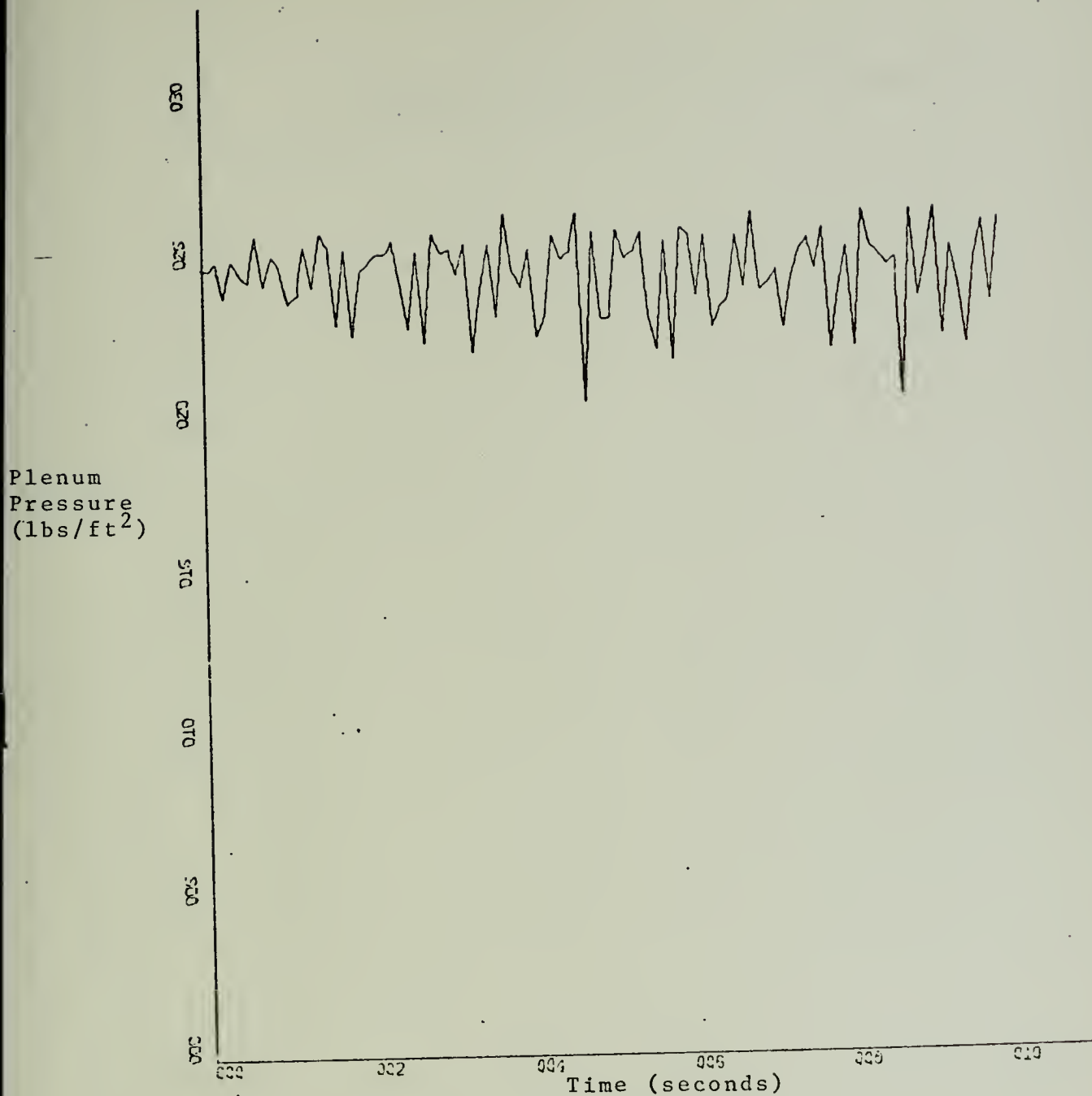


FIGURE 5

COMPUTER SIMULATION PLENUM PRESSURE VERSES TIME, SPEED 20 KNOTS  
ORIGINAL FAN MAPS, SEA STATE 1



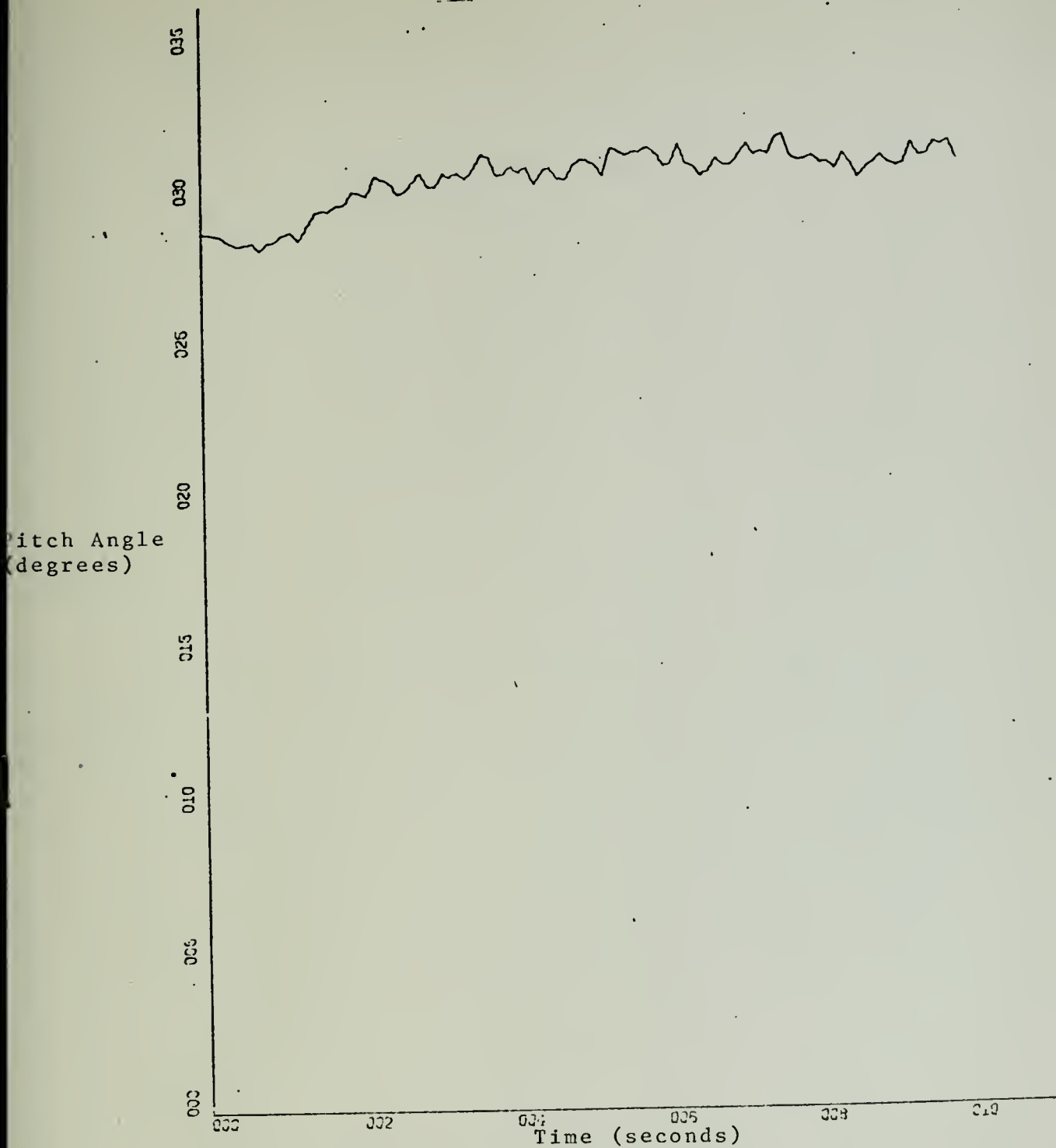


FIGURE 6

COMPUTER SIMULATION PITCH ANGLE VERSES TIME, SPEED 20 KNOTS  
ORIGINAL FAN MAPS, SEA STATE 1





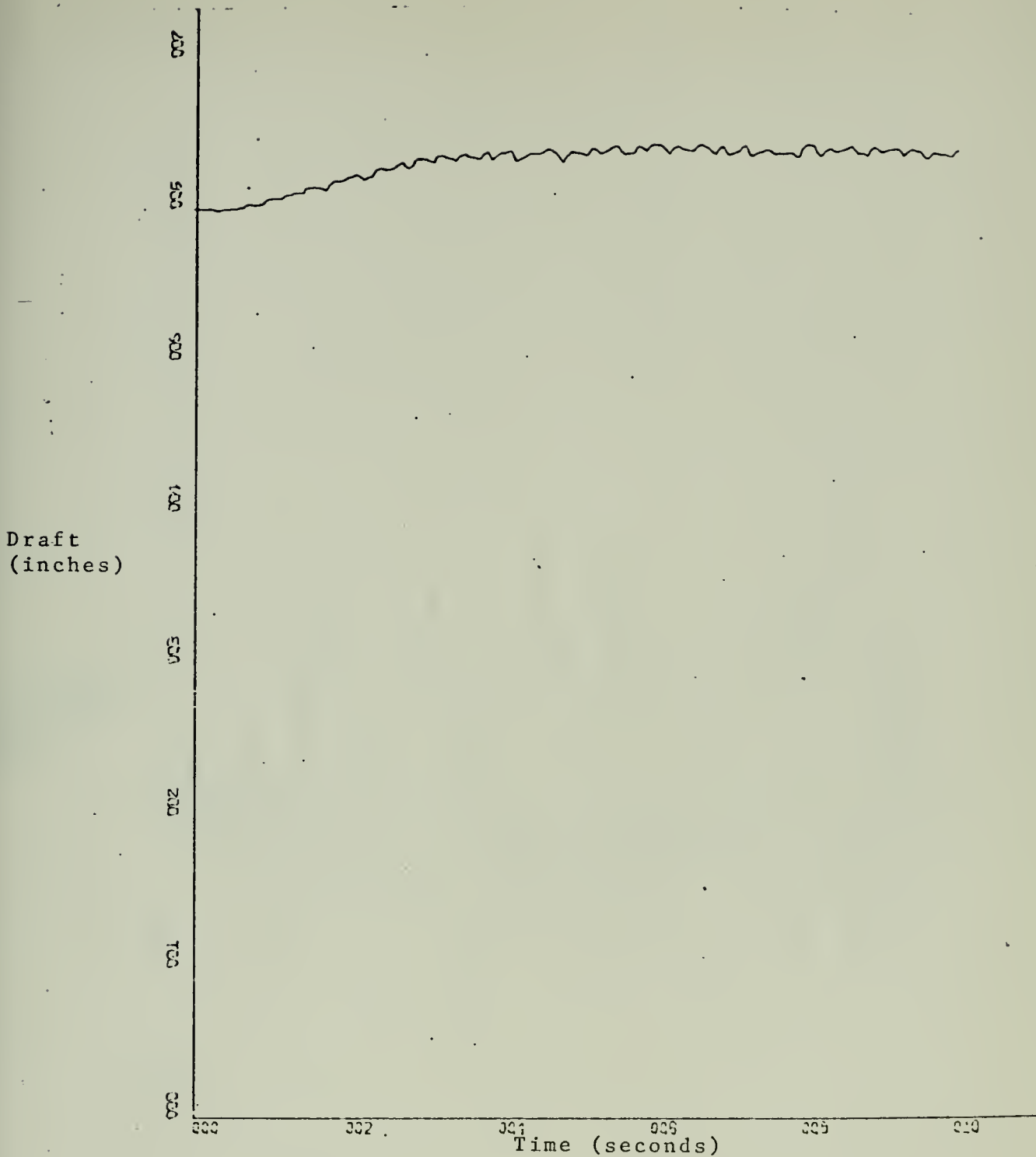


FIGURE 7  
COMPUTER SIMULATION C.G. DRAFT VERSES TIME, SPEED 20 KNOTS  
ORIGINAL FAN MAPS, SEA STATE 1



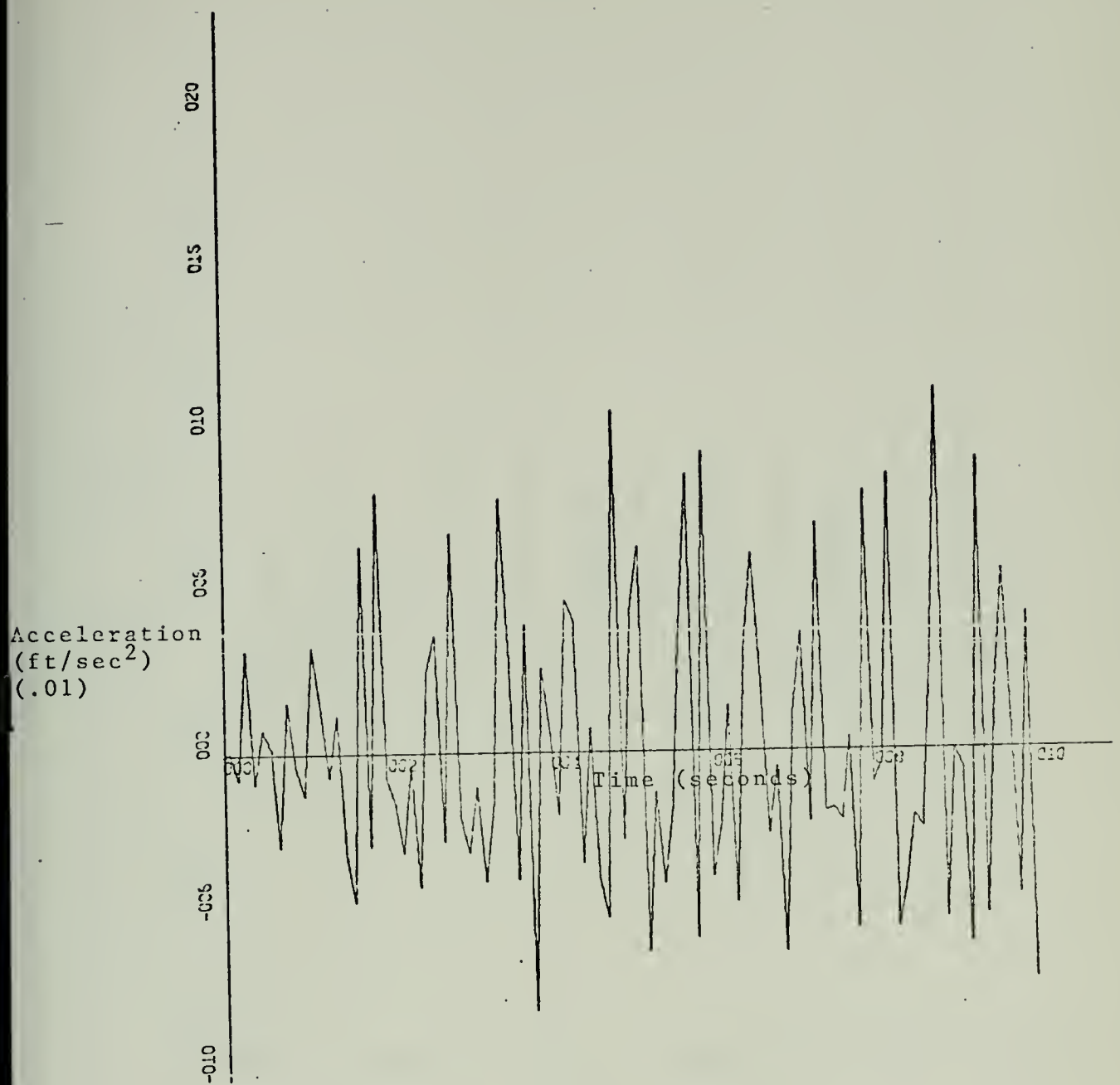


FIGURE 8

COMPUTER SIMULATION C.G. ACCELERATION VERSES TIME, SPEED 20 KNOTS  
ORIGINAL FAN MAPS, SEA STATE 1



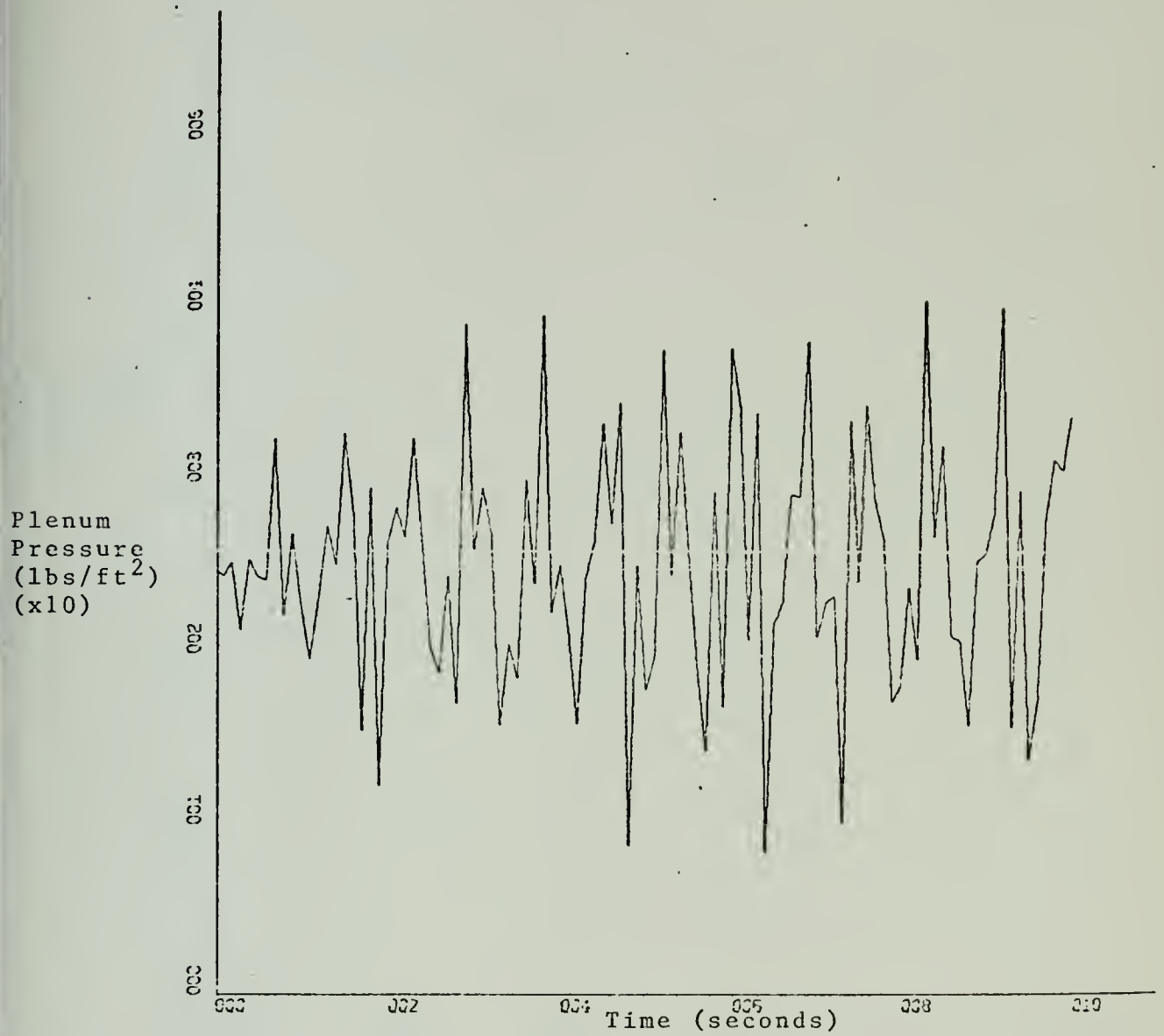


FIGURE 9

COMPUTER SIMULATION PLENUM PRESSURE VERSES TIME, SPEED 20 KNOTS  
NEW FAN MAPS, SEA STATE 1



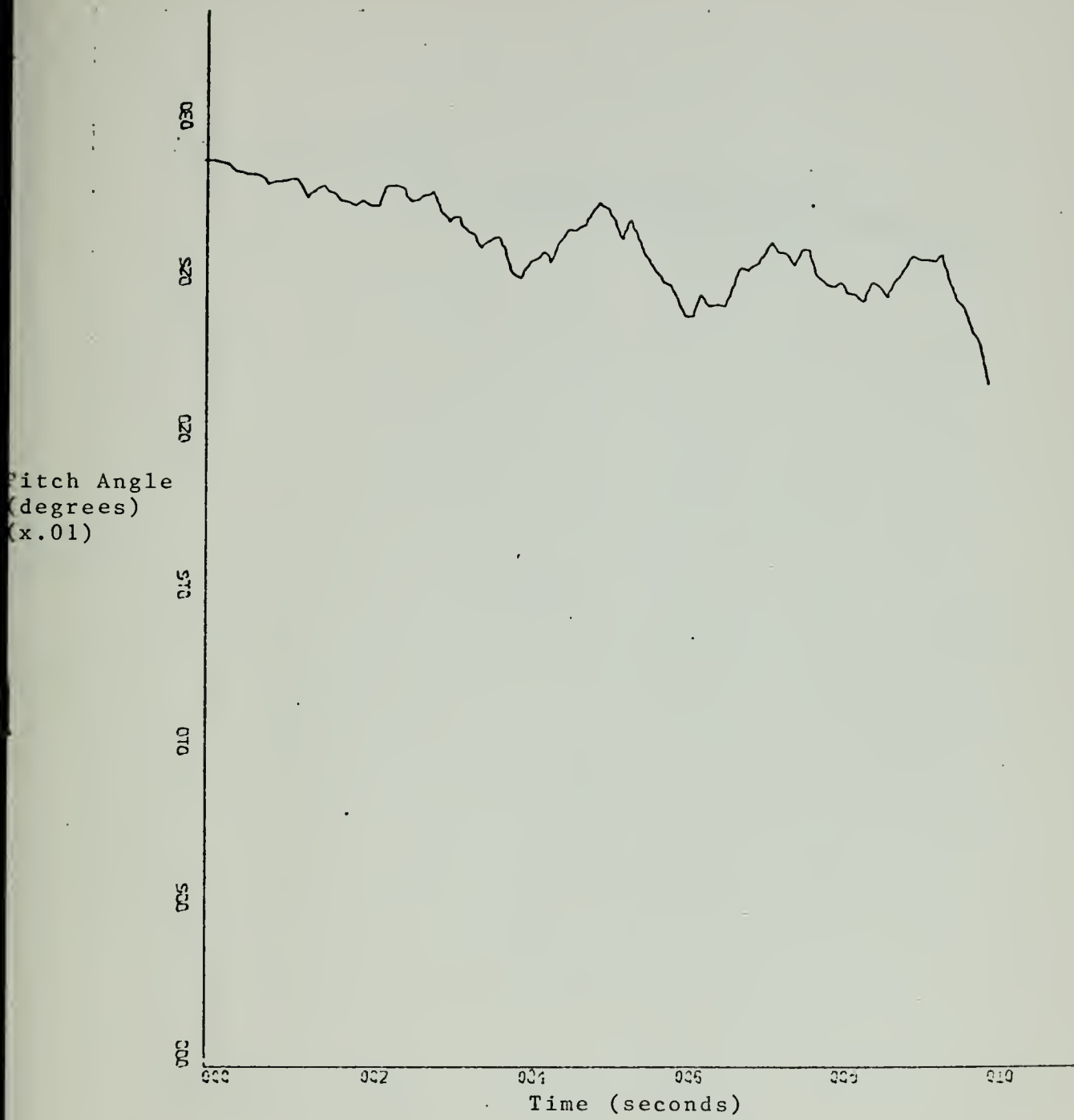


FIGURE 10  
COMPUTER SIMULATION PITCH ANGLE VERSES TIME, SPEED 20 KNOTS  
NEW FAN MAPS, SEA STATE 1





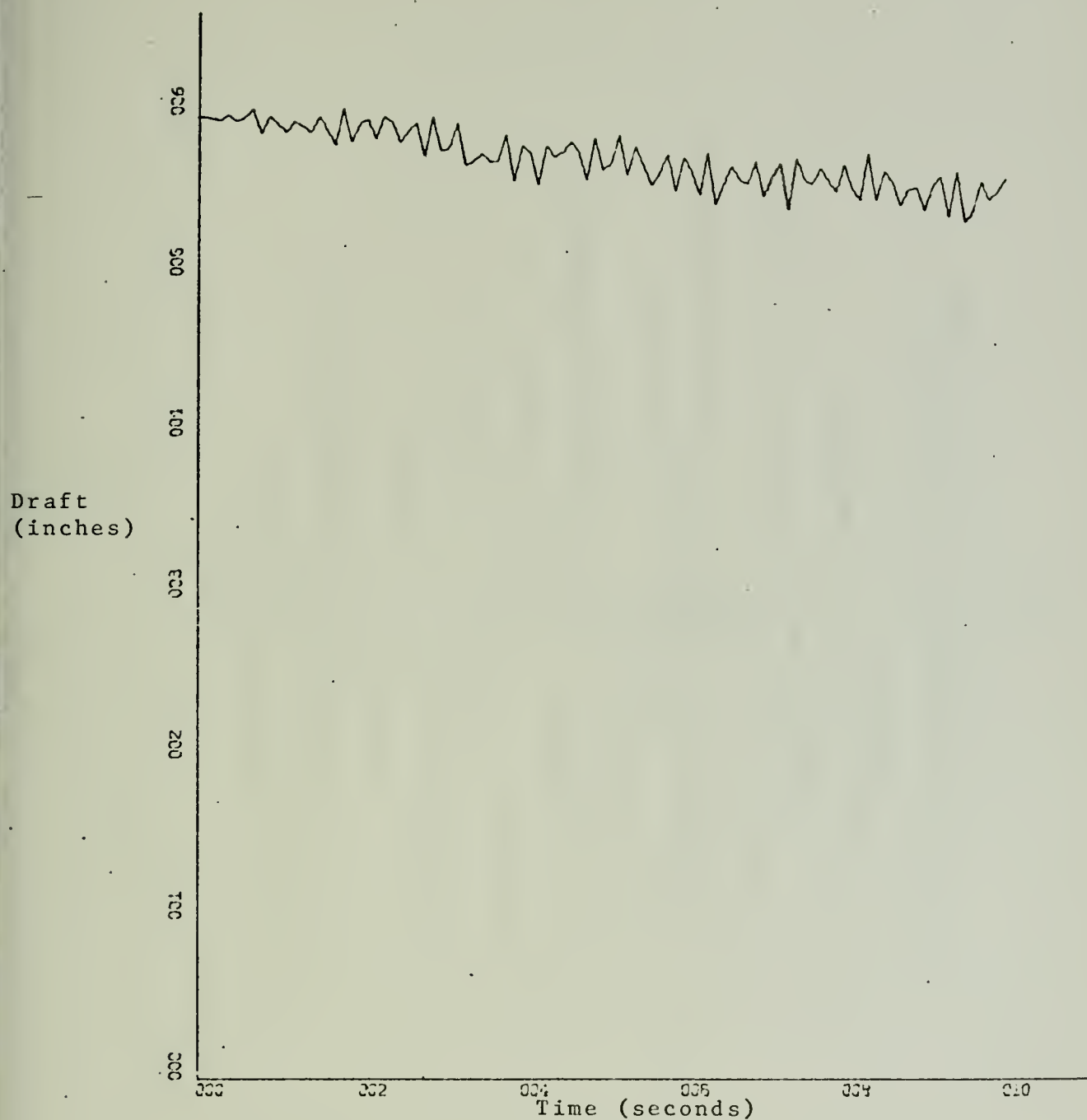


FIGURE 11  
COMPUTER SIMULATION C.G. DRAFT VERSES TIME, SPEED 20 KNOTS  
NEW FAN MAPS, SEA STATE 1



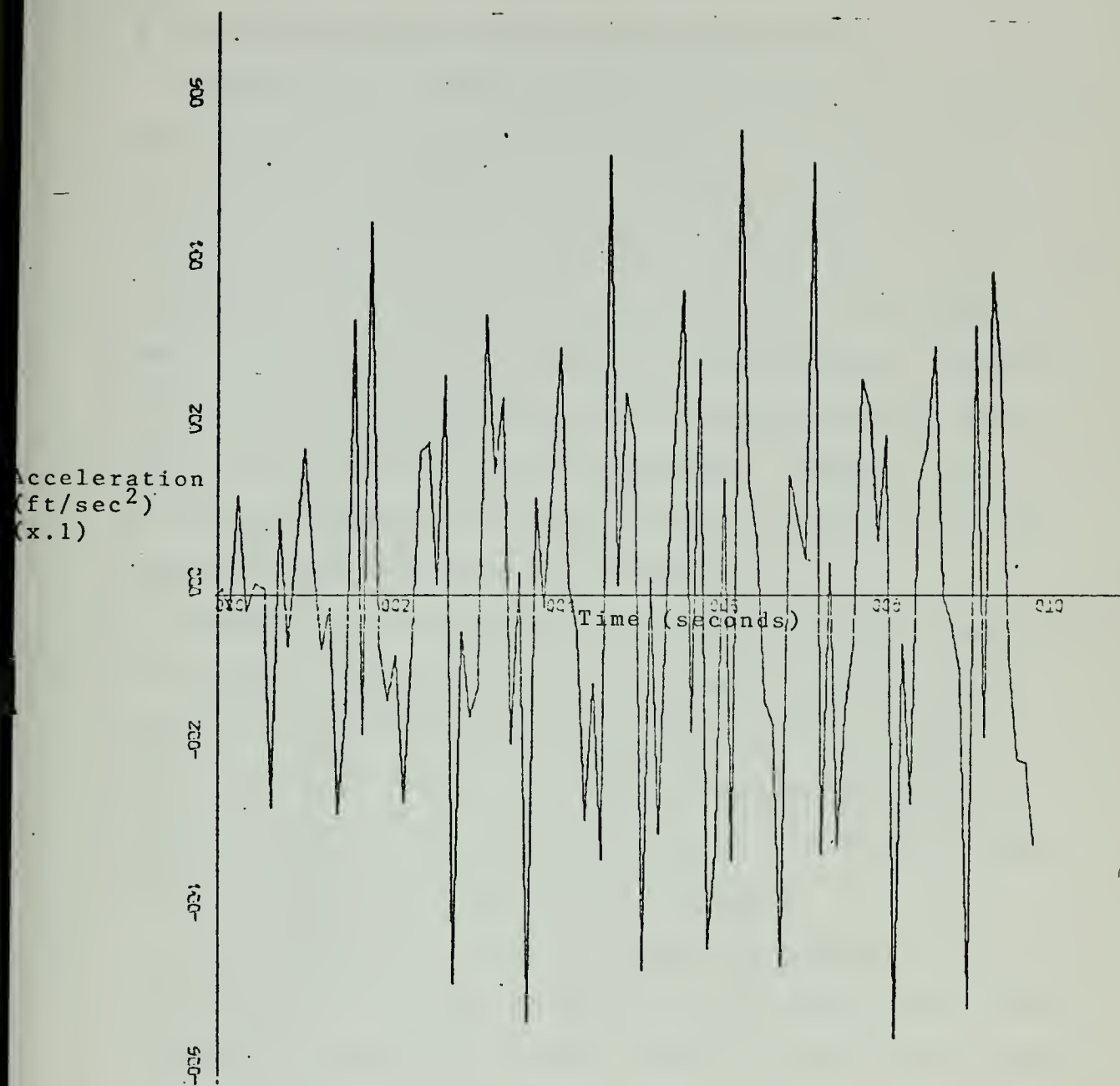


FIGURE 12

COMPUTER SIMULATION C.G. ACCELERATION VERSES TIME, SPEED 20 KNOTS  
NEW FAN MAPS, SEA STATE 1



### III. SEAL MODEL REFINEMENTS

#### A. INTRODUCTION AND BASIC MODELING TECHNIQUES

Through tests conducted aboard the XR-3 by the NPS test group headed by Associated Professor D.M. Layton of the Aeronautics Department it has been demonstrated that the forces generated by the seals have an appreciable effect on the overall performance of the test craft. By varying the lower travel limit of the bow seal and contouring its shape the steady state pitch angle can be changed as well as the thrust versus velocity characteristics. Although not as pronounced, changing the support cable length of the stern seal also affected craft trim conditions.

Because of the demonstrated steady state pitch sensitivity of the XR-3 to seal position limits as set by the support cables it was decided that more detailed modeling of the seals was needed before the overall response of the L&M computer model would reflect the behavior of the XR-3 under varying conditions of support cable length.

The original XR-3 seal modeling as presented in Ref. 3 was patterned after the rear seal in the L&M computer model of the Bell (100B) 100 ton CAB. This seal is of the "soft" pneumatic type and its representation is well covered by Kaplan, Bentson and Sargent in Ref. 2.

The pneumatic "soft" seal model is based on the assumption that this type of seal is unstiffened and non-rigid. The mass of the seal was considered so insignificantly small as



compared to the forces generated by the seal when it is in contact with the water as to have negligible effect on overall craft dynamics. The lifting forces generated by the seals were calculated by multiplying the wetted contact area of the seals by the pressure differential between the seal and the atmosphere for the bow seal and the plenum chamber and seal in the case of the stern seal.

Drag forces on the seals were considered to be due only to skin friction between the water and the seal. The equation used to compute these forces was

$$F_{x_{\text{seal}}} = - \frac{\rho u^2}{2} C_{df} A_{\text{seal}}$$

where  $\rho$  is the density of water,  $u$  the velocity of the craft and  $A_{\text{seal}}$  is the wetted surface of the seal.  $C_{df}$  is the drag coefficient and is calculated using the Schultz-Grünow formula

$$C_{df} = .427 / (\log_{10} Re - .407)^{2.64}$$

where  $Re$  is the Reynolds number computed based on the average wetted length of the seal and the Reynolds number is calculated by:

$$Re = \frac{u \times (\text{wetted length})}{1.28 \times 10^{-5}}$$

where  $1.28 \times 10^{-5} \text{ ft}^2/\text{sec}$  is the kinematic viscosity of the water.





The actual construction of the seals is well described in Ref. 3. Each seal consists of two pneumatic lobes separated by a common membrane. The membrane has limber holes in it to equalize the pressure between the lobes. The lower surface of the bottom lobe is shaped by twelve steel battens that act as stiffeners. These battens are spaced uniformly across the bottom surface at right angles to the hinge line. It is this surface that comes in contact with the water, and will hereafter be referred to as the "leading face" of the seal.

The forward edge of the leading faces is hinged near the top of the plenum chamber allowing the seal to pivot about this line when waves are encountered.

The pressure in the seals is maintained by axial fans. The air is delivered by ducts that discharge into the top of the upper lobe. The seals in turn vent to the main plenum by means of ducting. Back pressure in the vent ducting can be controlled by butterfly valves that can be manually adjusted. Normally the seals are operated so that they maintain about 1-2 PSF more pressure than the plenum.

Downward travel limits of the seals are controlled by adjustable support cables attached to the rear edge of each steel batten at the trailing edge of the seal's leading face. In addition a second support cable is attached to each stiffener approximately midway between the hinge line and the trailing edge. Figure 13 shows a cutaway of the seals, only two cables are drawn in for clarity.



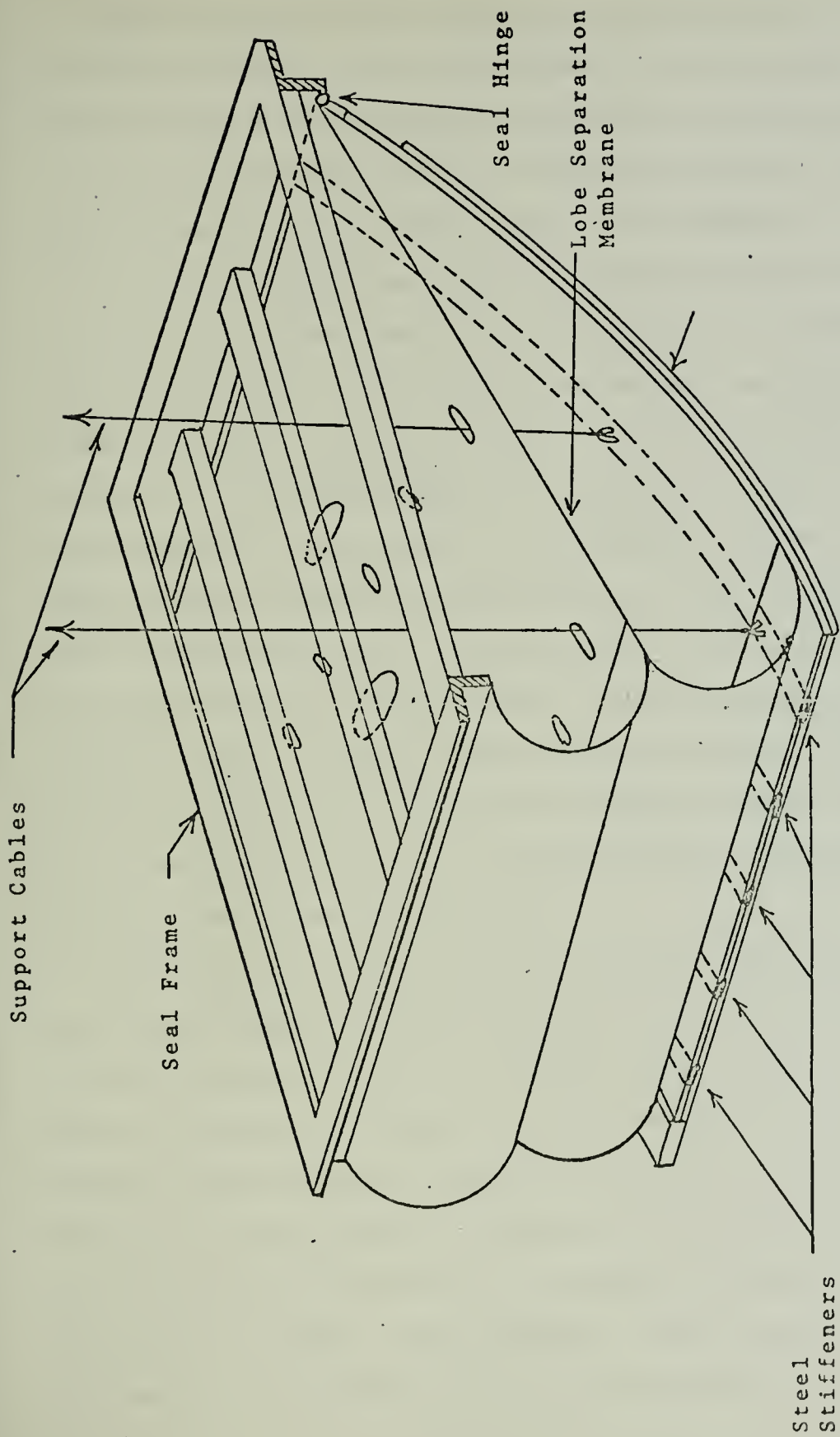


FIGURE 13  
CROSS SECTIONAL VIEW OF PNEUMATIC SEAL AS INSTALLED ON THE XR-3



Both the bow and the stern seal extend the width of the plenum chamber and are identical in construction. The leading faces are approximately 49 inches long from hinge line to trailing edge. The perpendicular distance from sidewall keels to the hinge line is 22.5 inches.

As stated before the original modeling of the seals did not take into account any of the seal's ability to flex or pivot on its hinge. In addition no attempt was made to model the support cables and their ability to affect craft attitude. In the new modeling the support cables have been incorporated. In the stern seal modeling only the rear support cable is modeled since this seal rarely comes in contact with the water. In the bow seal subroutine both the rear support cables and the center support cables have been included since this seal does contact the water. Before any attempt at revising the seal subroutines could be undertaken it was necessary first to study the action of the seals while the craft was actually underway.

The semi-rigid construction of the seal dictated a highly complex distributed parameter model of the seals be developed if the seals were to be fully modeled without any approximations. In addition to the fact that practically all of the physical characteristic parameters of the seal such as spring constants for the steel stiffeners and fabric flexibility were unknown such a model would require an inordinate amount of calculation time in the computer. Since extra computation time was to be avoided simplifying assumptions had to be made.



To be accurate these assumptions or approximations had to be based on actual observations of the seal or on previously made approximations whose effect has already been investigated.

In Ref. 2 the approximation of eliminating seal dynamics and the setting of seal pressure at a constant level above plenum pressure has been thoroughly investigated and was incorporated in the original model of soft pneumatic seals. These approximations have been continued in the present seal modeling.

The other modeling approximations made were based upon actual observations made of the seals while the XR-3 was in motion. These observations are described below:

1. For small water perturbations (approximately 3 inches) the bow seal flexed and appeared to pivot slightly about the center support cable causing the angle at the hinge line to slightly increase, but almost insignificantly.

2. For longer perturbations the seal both flexed as described above and then began to pivot on the hinge. After the seal rose about six inches no additional flexing took place.

3. The bow seal maintained contact with the water at all times and never gaped because of an inability to follow wave motion.

4. The bow seals penetration of the water was practically independent of water motion in relation to the craft, but appeared to be inversely related to the craft's velocity.





When the XR-3 was at rest penetration was about five to six inches and when traveling at 20 knots appeared to be approximately 1 inch.

5. The stern seal rode out of the water while the craft operated above "hump" speed. The height of the air gap thus created appeared to remain almost constant at four to five inches. Water rarely contacted the seal.

Using the above described observations and the preceding simplifying approximations concerning seal dynamics and pressures both the bow and stern seal were modified to reflect the action of the actual seals.

The approximation given in Ref. 2 of equating the wetted length of the seal with the water height above the sidewall keel at the seal's trailing edge location was eliminated. In its stead a two-dimensional "table of look up" was developed which gave wetted length as a function of the immersion depth of the seal's trailing edge in the water and the seal's trailing edge deflection height above the keel at the trailing edge location. In other words if the seal was deflected upwards because of wave motion or pitching motion of the craft the deflection height of the trailing edge would increase and the seal's leading face would become more parallel to the water's surface thereby increasing the wetted area of the seal.



The "table of lookup" was constructed using the information obtained from a graphical deflection model similar to the one presented in Figure 14. In this model the leading face of the seal is represented in varying amounts of deflection height from full down (point A) to full up against the seal framework (point B). Full down is zero deflection and is where the trailing edge of the seal is even with the bottom of the sidewall keel, full up is maximum deflection. This deflection height was divided into segments of one inch for ease of computation. Points were marked upon each leading face line which represented the surface of the water on the leading face under varying depths of trailing edge immersion. The distance along the leading face to the trailing edge from these points then represented the length of the leading face that was immersed in the water or the "wetted length". The points for similar immersion depths were connected for the varying seal deflection heights and these construction lines are labeled with their corresponding immersion depths in inches along the zero deflection height leading face. The construction line corresponding to an immersion depth of zero inches is, of course, congruent with the trailing edge of the seal since if the seal did not penetrate the water to at least some degree there could be no "wetted length" unless the leading face was exactly parallel to the water's surface, which never occurs. These construction lines were drawn for immersion depths of the trailing edge of 0 to 5 inches.



NOTE: length ① represents wetted length of seal with an immersion depth of one inch and a seal deflection height of five inches.  
 ② represents a wetted length of the seal when the deflection height is nine inches and the immersion depth is two inches.

seal hinge point

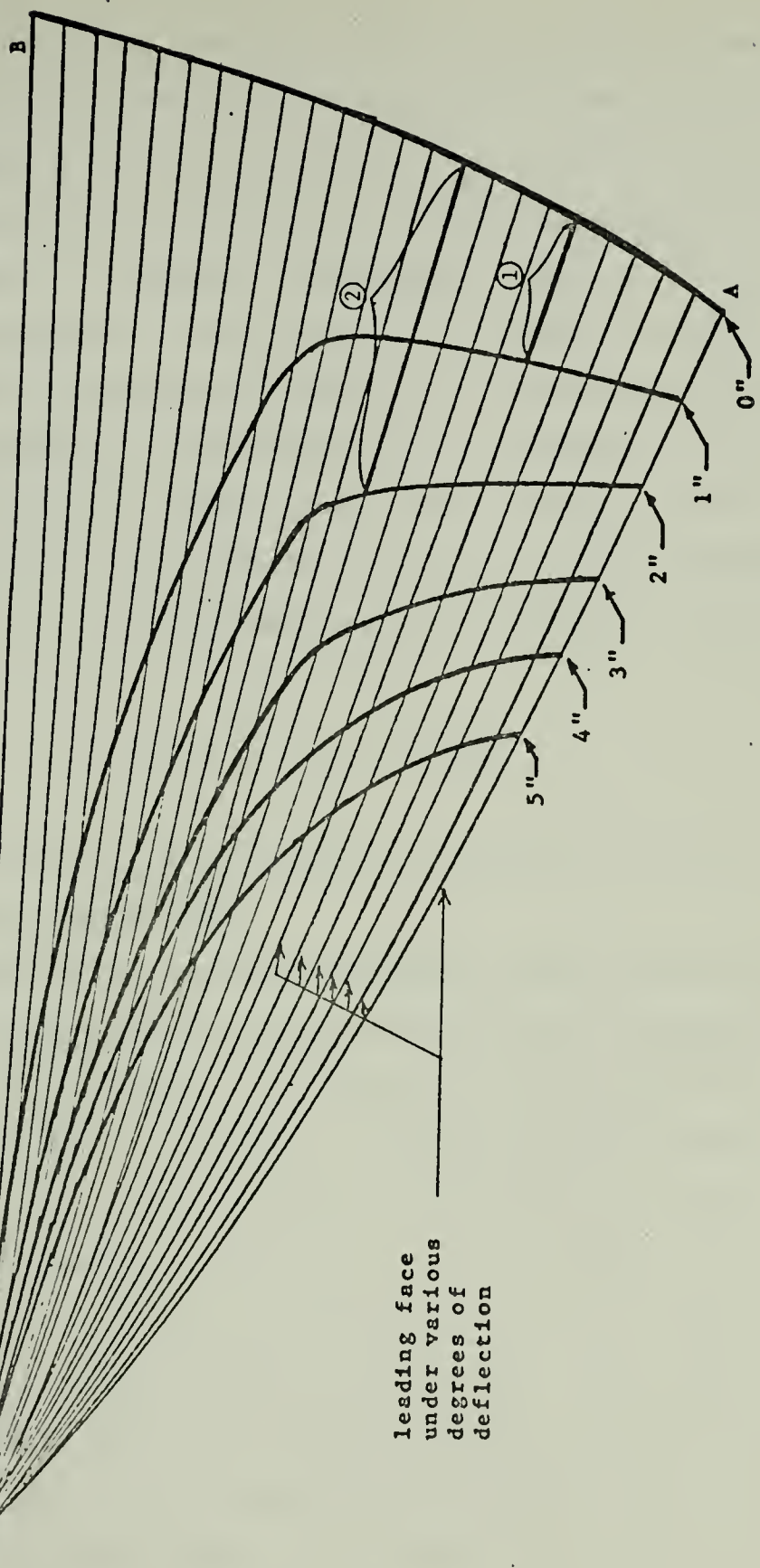


FIGURE 14

BOW AND STERN SEAL DEFLECTION MODEL ( NOT TO SCALE )



The actual immersion depth of the trailing edge is calculated based upon the observation that at rest the immersion depth was approximately 5.5 inches and while traveling at 20 knots was estimated at a little less than one inch. Since the hydrodynamic force on the seal is proportional to the square of the craft's velocity the immersion depth was assumed to be approximately inversely proportional to some factor of the square of the speed.

Using 5.5 inches as the known immersion depth at zero speed and .75 inches at 20 knots, the following empirical formula was derived which gives reasonable results

$$D(\text{in.}) = 5.5 / (1 + \frac{u}{25})^2$$

where D(in.) is the depth in inches and u is the velocity in feet per second.

Using the calculated immersion depth and the seals calculated deflection height the table is entered to give the wetted length. This table of look up is presented graphically in Figure 15. The non-linear nature of the curves is readily apparent. An important aspect of this table apparent in Figure 15 is that within about the first ten inches of seal deflection the wetted length of the seal remains fairly constant, especially if the craft is operating at speeds where the immersion depth is approximately one inch. This figure also shows that the maximum wetted length is equal to the length of the leading face (just over 48 inches).





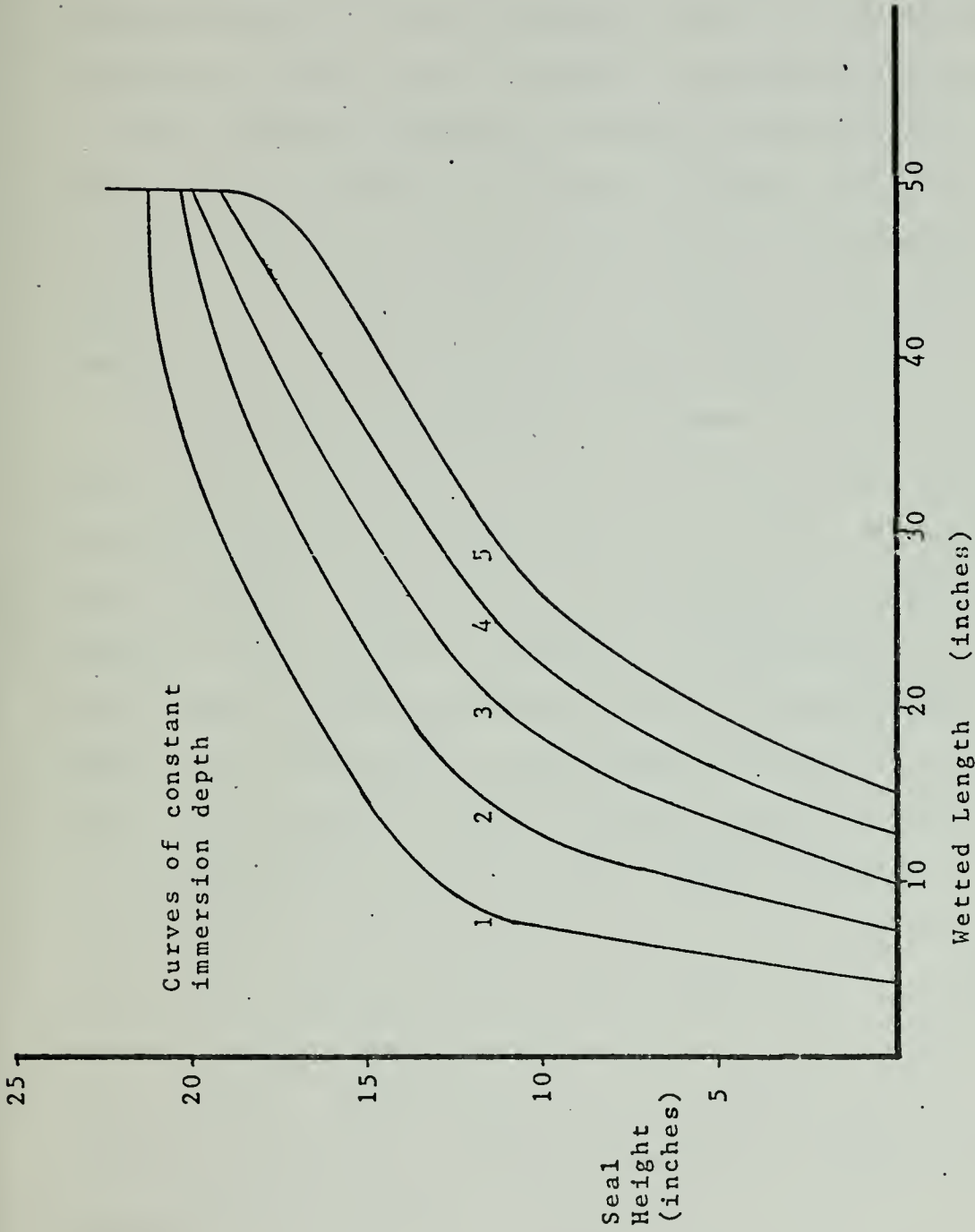


FIGURE 15  
SEAL TRAILING EDGE HEIGHT ABOVE KEEL VERSES SEAL WETTED LENGTH



As the seal deflects and becomes more horizontal the wetted surface area becomes greater given a constant immersion depth.

This same "table of look up" is provided in the stern seal modeling but because the seal does not ride in the water an assumed "depth" had to be used as an entering argument.

The assumption was made that since the stern seal does not ride on the water its lifting force has to be the result of some form of air pressure. This force could only be generated by the impingement of air particles on the seal's leading face as they rushed to escape underneath the seal.

At this point an assumption was made that the effective wetted area occurred where the kinetic energy in the air mass was approximately one quarter that of the air escaping underneath the seal. As the air in the plenum is at such a pressure that it can be considered incompressible this would occur where the cross-sectional area was approximately two times the cross-sectional area beneath the seal. As the width of the plenum chamber is constant and the gap height is approximately 4.5 inches at all times the point on the seal where the cross-sectional area is two times the gap area is the point along the leading face where the height from the seal to the water is two times the gap height or about 9 inches. Subtracting the gap height gives an effective "phantom" immersion depth of 4.5 inches; this was rounded to five inches.



Lift forces generated by the stern seal were considered to be the product of the seal area found by using the above phantom immersion depth and the seal deflection height, and the pressure differential between the stern seal and plenum chamber.

The above lifting force calculation has only minimal effect on simulated performance of the XR-3 since the pressure between the seal and the plenum chamber is normally only one to two PSF. The drag forces on the stern seal are calculated in the same manner as they are in the bow seal subroutine but are subsequently set to zero since the seal rarely contacts the water.

#### B. BOW SEAL MODELING

Contained herein is a detailed analysis of the actual bow seal subroutine. It is coded in standard FORTRAN. By reviewing the actual subroutine the actual approximations used in the routine may be understood. A full listing of the BOWSL subroutine is contained in Appendix A along with the required entries in the data input statements.

```
(1) DO 1 J=1,11
(2) GAP(J) = 0.0
(3) ELSKI(J) = 0.0
(4) WETLEN(J) = 0.0
(5) ELSKID(J) = 0.0
(6) 1 CONTINUE
```

The above statements (1 through 6) zero all variable arrays that will be used every time BOWSL is entered. GAP(J) is the height of the air gap at each station along the bow seal.



ELSKI(J) is the water height above the keel at the trailing edge of the seal. WETLEN(J) is the wetted surface length at each station. ELSKID(J) is the deflection height of the seal trailing edge measured from the bottom of the keel of the craft.

```
(7)  ALBS = 0.0
(8)  FX = 0.0
(9)  FY = 0.0
(10) FZ = 0.0
(11) FK = 0.0
(12) FM = 0.0
(13) FN = 0.0
```

The preceding seven statements initialize the single valued variables that are computed each time BOWSL is entered. ALBS is leakage area of the bow seal. FX is the forces parallel to the craft's axis of symmetry (centerline). FY is the horizontal forces perpendicular to the FX forces. FZ is the vertical forces. FK, FM, FN are the moments about the Z axis, Y axis and X axis respectively.

```
(14) DELPBG = PBS - PB
(15) IF (DELPBG.LT.0.0)DELPBG=0.0
```

Equation 14 computes the pressure differential between the plenum chamber (PB) and the seal (PBS). This differential is actually fixed in INCON as an entering argument. Equation 15 assures that the seal differential pressure is never negative. This is reasonable since the seals vent to the chamber.





(16)       $ARGO = ELMAXB / CORLEN$   
(17)       $ANGO = ARSIN(ARGO)$   
(18)       $X1 = XBS + ZBS * THETA - CORLEN * COS(ANGO)$

The three equations above (16-18) establish the moment arm in the X direction from the craft center of gravity to the trailing edge of the bow seal. ELMAXB is the rear cable length. CORLEN is the chord length of the bow seal. XBS is the distance from the center of gravity to the bow. ZBS is the vertical distance of the bow hinge line below the center of gravity. Theta is the pitch angle of the craft.

(19)       $Z1 = -Z - ABS + XBS * THETA - ELMAXB * COS(THETA)$

Equation (19) establishes the moment arm in the -Z direction to the water's surface through which the drag forces act to create a moment about the Y axis.

(20)       $DPTHFT = (5.5 / (1. + (U/25.))) ** 2.0 / 12.0$

Equation (20) calculates the immersion depth of the seal based upon craft velocity, u.

(21)       $IF(CENCAB.GT.1.1875)CENCAB=1.1875$

Logical statement (21) sets the maximum length of the center support cable to 3 inches more than the maximum rear cable length, ELMAXB.



(22) DO 3 K=1,N

⋮

3 CONTINUE

The above loop calculates for each seal partition point the water height above the keel  $ELSK1(K)$ , the wetted length,  $WETLEN(K)$ , and the seal deflection height  $ELSKID(K)$  in preparation to calculating the forces and moments.

(23) DPFT(K) = DPTHFT

Equation (23) initializes the immersion depth of the seal.

(24)  $ELSK1(K) = (ETA(3,K) - DTABX(K) * (XX(3,K) - X1) - Z1) + YY(3,K) * PHI + XLXPVW * WATSLP$

Equation (24) establishes the water height above (or below) the keel at the bow.  $ETA(3,K)$  is the height of the water at the center of gravity above mean.  $DTABX(K)$  is the correction factor for moving this height away from the C.G. (Center of Gravity).  $(XX(3,K) - X1)$  is the distance the correction factor has to act on.  $Z1$  is the height of the keel in relation to the C.G.  $YY(3,K)$  is the displacement of the partition from the craft center line.  $PHI$  is the roll angle.  $XLXPVW * WATSLP$  is the correction factor for the water slope caused by the plenum pressure acting for a finite period.



(25) IF(ELSKI(K).GT.HINGHT) ELSKI(K)=HINGHT

Equation (25) limits the water height to the hinge height of the bow seal.

(26) IF((HINGHT-ELSKI(K)+DPFT(K)).GE.ELMAXB)  
DPFT(K)=ELMAXB-HINGHT+ELSKI(K)

Equation (26) adjusts the immersion depth of the seal so that the seal can go no lower than that permitted by the rear cable ELMAXB.

(27) IF(DPFT.LT.0.0) DPFT=0.0

DPFT is used in computing DPIN which is an entering argument into the wet length table BWSL. Therefore equation (27) limits this argument to a minimum value of zero.

(28) ELSKID(K)=(ELSKI(K)-DPFT(K))\*12.0

Equation (28) calculates the deflection height of the seal (ELSKID(K)) in inches based upon water height, ELSKI(K) and the immersion depth DPFT(K).

(29) IF((HINGHT-ELSKID(K)/12.0).GE.ELMAXB)  
ELSKID(K)=(HINGHT-ELMAXB)\*12.0

Equation (29) limits the downward travel of the bow seal to ELMAXB the rear cable length and adjusts the deflection height ELSKID(K) to reflect this lower limit.



```

(30) DPIN=DPFT(K)*12.0
(31) MM=DPIN
(32) MM1=MM+1
(33) MM2=MM1+1
(34) DINC=DPIN-MM

```

The equations above, (30) through (34), establish parameters for entering the bow seal wetted length array, BOWSL. DPIN is the immersion depth in inches, MM1 is the lower limit table calling integer, MM2 is the upper table calling integer and DINC is the incremental difference.

```

(35) GAP(K)=-ELSKI(K)+(HINGHT-ELMAXB)

```

Equation (35) computes the air gap height based on water height ELSKI(K) which is positive upwards and the limit of the seal travel (HINGHT-ELMAXB).

```

(36) IF(GAP.LT.0.0) GAP=0.0

```

Equation (36) limits the gap to positive values.

```

(37) IF(ELSKID(K).GE.0.0) GO TO 2
(38) WETLEN(K)=ELSKI(K)
(39) GO TO 3

```

Equations (37) through (39) set the wet length equal to the water height if it is negative. This computation is used in case one seal partition point has a negative value while the others on either side are positive.





```

(40)    MM3=ELSKID(K)
(41)    MM4=MM3+1
(42)    MM5=MM4+1
(43)    DLINC=ELSKID(K)-MM3

```

Equations (40) through (43) establish the final two entering arguments for retrieving the four points needed from BWSL to compute the wetted length. ELSKID(K) is the deflection height of the seal. MM4 is the lower entering integer based upon the deflection height, MM5 is the upper integer. DLINC is the incremental difference used for linear interpolation.

```

(44)    BWSL1=BWSL(MM1,MM4)
(45)    BWSL2=BWSL(MM1,MM5)
(46)    BWSL3=BWSL(MM2,MM4)
(47)    BWSL4=BWSL(MM2,MM5)
(48)    BWSLA1=(BWSL2-BWSL1)*DLINC+BWSL1
(49)    BWSLA2=(BWSL4-BWSL3)*DLINC+BWSL3
(50)    WETLEN(K)=((BWSLA2-BWSLA1)*DLINC+BWSLA1)/12.0

```

Equations (44) through (50) identify the four points of the BWSL array which bracket the actual value of wetted length. Linear interpolation is used twice to find the average based on deflection height and once to find the final wetted length. The array BWSL was calculated in inches; thus, to convert to feet the final average is divided by 12.0.

```

(51)    DO 8 J=1,N
          :
          8 CONTINUE

```

This loop makes all the force calculations based upon wetted length and seal position calculated previously. In



addition it calculates the leakage area based upon the steady state leakage area and the variable gap heights.

```
(52)    WETLAV=(WETLEN(J+1)+WETLEN(J))/2.0
(53)    IF(WETLAV.LE..001)GO TO 6
(54)    DPFTAV=(DPFT(J+1)+DPFT(J))/2.0
(55)    ELSKIA=(ELSKI(J+1)+ELSKI(J))/2.0
(56)    ELSKDA=(ELSKID(J+1)+ELSKID(J))/2.0
```

Equations (52) and (54) through (56) average the wetted length, immersion depth, water height and deflection height respectively, for each seal segment based on the values calculated for the stations on either side.

Equation (53) routes the program around the remaining force calculations if the wetted length of the seal is zero or insignificant for calculation.

```
(57)    SEALHT=HINGHT-ELSKDA
```

Equation (57) is the calculation of the distance between the top of the seal's supporting frame and the bottom of the trailing edge of the seal.

```
(58)    DIFF=2.0*CENCAB-(SEALHT+0.5)
(59)    IF(DIFF.GT.0.5) DIFF=0.5
```

The DIFF equation (58) calculates the spring distance of the steel battens based upon the center support cable length CENCAB and the position of the seal, SEALHT.

Equation (59) limits the spring movement to .5 feet or six inches, the point where rigid body analysis comes into full effect.



```

(60)   ARM1B(J)=X1+WETLAV/2.0
(61)   ARM2B(J)=ZS-ELSKIA+DPFTAV/2.0

```

Equations (60) and (61) calculate the moment arms in the X and Z direction respectively based upon the length to the trailing edge of the bow seal, X1, and half the wetted length, WETLAV/2.0, for ARM1B. ARM2B is based upon the height of the center of gravity ZS, the water height, ELSKIA and half the immersion depth of the seal, DPFTAV/2.0.

```

(62)   IF(DIFF.GE.0.25) GO TO 4
(63)   DFBS(J)=-DELP*DELYBS*WETLAV
(64)   GO TO 5

```

Equations (62) through (64) calculate the vertical force acting on the segment if the deflection difference is less than .25 feet or three inches. If the deflection difference is greater than .25 or 3 inches the vertical force equation has a spring constant term in it acting upon the moment summations about the hinge line.

```

(65)   4 FORLEN=XBF-WETLAV
(66)   IF(FORLEN.EQ.00) GO TO 5
(67)   ARGW=(HINGHT-ELSKIA)/FORLEN
(68)   IF(ARGW.GT.1.0)ARGW=1.0
(69)   ANGW=ARSIN(ARGW)
(70)   FORCOS=COS(ANGW)
(71)   GO TO 6
(72)   5 FORCOS=0.0

```

Equations (65) through (72) calculate the length of the seal not in contact with the water, FORLEN, and the angle which this length makes with the water ANGW. From the angle the cosine of ANGW is calculated, FORCOS, for future use in calculating the vertical moments about the hinge line.



```

(73)  DFBS(J)=-DELP*DELYBS*WETLAV-DELP*FORLEN*DELYBS
        *FORCOS*(FORLEN*0.5*FORCOS)/
        FORLEN*FORCOS+WETLAV/2.0))*
        ((DIFF-0.25)*4.0)

```

The above equation calculates the vertical force acting upon the bow seal by summing vertical moments about the hinge line and equating it to the moment created by one vertical force vector acting on the midpoint of the wetted surface. The term "(DIFF-0.25)\*4.0" introduces a spring distance of three inches through which the vertical force transitions from being only based upon the product of the wetted area and the pressure differential to one based upon equalizing moments about the hinge line. After the seal bends this three inches it is assumed to be completely rigid and therefore if the seal is not undergoing accelerations, the moments must balance about the hinge line.

```

(74)  ARG=0.5*RHO*U*U*WETLAV*DELYBS
(75)  RESKI=U*WETLAV/ENU
(76)  CDTSKI=0.427/(ALOG10(RESKI)-0.407)**2.64
(77)  TSKIB(J)=-ARG*CDTSKI

```

The above four equations calculate the drag forces of the seal based upon the previously discussed Schultz-Grunow formula. RESKI is the Reynolds number, CDTSKI is the drag coefficient and TSKIB(J) is the drag force on the segment.





```

      7 CONTINUE
(78)  FX=FX+TSK1B(J)
(79)  FZ=FZ+DFBS(J)
(80)  FK=FK+DFBS(J)*YAVGB(J)
(81)  FM=FM-DFBS(J)*ARM1B(J)+TSKB(J)*ARM2B(J)
(82)  FN=FN-TSK1B(J)*YAVGB(J)
(83)  ALBS=ALBS+GAP(J)+GAP(J+1))*DELYBS/2.0

```

Equations (78) through (83) calculate the forces and moments for each segment and sums them to give total forces and moments. YAVGB(J) is the average distance off centerline of the individual segment.

```

(84)  8 CONTINUE
(85)  ALBS=ALBS+BLEAK
(86)  SQFAC=SQRT(2.*ABS(PBAR)/RHOINF)
(87)  QL=CFBS*ALBS*SQFAC*SIGN(1.,PBAR)

```

The last equations calculate the flow rate of air based upon the leakage area ALBS and the pressure differential between the plenum chamber and the atmosphere. BLEAK is the seal leakage entered in INCON to account for slight leakage where the seals do not quite maintain contact with the sidewall.

The remaining statements of subroutine BOWSL give the following values as printed output if the bow seal print switch is on, GAP, WETLEN, FX, FY, FZ, FK, FM, and FN.

### C. STERN SEAL MODELING

The stern seal subroutine is covered in the same manner as the bow seal subroutine. The complete listing of the stern seal subroutine is contained in Appendix B along with instructions on the proper entries to be used on the data cards.



```

(1)      DO 1 J=1,11
(2)      GAP(J)=0.0
(3)      ELSKI(J)=0.0
(4)      ELSKIL(J)=0.0
(5)      AIRLEN(J)=0.0
(6)      1 CONTINUE

```

The above loop and equations zero all variable arrays that will change each time subroutine STNSL is entered as was the case in the bow seal subroutine.

```

(7)      EFDEP = 6.0

```

Equation (7) establishes the effective depth of the seal at five inches. This figure is used as an entering argument in the stern seal contour mapping array CTNSL.

```

(8)      ALSS=0.0
(9)      FX=0.0
(10)     FZ=0.0
(11)     FK=0.0
(12)     FM=0.0
(13)     FN=0.0
(14)     AGAP1=0.0
(15)     AGAP2=0.0
(16)     AGAPA1=0.0

```

The nine equations above zero all single valued variables that are computed each time STNSL is entered.

```

(17)     DELP=PSS-PB
(18)     IF(DELP.LT.0.0) DELP=0.0

```

The two statements above fix the pressure differential between the plenum (PB) and the stern seal (PSS). Equation (17) is first used to arrive at the difference between these two quantities and the logical IF statement is used to insure all values are non-negative. As in the bow seal



subroutine this is logical since the air supplied to the stern seal vents into the plenum chamber.

$$(19) \quad \text{PBAR} = \text{PB} - \text{PINF}$$

This equation establishes the pressure differential between the plenum (PB) and the atmosphere. It is used in computing leakage flow rates.

$$(20) \quad \text{SINDIF} = \text{SINTH} - \text{COSTH} * \text{THETA}$$

$$(21) \quad \text{COSDIF} = \text{COSTH} + \text{SINTH} * \text{THETA}$$

The above equations (20) and (21) establish the angle of the XR-3 with respect to the horizontal and the vertical, respectively.

$$(22) \quad \text{X1} = \text{XSS} + \text{ZSS} * \text{THETA} - \text{XLF} * \text{SINDIF}$$

$$(23) \quad \text{Z1} = (-\text{Z} - \text{ZSS} + \text{XSS} * \text{THETA} - \text{ELMAXS} * \text{COS}(\text{THETA}))$$

The above two equations establish lengths in the X and Z directions which are used to calculate the water height above the keel at the stern seal location.

$$(24) \quad \text{N} = \text{NSTA}(4)$$

$$(25) \quad \text{DO } 2 \text{ K} = 1, \text{N}$$

2 CONTINUE

The above loop is used to establish the gap at each station and the phantom "wetted length" of the seal. NSTA(4) is the number of stations chosen for the seal and can be up to eleven, thereby defining ten seal segments.



```

(26)   ELSKI(K)=(ETA(4,K)-DETADX(K)*(XX(4,K)-X1)
        -Z1)+YY(4,K)*PHI
(27)   IF(ELSKI(K).GT.HINGHT) ELSKI(K)=HINGHT

```

Equation (26) computes the height of the water above the keel at the stern seal location. ETA(4,K) is a length correction factor that is dependent on seal shape. Since in the case of the XR-3 the seal is flat across the hinge line this term is zero. DETADX(K) is a wave correction factor that is multiplied by the seal distance from the center of gravity (XX(4,K)-X1) to give the wave height at the stern seal location. The logical IF statement limits the water height to the top of the seal.

```

(28)   ELSKIL(K)=ELSKI(K)+GPS
(29)   IF(ELSKIL(K).GT.HINGHT) ELSKIL(K)=HINGHT
(30)   IF(ELSKIL(K).LT.(HINGHT-ELMAXS))
        ELSKIL(K)=HINGHT-ELMAXS

```

ELSKIL(K) is the height of the trailing edge of the stern seal above the keel. It is measured in feet. GPS is the air gap height that was observed to be constant under normal running conditions. It is .4644 feet. The logical IF statement (29) establishes the upper limit of seal deflection where it is stopped by the seal supporting framework. The second logical IF statement establishes the lower limit of seal deflection height.

```

(31)   GAP(K)=-ELSKI(K)+(HINGHT-ELMAXS)
(32)   IF(GAP(K).LT.0.0)GAP(K)=0.0

```

The equation (31) and logical IF statement (32) establish the gap height below the lower stop limit set by the support cable length ELMAXS.





```

(33)    MM1=ELSKIL(K)*12.0
(34)    MM2=MM1
(35)    MM3=MM2+1
(36)    DLINC=ELSKIL(K)*12.0-MM1
(37)    STNSL1=CTNSL(MM,MM2)
(38)    STNSL2=CTNSL(MM,MM3)
(39)    AIRLEN(K)=((STNSL2-STNSL1)*DLINC+STNSL1)/12.0

```

Equations (33) through (35) establish the entering arguments of the seal contour array CTNSL in the same manner as was done in the bow seal subroutine. AIRLEN(K) is the phantom "wetted length" and is given the name AIRLEN because the seal is supported by air.

```

(40)    N=NSTA(4)-1
(41)    DO 5 J=1,N
        5 CONTINUE

```

The above loop accomplishes the actual force and moments of each seal segment and totals the forces and moments. It also computes the average gap height based upon the gap heights of the individual stations.

```

(42)    ELSKIA=(ELSKI(J+1)+ELSKI(J))/2.0
(43)    ELSKLA=(ELSKIL(J+1)+ELSKIL(J))/2.0
(44)    AIRLAV=(AIRLEN(J+1)+AIREN(J))/2.0

```

The three above equations average the water height above the keel, ELSKIA; the average seal deflection height ELSKLA, and the average phantom wetted length AIRLAV.

```

(45)    AGAP=ELSKLA-ELSKIA
(46)    AGAP1=AGAP

```

Equation (45) establishes the average height of the air gap at the seal segment. AGAP1 is a variable used in further calculations.



```
(47) IF(AGAP.LT.GPS)AGAP=GPS
(48) IF(AGAP1.GT.GPS)AGAP1=GPS
```

The above logical IF statements establish the lower limit for AGAP at .4644 feet at the maximum value of AGAP1 at .4644 feet.

```
(49) ARM1S=XX(4,J)+ELSKIA/2
(50) ARM2S=ZS-ELSK1A
```

The above equations (49) and (50) calculate the moment arms through which the vertical lifting force acts to create the major component of the FM moment about the Y axis; the second equation creates the moment arm with respect to the C.G. through which the drag forces act.

```
(51) DFSS(J)=-DELP*DELYSS*AIRLAV/(GPS/AGAP)**2.0
```

Equation (51) calculates the vertical force acting upon the seal and with the term  $(GPS/AGAP)**2.0$  allows for this force to decrease with the square of the ratio of the actual gap width AGAP and the nominal width GPS. This is based on the assumption that the air exiting beneath the stern seal supports the stern seal and that the lift forces generated by the exiting air are inversely proportional to their velocity.



```

(52) ARG=.5RHO*U*U*AIRLAV*DELYSS
(53) RESKI=U*AIRLAV/ENU
(54) CDTSKI=.427/(ALOG10(RESKI)-.407)**2.64
(55) TSKIS(J)=-ARG*CDTSKI
(56) TSKIS(J)=0.0

```

Equations (52) through (55) calculate the theoretical drag forces based upon the average phantom wetted length AIRLAV as if the seal was actually in contact with the water. The Schultz Grunow formula is used as in the bow seal routine to calculate the drag forces based upon the Reynold's number which is based on AIRLAV the average "wetted" length. Equation (56) removes this drag calculation since the seal is presumed to ride on a cushion of air and is hence negligible.

```

(57) FX=FX+TSKIS(J)
(58) FZ=FZ+DFSS(J)
(59) FK=FK+DFSS(J)*YAVGS(J)
(60) FM=FM-DFSS(J)*ARM1S(J)+TSKIS(J)*ARM2S(J)
(61) FN=FN-TSKIS(J)*YAVGS(J)

```

The five equations above calculate the forces and moments of each segment and sums them for all the segments to give the total seal forces and moments.

```

(62) ALSS=ALSS+(GAP(J)+GAP(J+1))*DELYSS/2.0
(63) AGAP2=AGAP2+AGAP1
(64) AGAP1=AGAP2/J

```

The above equation (62) calculates the total gap area ALSS that is due to the seal reaching the downward limit of its travel and the gap thus increasing past its nominal value of .4644 feet. Equations (63) and (64) calculate the



average gap height including the nominal .4644 height and allows the nominal gap to close if the seal is slammed against its upper limit, the upper seal support framework.

$$(65) \quad ALSS = ALSS + ALEAK * (AGAPAL / GPS)$$

Equation (65) calculates the leakage area under the seal. ALSS is the leakage area due to the gap width increasing beyond the nominal .4644 feet. The term ALEAK is the nominal leakage area of 3.79 square feet normally observed. Multiplying ALEAK by AGAPAL/GPS allows this nominal leakage area to decrease if the seal is limited in its upward travel.

$$(66) \quad SQFAC = \sqrt{2 * ABS(PBAR / RHOINF)}$$
$$(67) \quad QL = CFSS * ALSS * SQFAC * SIGN(1., PBAR)$$

Equations (66) and (67) calculate the flow rate based upon the leakage area and the pressure differential between the plenum and the atmosphere. The equation assumes orifice type leakage.

The remaining statements give print outputs of the terms GAP, AIRLEN, FX, FY, FZ, FK, FM and FN if the stern seal print switch is on.





#### IV. DATA ANALYSIS OF ACTUAL CRAFT TRANSIENT MOTION AND COMPUTER SIMULATION

##### A. INTRODUCTION

In order to verify the modeling changes made in the seals, data was collected on the XR-3 test craft for conditions of induced transient motion in pitch and roll. To induce roll action the test craft was sallied by shifting body weight laterally near the C.G. until maximum oscillations built up, then the forcing action was stopped. For pitch oscillations the chase boat was veered across the path of the XR-3 to produce a wave front with its wake. By having the XR-3 pass over the wake it was intended to induce a transitory pitch oscillation.

These attempts to produce a transient response cannot be viewed as entirely successful. The principal reason for the limited success was that it was extremely difficult to induce a large enough perturbation in either pitch or roll so that the normal background oscillations could be ignored. Figures 16, 17 and 18 are graphs of the roll and pitch motions<sup>2</sup> of the XR-3 when making its twenty knot calibration. The magnitude and frequency of the steady state pitch

---

<sup>2</sup>Figure 17 depicts the actual pitch angle of the test craft. Figure 18 is the same data with the steady state average pitch angle removed. This was done on all data to facilitate the measurement of the pitch oscillations superimposed on the steady state value of pitch angle.



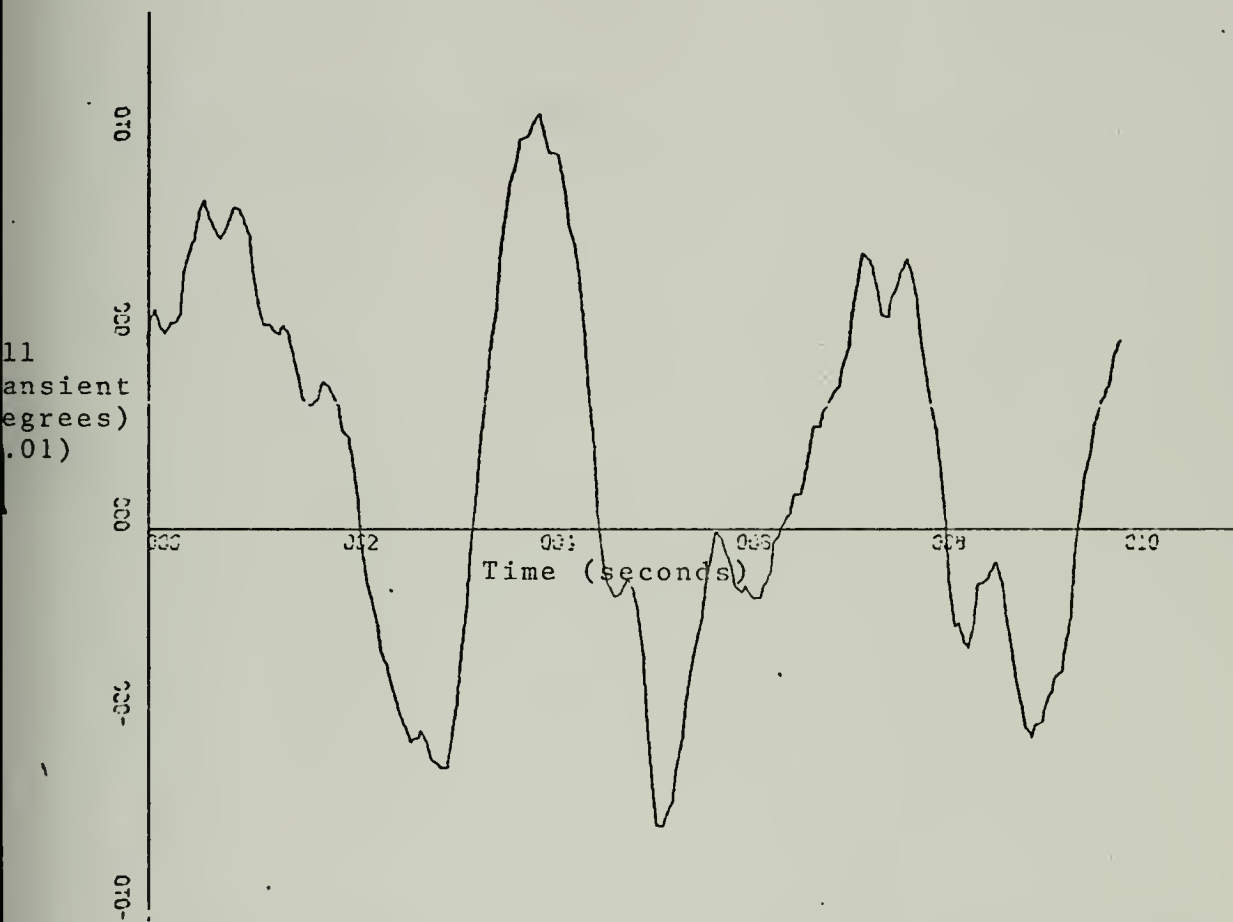


FIGURE 16

ROLL MOTION VERSES TIME, VELOCITY 20,429 KNOTS



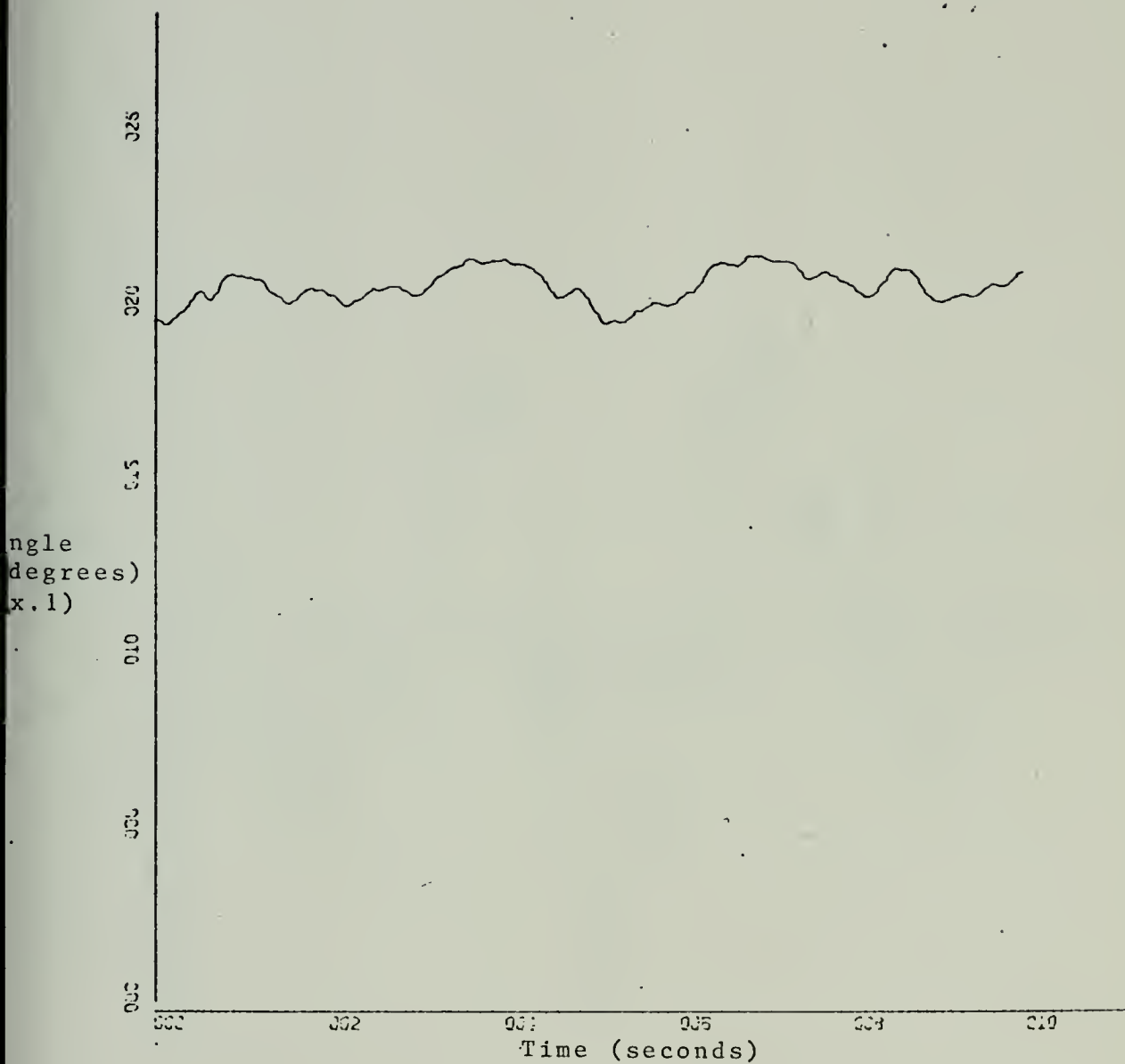


FIGURE 17

PITCH VERSES TIME, VELOCITY 20.429 KNOTS



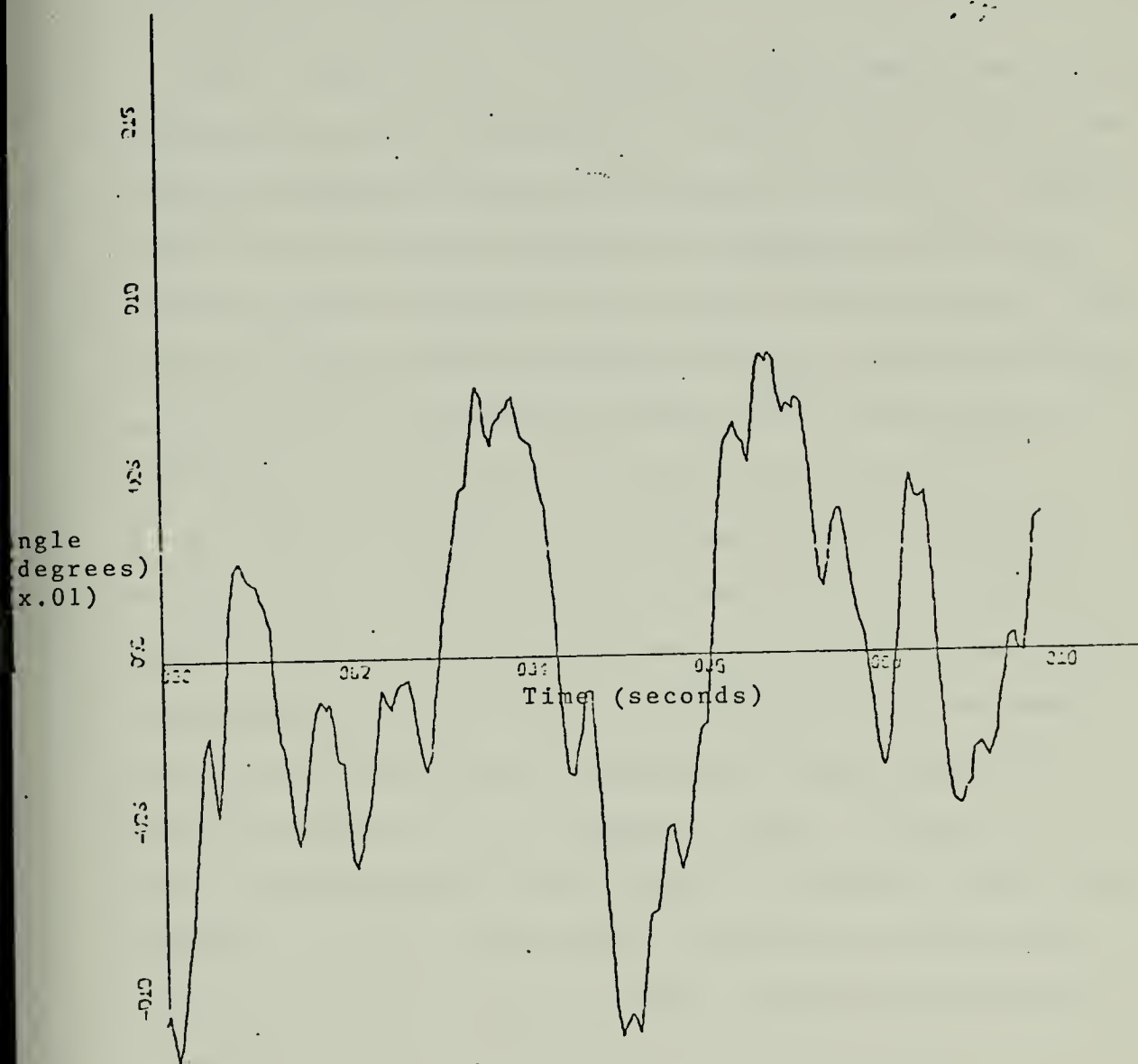


FIGURE 18

PITCH MOTION VERSES TIME, VELOCITY 20.429 KNOTS





oscillation shown in Figure 18 is approximately .08 degrees and .295 Hz respectively. The steady state magnitude of the roll motion shown in Figure 16 was approximately .075 degrees and its frequency was approximately the same frequency of the pitch motion, .295 Hz.

These steady state oscillations appear quite small until it is realized that the maximum roll perturbation that was able to be induced during any run was only about .4 degrees. Lower ratios between induced and background oscillations were the norm for both roll and pitch induced motion. The background oscillations in pitch and roll therefore could not be ignored when analyzing data, and deleteriously affected the measurement of decay time constants.

As stated before the attempt was made to introduce separately pitch and roll motion into the test craft and then record the transient response after the forcing action had passed or was stopped. After studying the processed data it was evident that it had been nearly impossible to affect transients in one variable (either pitch or roll) without introducing at least some oscillations in the other variable. In introducing pitch oscillations roll motion was greatly affected. This was caused because the wave front caused by the chase boat's wake always struck the test craft at an oblique angle and not perpendicular to the axis of symmetry of the craft. Only during those runs where the XR-3 was sallied was some modicum of success achieved in



isolating roll transient motion. The one run included in this report where sallying was used to induce roll transients is the one conducted at 11.79 knots. During the other two runs included (15.93 and 19.45 knots) the wake crossing method was used to force oscillations. This resulted in runs in which both roll and pitch transients could be studied at the same time.

In making comparison between the recorded data and that of the computer simulations both the original XR-3 model as presented in Ref. 3 and the new model which incorporates the new fan maps, new bow and stern seals and a water slope correction were used. This last modification is one which has been incorporated into the XR-3 program by LCDR G. T. Forbes, USN during his concurrent study and is reported in Ref. 5. The water slope modification is used to correct the water level in the plenum chamber based upon the fact that increased pressure in the plenum will tend to displace water after it comes in contact with the bow seal and passes into the chamber. This displacement since it does not take place instantaneously is a function of both time and pressure and hence results in a "slope" in the water as it passes through the plenum chamber. The purpose of using both the original and the new models was to gain an appreciation of the effects of the modeling changes made.

During all the runs made at Lake San Antonio with the XR-3 the water conditions were fairly calm, but the steady



state roll and pitch oscillations were always present in the processed data as reported previously. Figures 19 through 35 which are the graphs for all the runs clearly show this oscillation in both pitch and roll. Again it is emphasized that these oscillations precluded exact measurements of the decay time constants.

The method used to induce roll and pitch transient oscillations in the computer models was to offset the initial roll and pitch angle from the known steady state angles when the program was executed. These offsets would then decay as the craft returned to the steady state conditions for that speed. The magnitude of these offsets were taken from the recorded data. The point in time where this data was taken is marked on each graph of the test craft's recorded data by a dashed vertical line.

From known loading conditions the craft's weight during these runs was 6050 lbs. Its center of gravity was located 10.08 feet forward of the transom. Average plenum pressure was not available as this data was not recorded. The plenum pressure was assumed to be the nominal 24.86 PSF as reported in Ref. 3.

These inputs in the case of the original [Ref. 3] XR-3 model caused the craft to have a negative steady state trim angle which is readily apparent when looking at the graphs of the simulation runs of the original model (see Figures 22 through 28 for simulation runs at 15.93 knots).



Although it was recognized that this negative trim angle was not realistic the initial conditions were not varied to get a positive trim angle because it was desired to test each model with exactly the same physical characteristics. The actual value of the steady state trim was not the quantity that was to be studied. The quantity that was of interest was the transient response of the model as it arrived at that steady state value after an initial offset.

## B. RUN DATA ANALYSIS

The first run was a calm water transient roll motion study at 11.79 knots. In this run the pitch offset was considered negligible. The roll induced oscillation was measured to have a negative magnitude of approximately .3 degrees. This roll offset was entered into both models with the following results. The decay time constant for roll motion was 4.6 seconds for the original XR-3 model and 5.6 seconds for the new model. The oscillation frequency was .752 Hz for the original XR-3 and .714 Hz for the new. Measured data gave the actual boat a frequency of roll oscillation of .29 Hz and a decay time constant of less than 1 second.

The second run was at 15.93 knots in calm water. This run had both roll and pitch perturbations. They were minus .25 degrees for pitch and a negative .27 degrees for roll. With these offsets the new XR-3 model gave a roll time constant of 4.1 seconds and a pitch time constant of





3.4 seconds. The frequencies of oscillation for the new model were .72 Hz for roll and .44 Hz for pitch. These same quantities were measured on the old model to be 3.1 seconds and 5.0 seconds for the roll and pitch time constants respectively, and in order, .76 Hz and .50 Hz for the roll and pitch frequencies. The same measured quantities from the recorded data gave something less than one second for both the roll and pitch time constants and .25 Hz and .22 Hz for the oscillation frequencies for roll and pitch.

The last calm water data was taken at 19.45 knots. The measured pitch offset was a positive .12 degree and a positive .45 degree for the roll offset. Again these values were imposed upon the initial steady state trim conditions to achieve a transient response.

From the two computer simulations the following results were obtained. Original model roll frequency - .76 Hz, roll decay time constant - 2.7 seconds, pitch frequency - .50 Hz, pitch time constant - 4.6 seconds. New model roll frequency is .72 Hz and decay time constant 4.3 seconds. Pitch frequency is .42 Hz and decay time constant is 4.4 seconds. The same data from the recorded tapes gave a pitch frequency of .28 Hz and with decay time constant of less than one second. Roll frequency was measured to be .28 Hz, and the roll decay time constant was estimated at less than one second.



From the above data taken on the three runs and the computer simulations thereof it is evident that the computer model neither in the original form nor in its new form accurately predicts roll or pitch transient motion under the conditions studied. Decay time constants for pitch and roll were generally four times too long in both simulation models. Pitch and roll frequencies of the computer models were generally too high by a factor of two. Table III gives this transient behavior of the XR-3 and both simulation models in tabular form.

Figure 19 is the actual roll response data for Run 1 collected at 11.79 knots. Figures 20 and 21 are the computer simulation runs for the original and new model for this run depicting roll response. Recorded pitch and roll motion for Run 2 (15.93 knots) is given in Figures 22, 23 and 24 and the original model computer simulation of roll and pitch is in Figures 25 and 26 respectively. The response of the new model for Run 2 is recorded in graphs 27 and 28. Recorded data for Run 3 is given in Figures 29 through 31 with the computer model's simulations of pitch and roll given in Figures 32 through 35.

#### C. SIMULATION STUDIES OF THE TWO MODELS

In an effort to gain better knowledge of the total effect of the new modeling, both the old and the new models were given a positive three degree pitch offset from steady state calm water conditions. Both models were set at the



TABLE III. CALM WATER FORCED OSCILLATIONS RESPONSE

Run 1, Speed 11.79 knots

Variable	Measured XR3	Simulated	
		Original Model	New Model
Roll Frequency	.29 Hz	.752 Hz	.714 Hz
Roll decay time constant	<1 sec	4.6 sec	5.6 sec
Pitch Frequency	-	-	-
Pitch decay time constant	-	-	-

Run 2, Speed 15.93 knots

Variable	Measured XR3	Simulated	
		Original Model	New Model
Roll Frequency	.25 Hz	.76 Hz	.72 Hz
Roll decay time constant	<1 sec	3.1 sec	4.1 sec
Pitch Frequency	.22 Hz	.50 Hz	.44 Hz
Pitch decay time constant	<1 sec	5.0 sec	3.4

Run 3, Speed 19.45 knots

Variable	Measured XR3	Simulated	
		Original Model	New Model
Roll Frequency	.28 Hz	.76 Hz	.72 Hz
Roll decay time constant	<1 sec	2.7 sec	4.3 sec
Pitch Frequency	.28 Hz	.50 Hz	.42 Hz
Pitch decay time constant	<1 sec	4.6 sec	4.4 sec



Roll  
transient  
(degrees)  
(x.1)

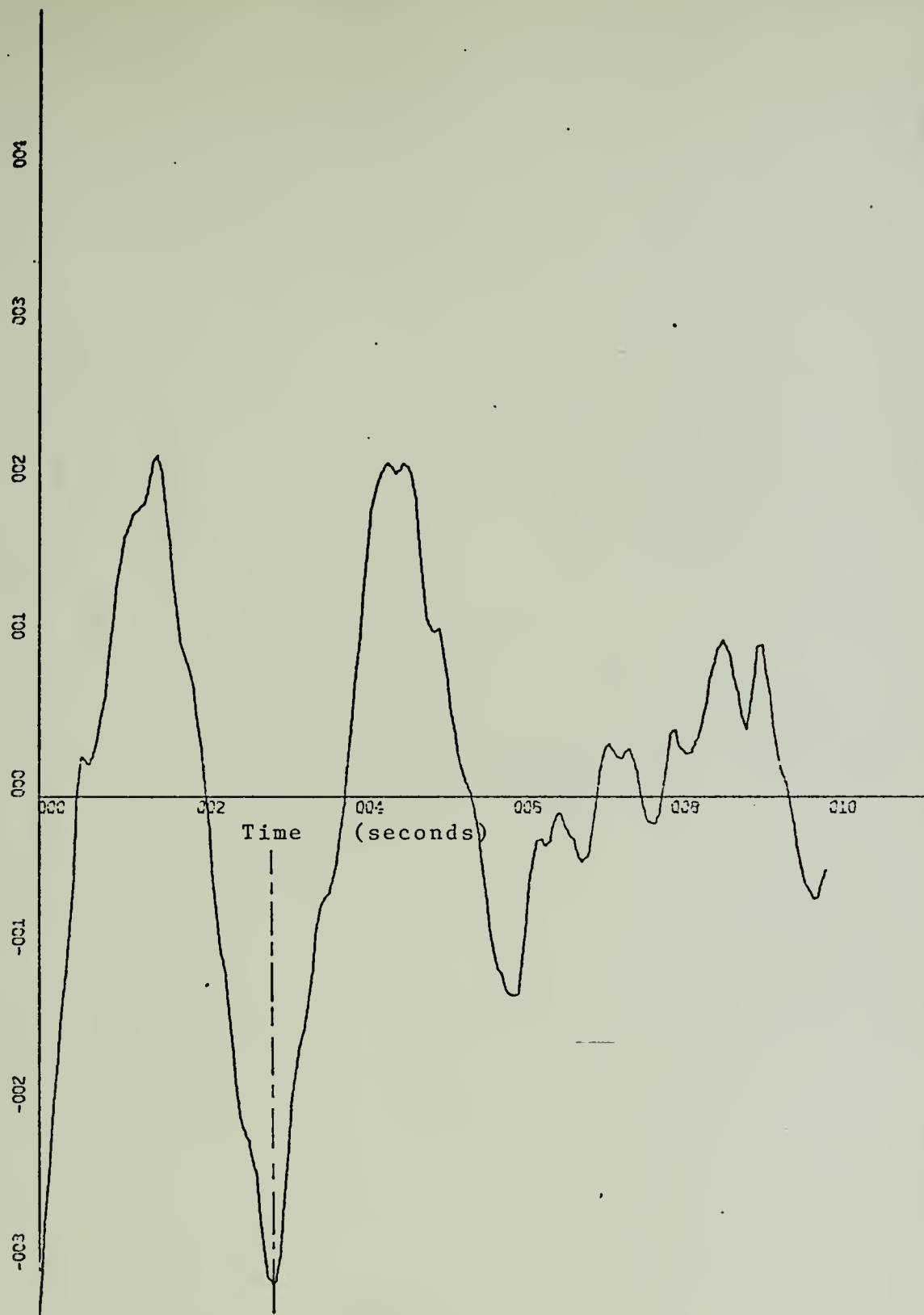


FIGURE 19  
ROLL TRANSIENT VERSES TIME, VELOCITY 11.79 KNOTS





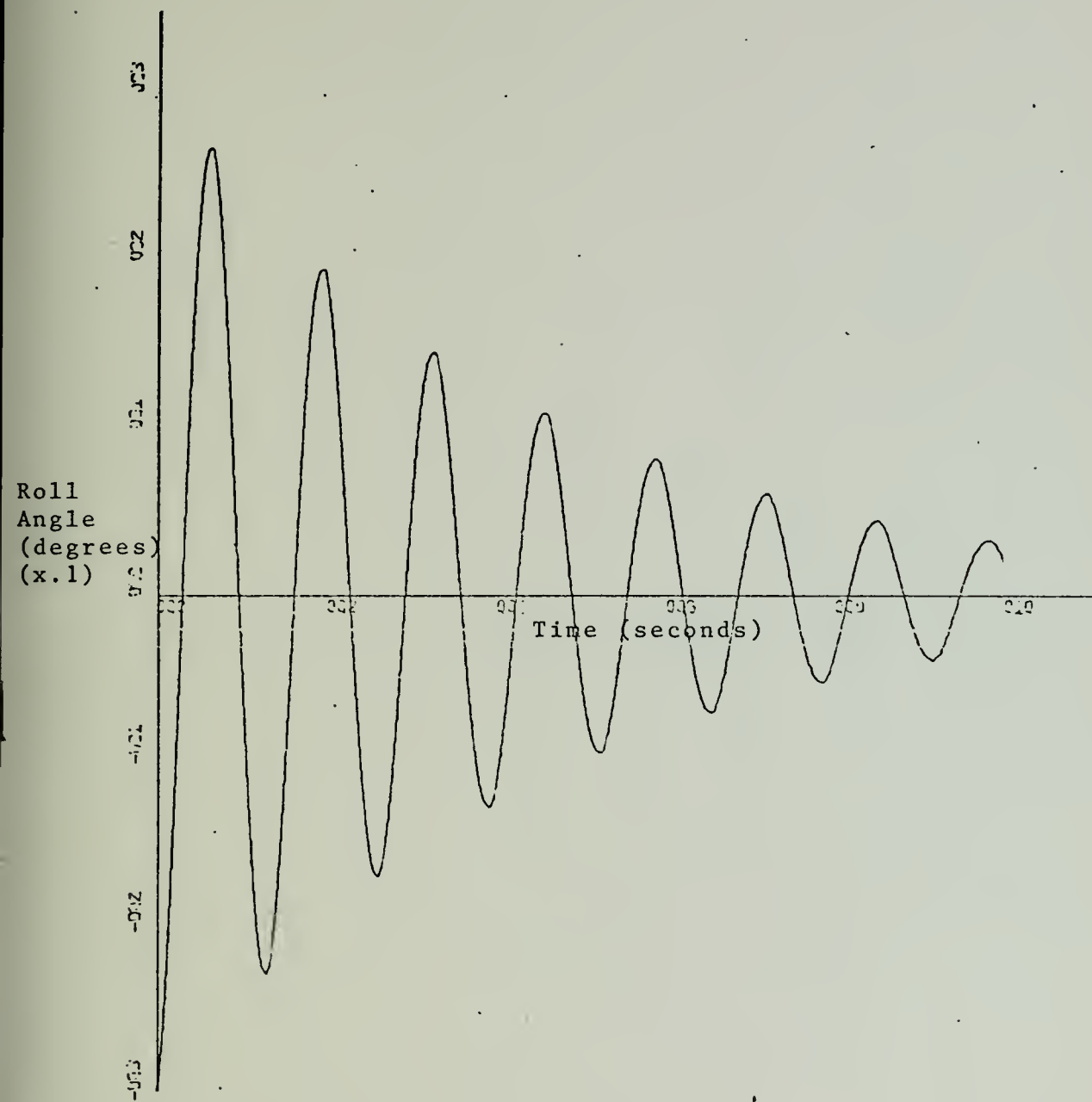


FIGURE 20

COMPUTER SIMULATION ROLL ANGLE VERSES TIME, 11.79 KNOTS  
ORIGINAL XR-3



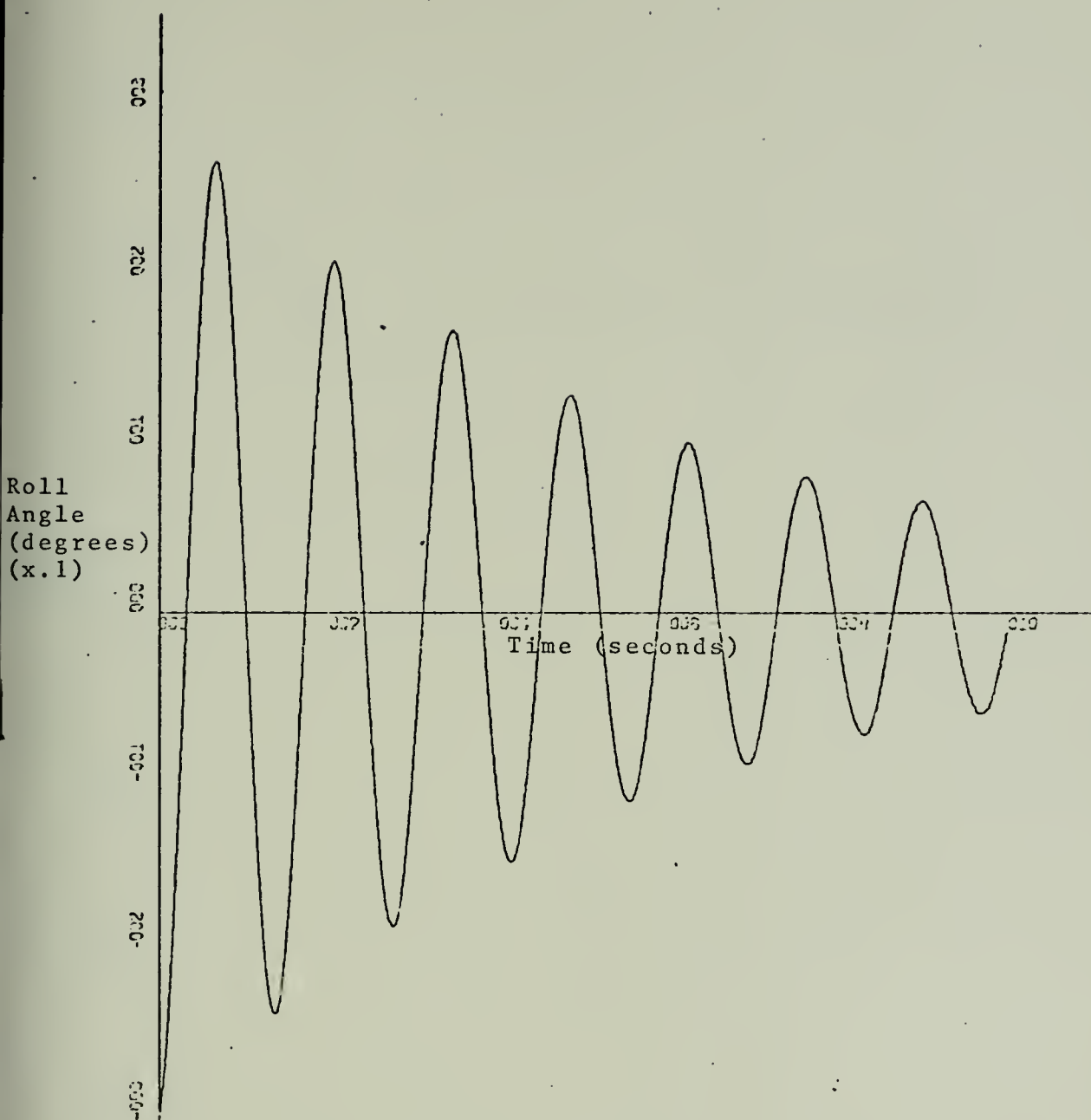


FIGURE 21

COMPUTER SIMULATION ROLL ANGLE VERSES TIME, 11.79 KNOTS  
NEW XR-3



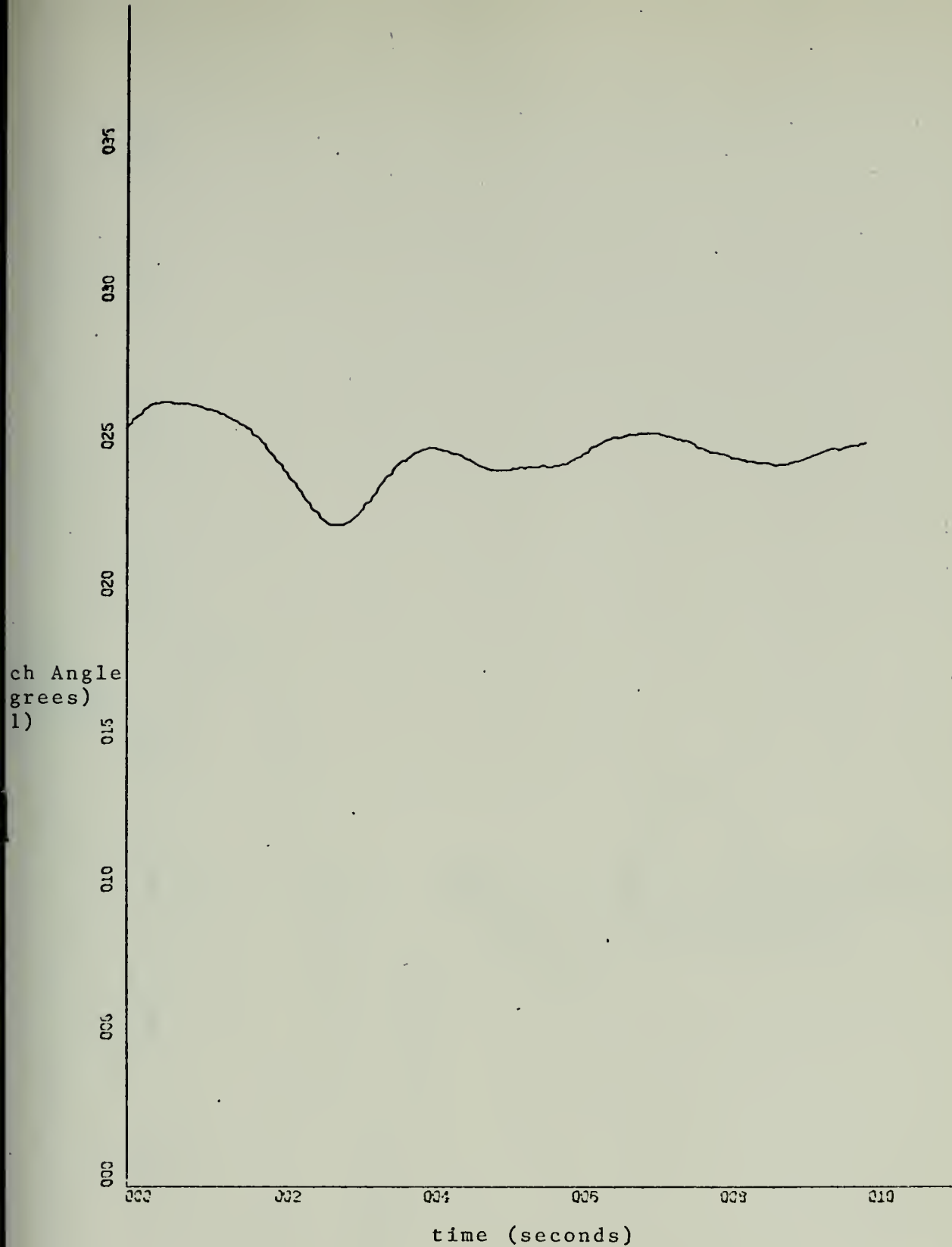


FIGURE 22  
PITCH VERSES TIME, VELOCITY 15.93 KNOTS



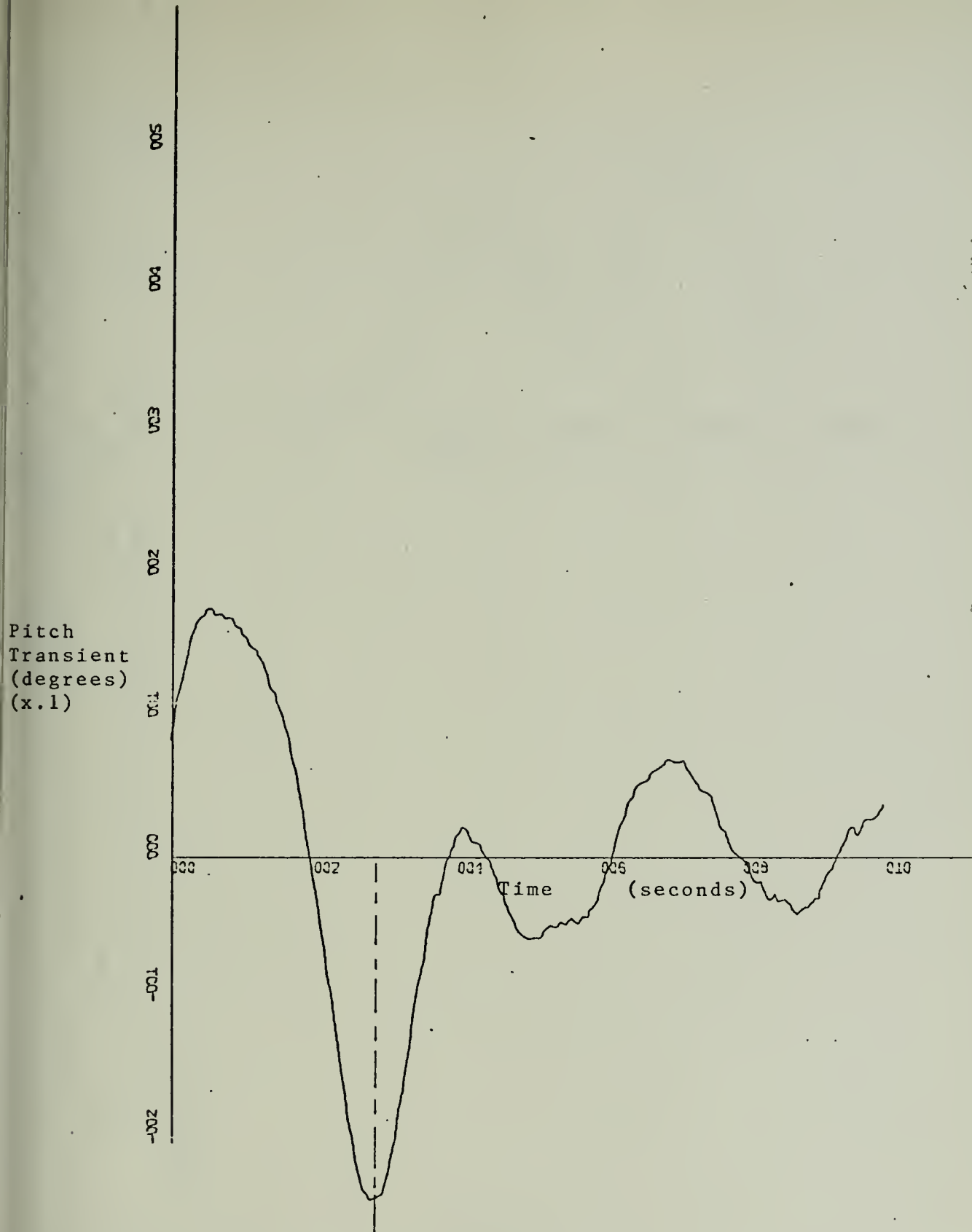


FIGURE 23  
PITCH TRANSIENT VERSES TIME, VELOCITY 15.93 KNOTS





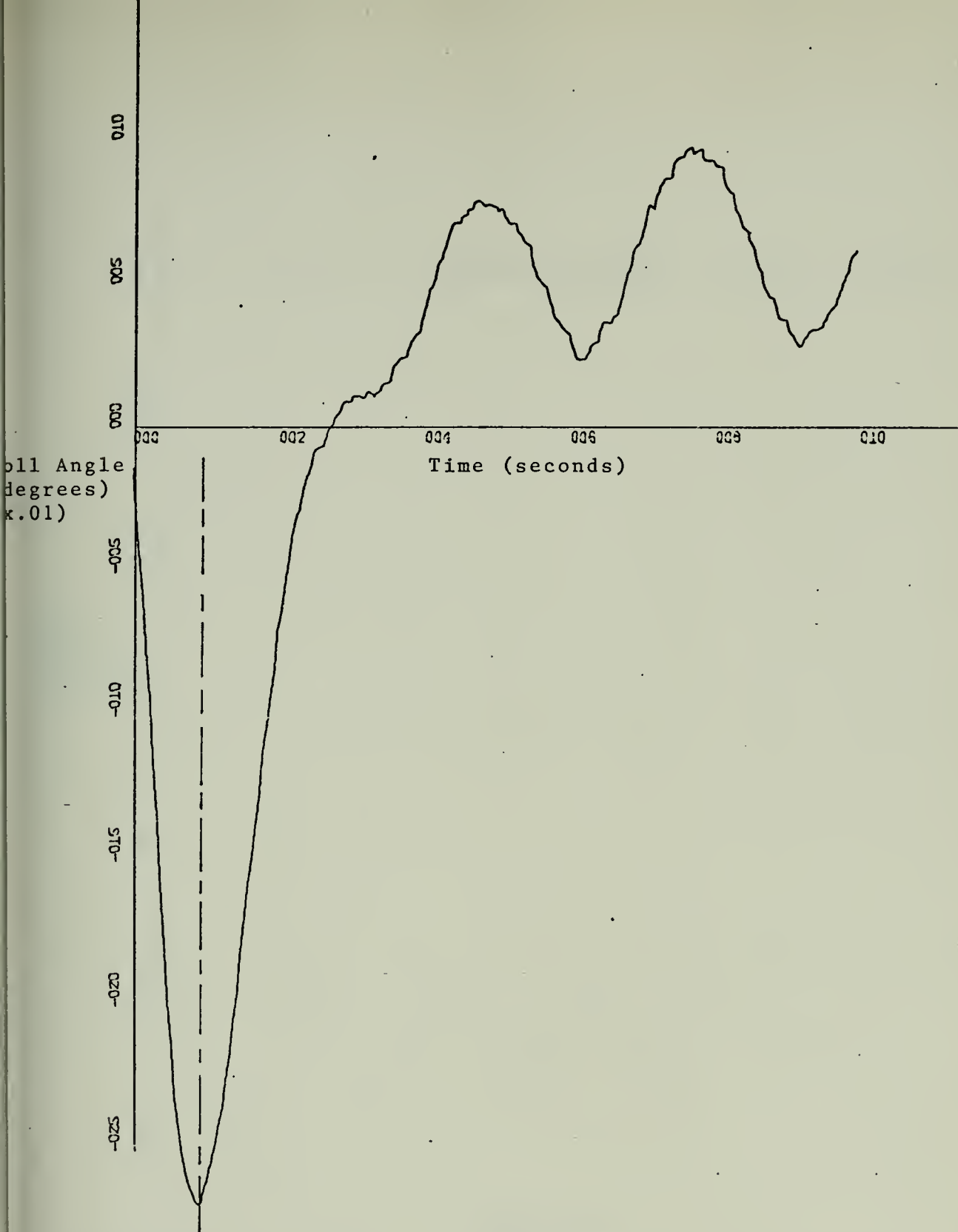


FIGURE 24  
ROLL TRANSIENT VERSES TIME, VELOCITY 15.93 KNOTS



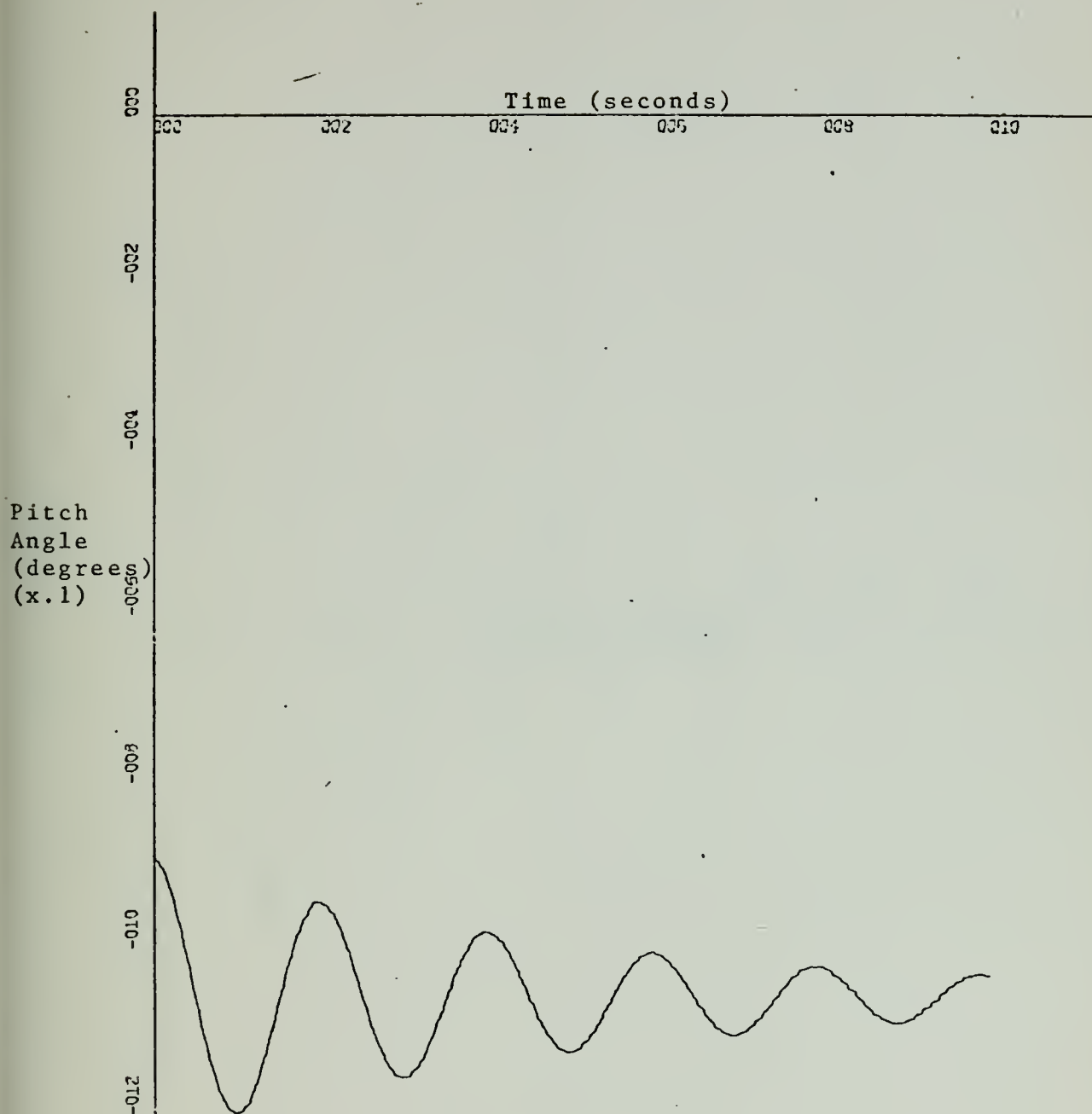


FIGURE 25  
COMPUTER SIMULATION PITCH ANGLE VERSES TIME, 15.93 KNOTS  
ORIGINAL XR-3



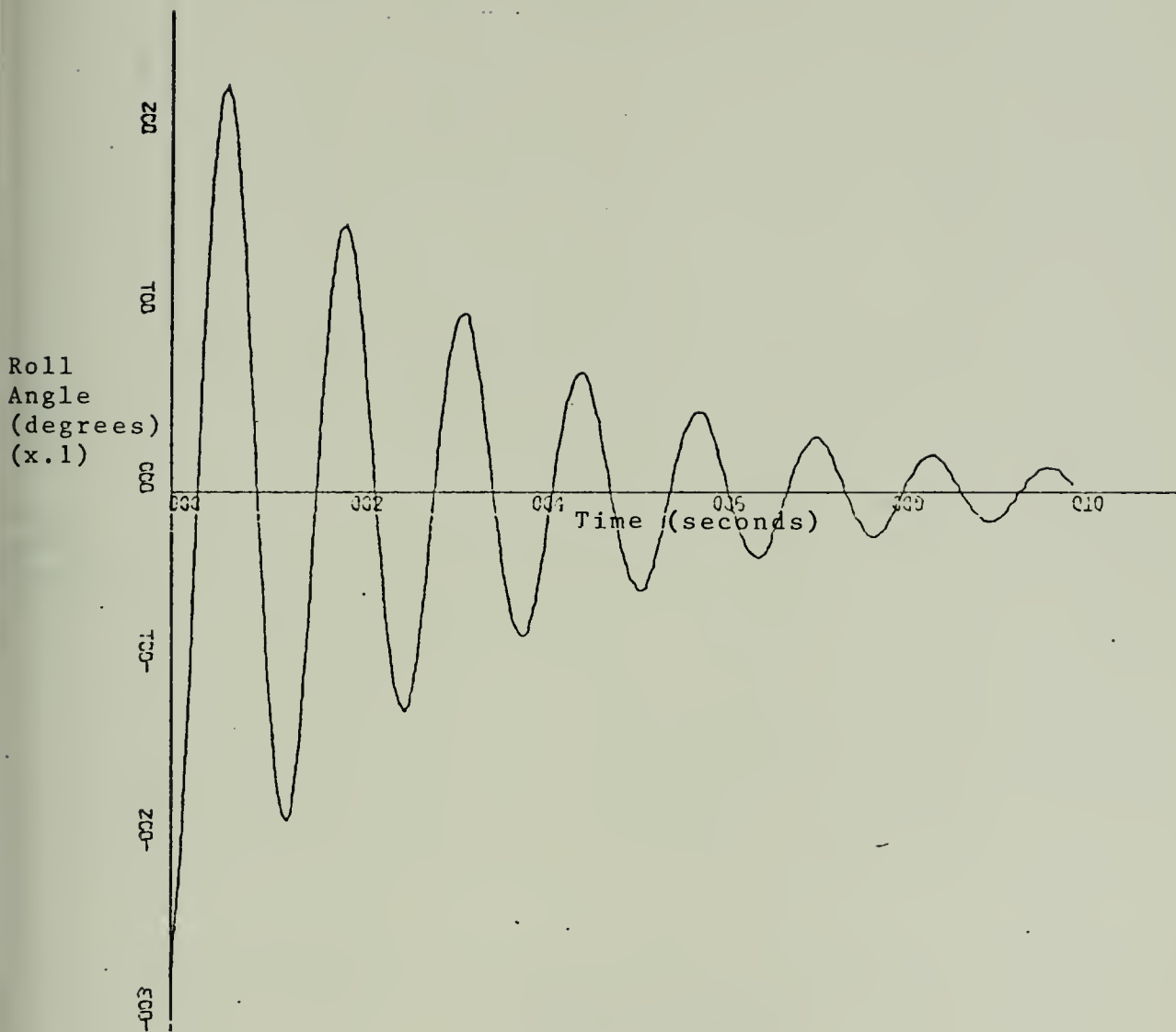


FIGURE 26

COMPUTER SIMULATION ROLL ANGLE VERSES TIME, 15.93 KNOTS  
ORIGINAL XR-3



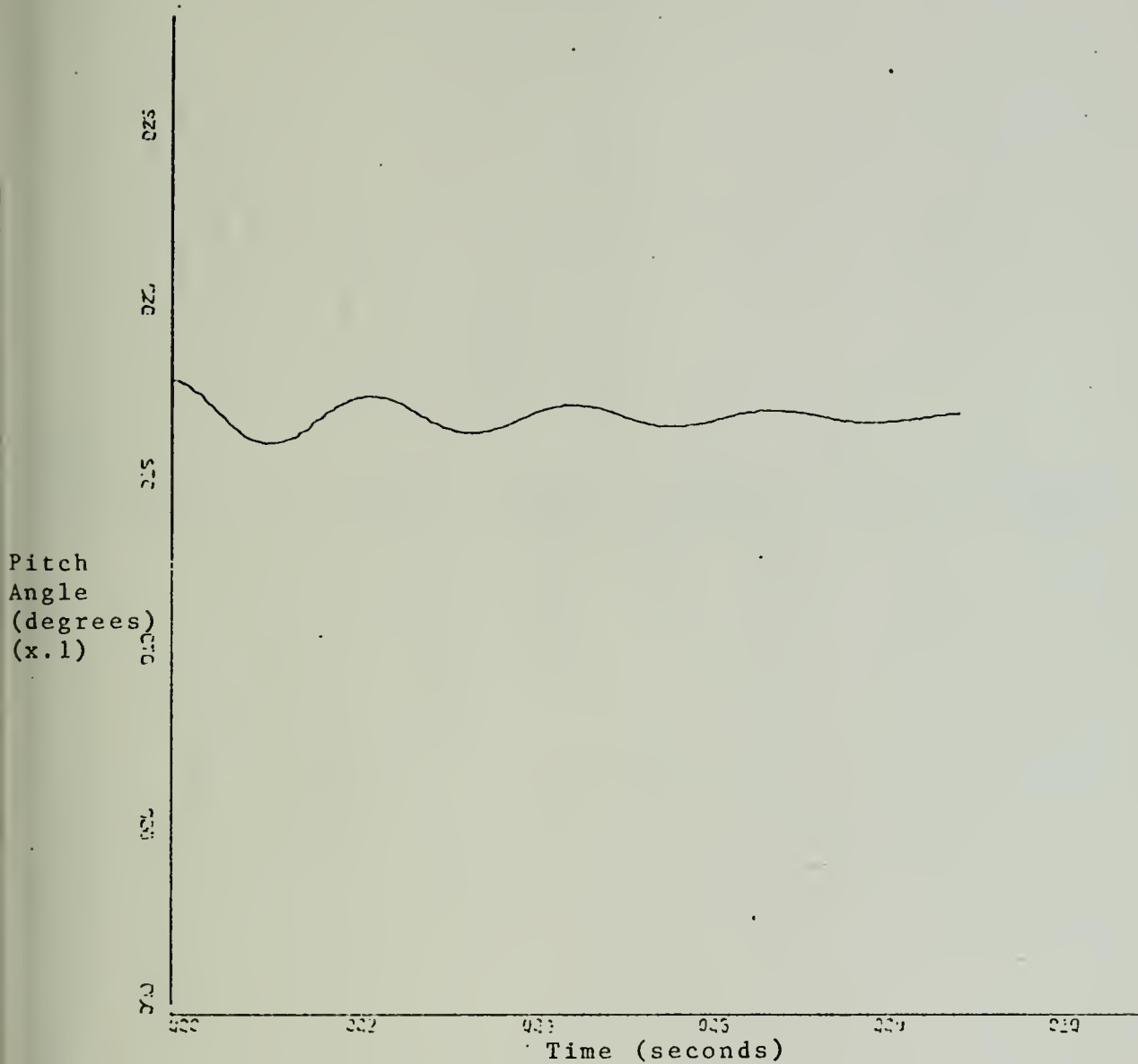


FIGURE 27  
COMPUTER SIMULATION PITCH ANGLE VERSES TIME, 15.93 KNOTS  
NEW XR-3





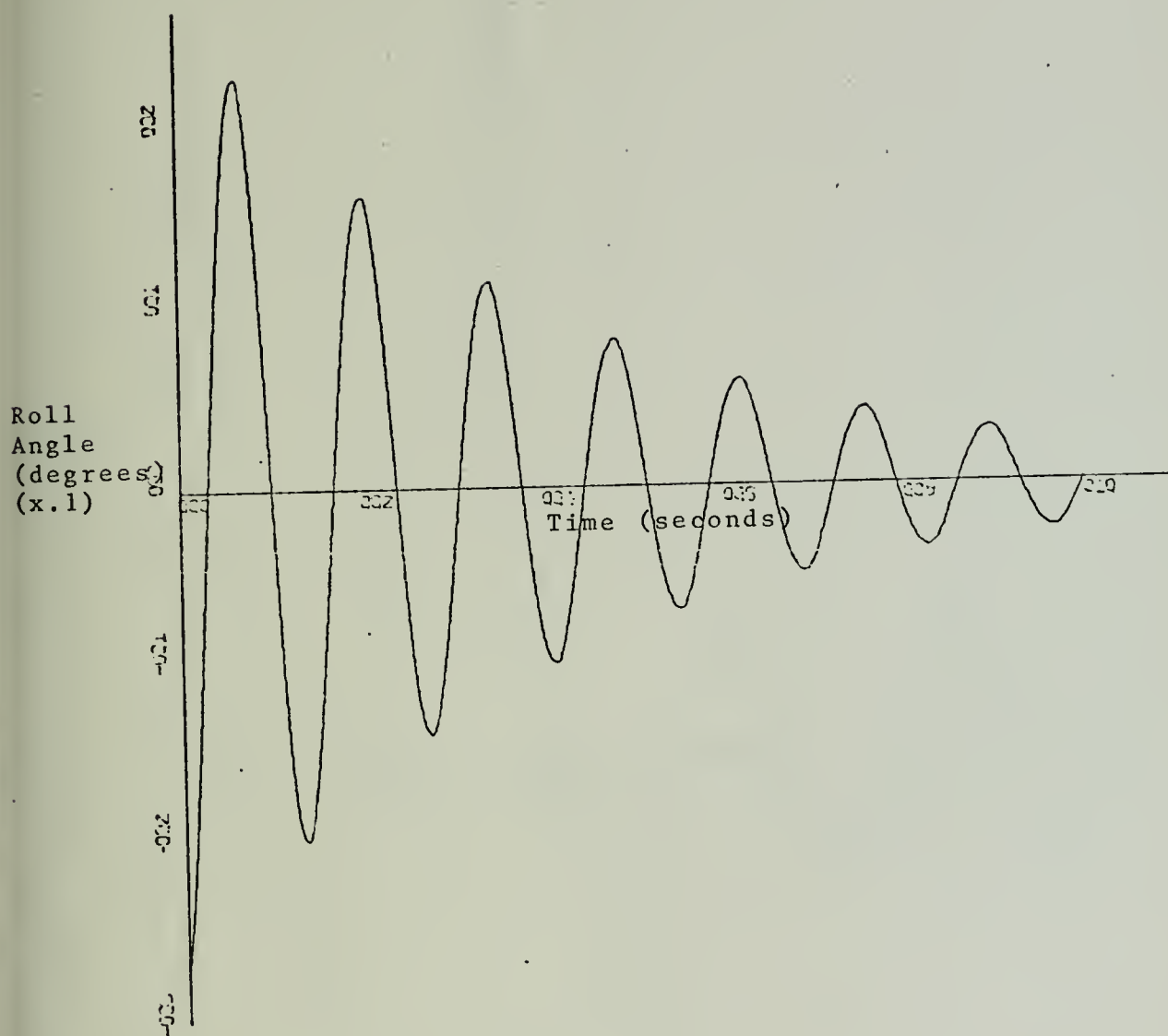


FIGURE 28  
COMPUTER SIMULATION ROLL ANGLE VERSES TIME, 15.93 KNOTS  
NEW XR-3



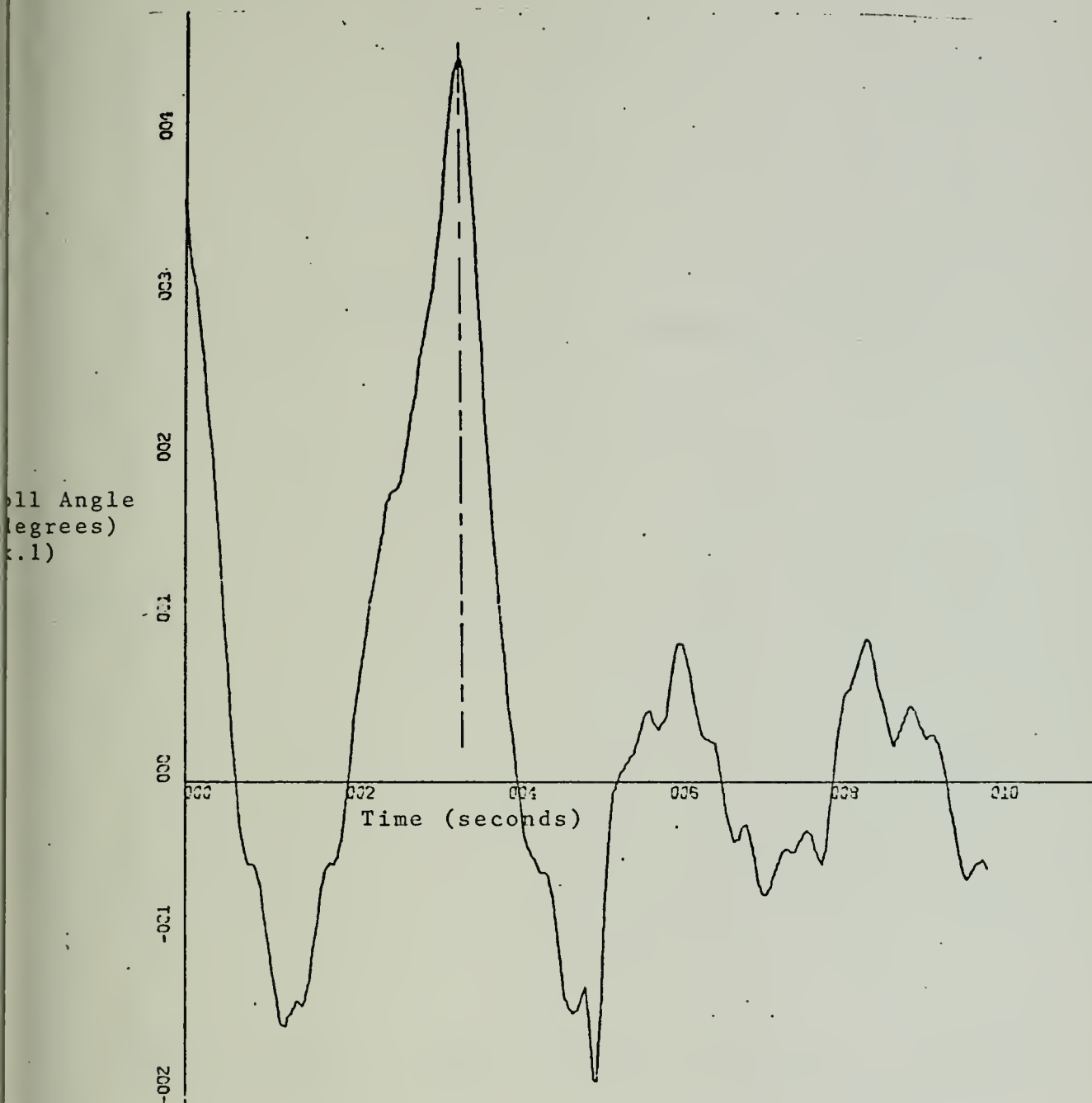


FIGURE 29  
ROLL TRANSIENT VERSES TIME, VELOCITY 19.45 KNOTS



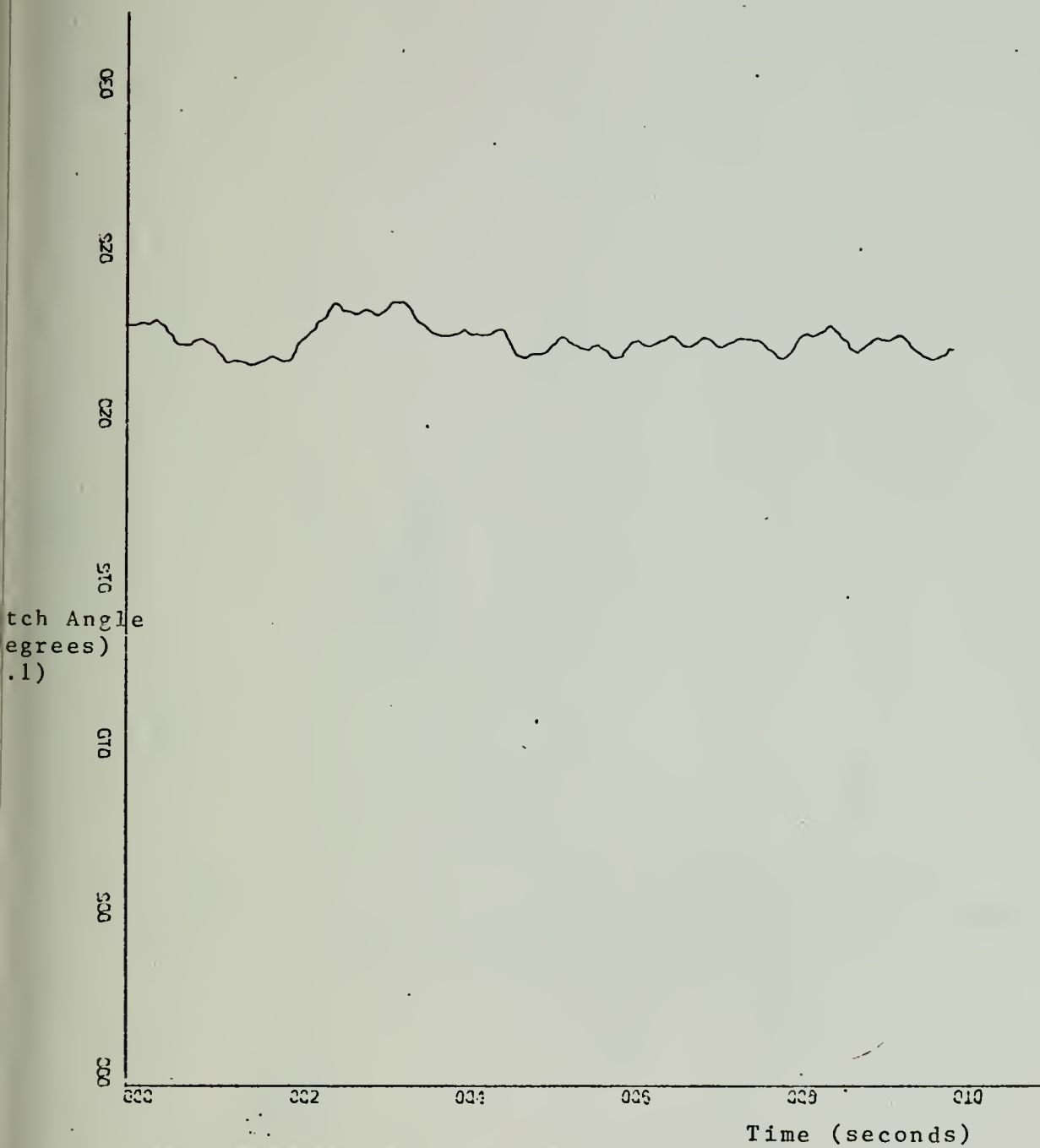


FIGURE 30  
PITCH VERSES TIME, VELOCITY 19.45 KNOTS



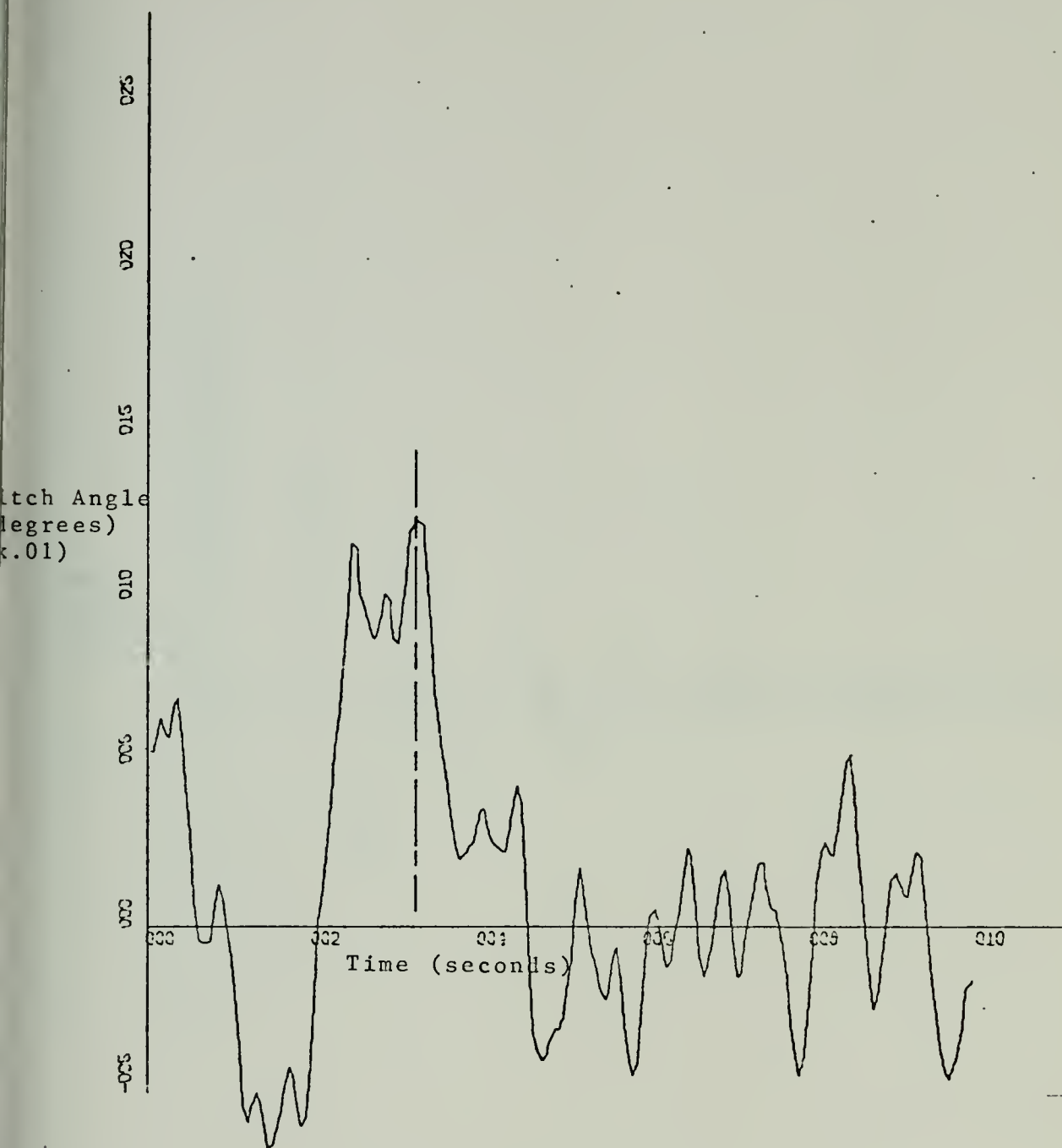


FIGURE 31

PITCH TRANSIENT VERSES TIME, VELOCITY 19.45 KNOTS





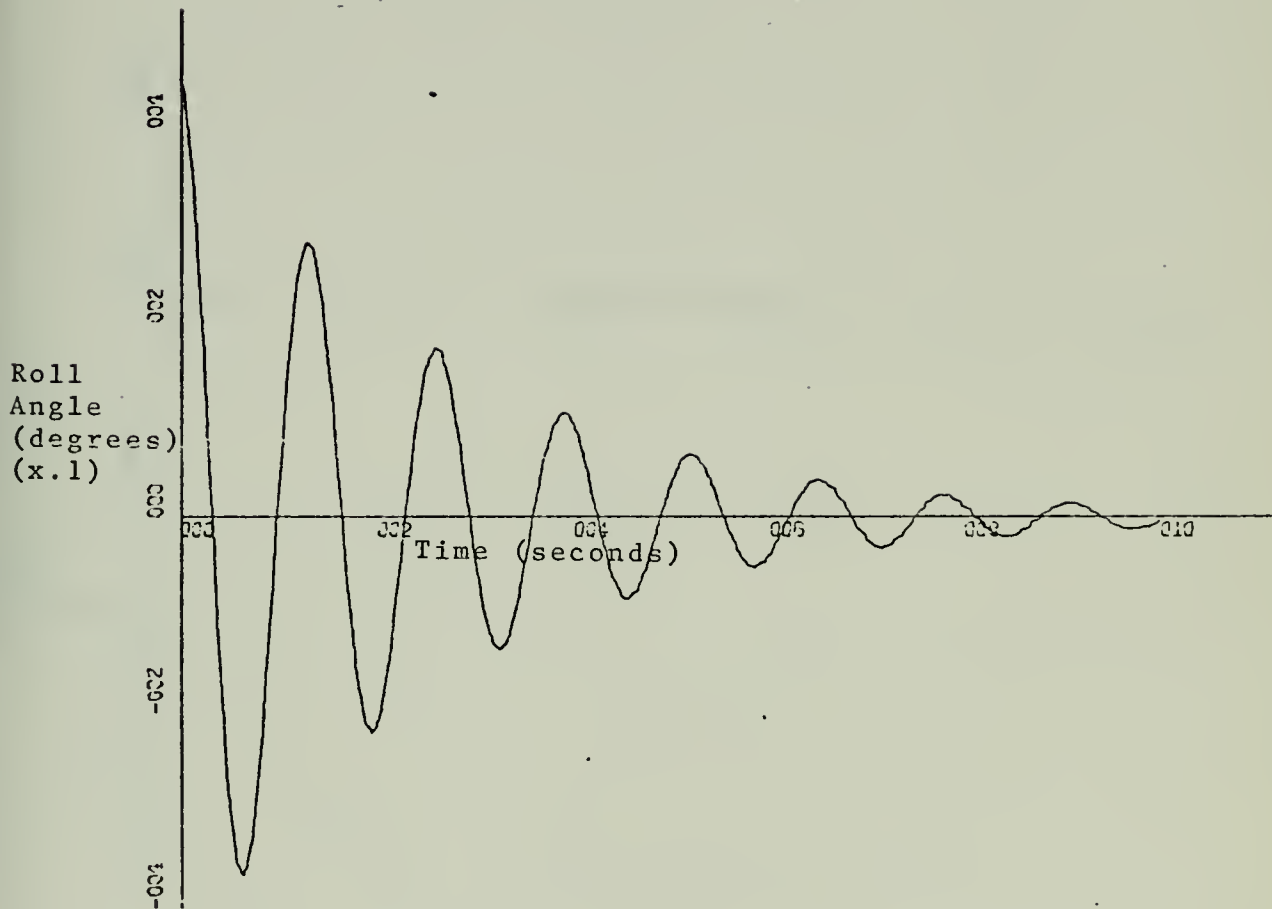


FIGURE 32

COMPUTER SIMULATION ROLL ANGLE VERSES TIME, 19.45 KNOTS  
ORIGINAL XR-3



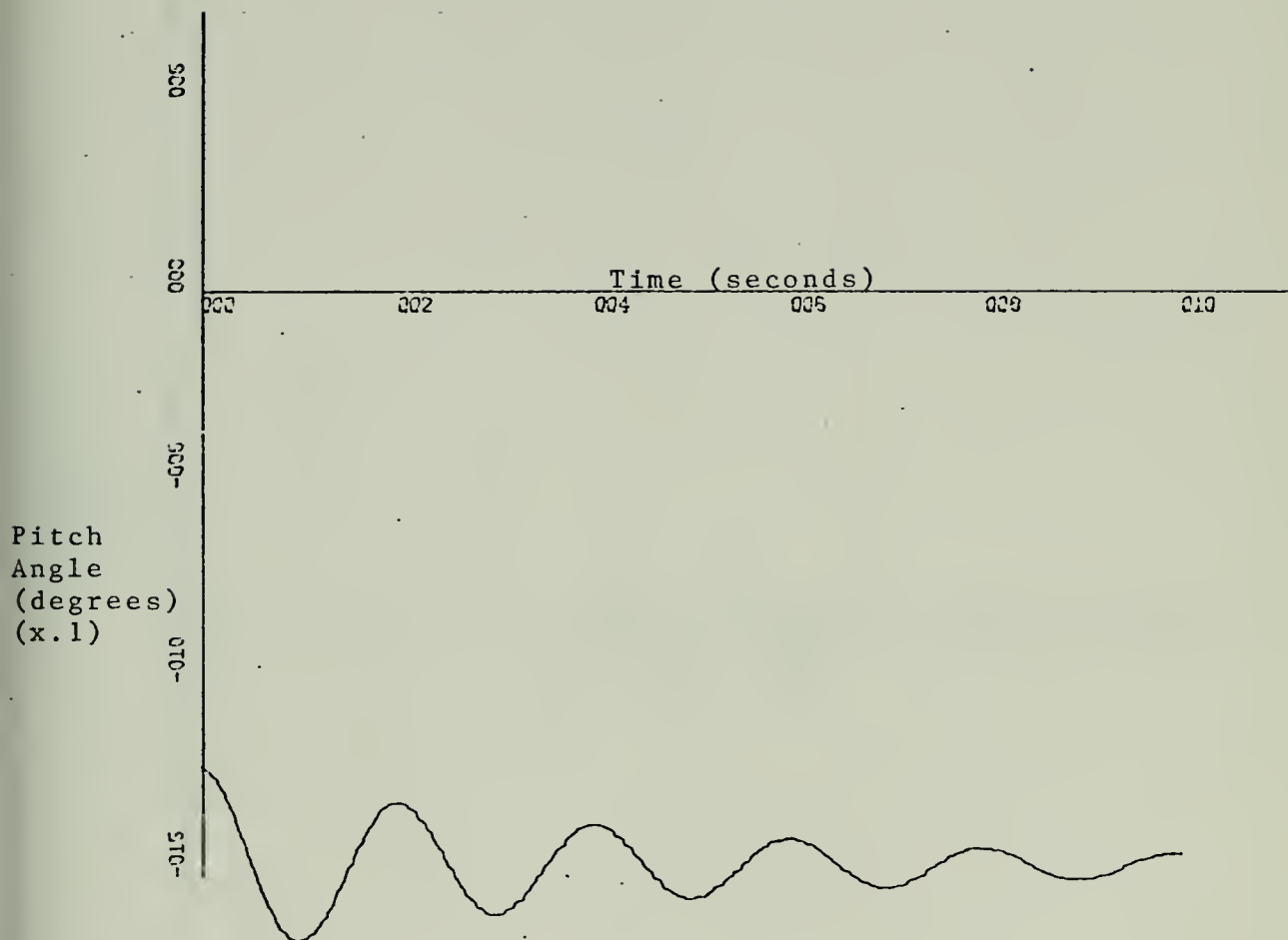


FIGURE 33

COMPUTER SIMULATION PITCH ANGLE VERSES TIME, 19.45 KNOTS  
ORIGINAL XR-3



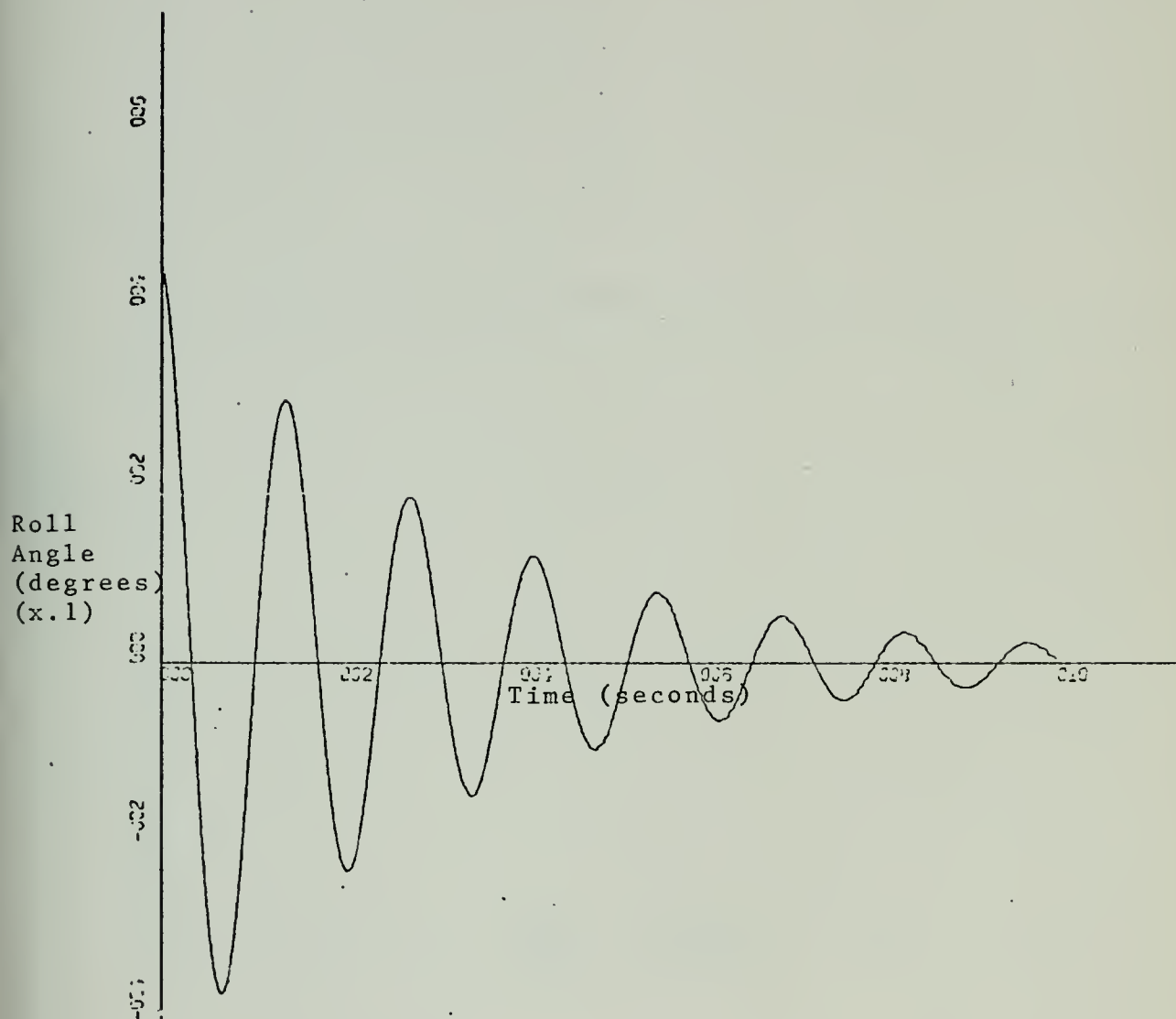


FIGURE 34

COMPUTER SIMULATION ROLL ANGLE VERSES TIME, 19.45 KNOTS  
NEW XR-3



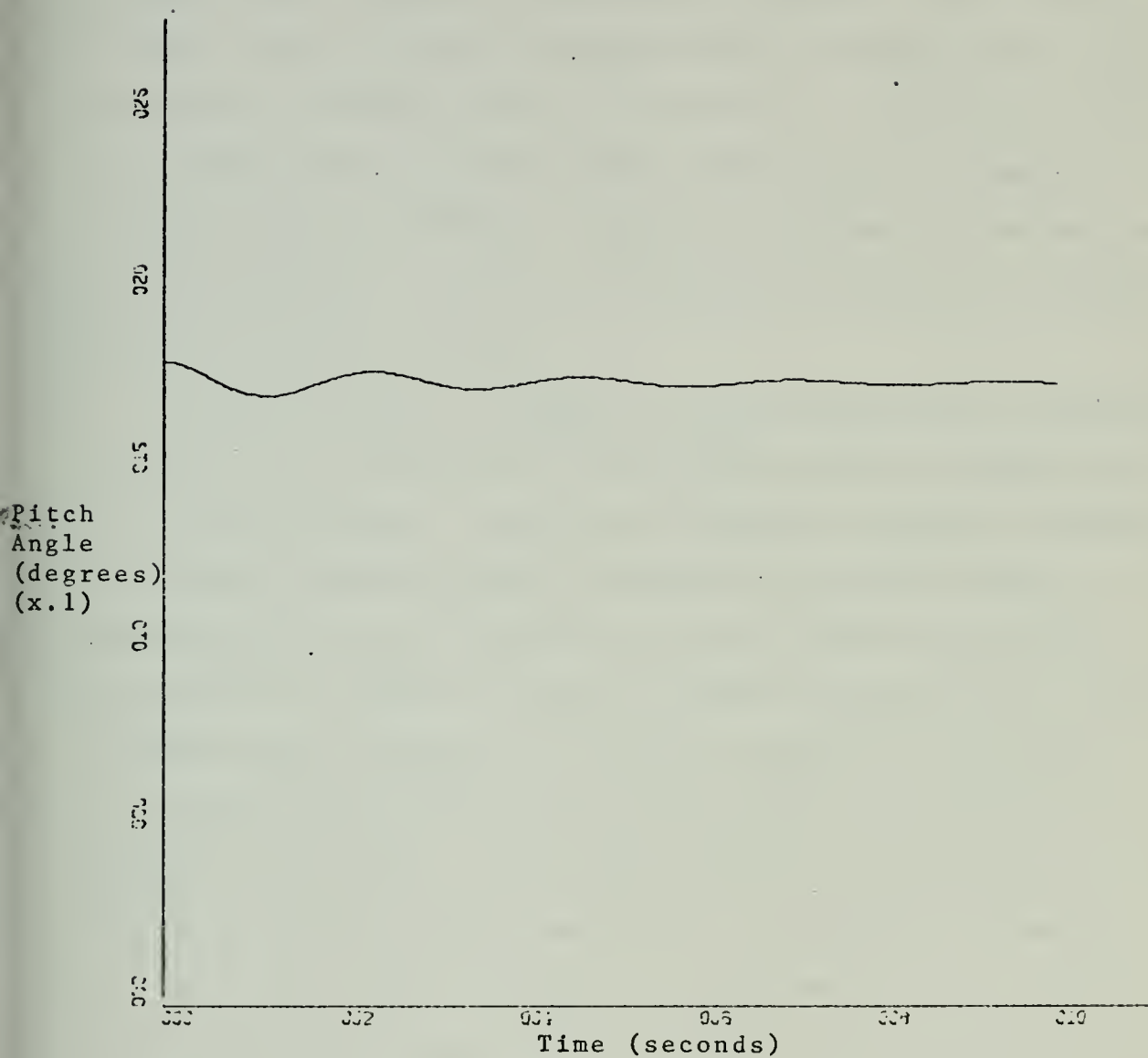


FIGURE 35

COMPUTER SIMULATION PITCH ANGLE VERSES TIME, 19.45 KNOTS  
NEW XR-3





same initial conditions that they were during the 19.45 knot run except for the offset. In the case of the new model this raised the bow approximately six inches and since the steady state condition gave the bow a depth of about three inches with the positive steady state pitch angle this caused air gaps to appear beneath the bow seal. In the case of the old model where the steady state pitch angle was negative no air gaps were created. Figures 36 through 38 present the original model's response and Figures 39 through 41 present the new model's response.

As can be seen in Figure 40, the air gap on the new model caused wide fluctuations in the plenum pressure during the first half-second. This loss of pressure permitted the boat to rapidly sink as shown in Figure 41 until the plenum pressure built up. When the air gaps closed and the boat continued to settle the plenum pressure rapidly rose as the plenum volume decreased. The boat exponentially returned to steady state draft levels as the pitch motion shown in Figure 39 died down. The pitch motion of the new model shows the effect of the new seals. The downward movement of the bow as seen in Figure 39 is severely limited as the bow seal wetted length becomes greater and the effect of the rigid body analysis comes into play. The first negative overshoot is limited to 34 percent of the original effect. The initial decay time constant is 2.5 seconds and the pitch frequency is .63 Hz which because of the nonlinearity



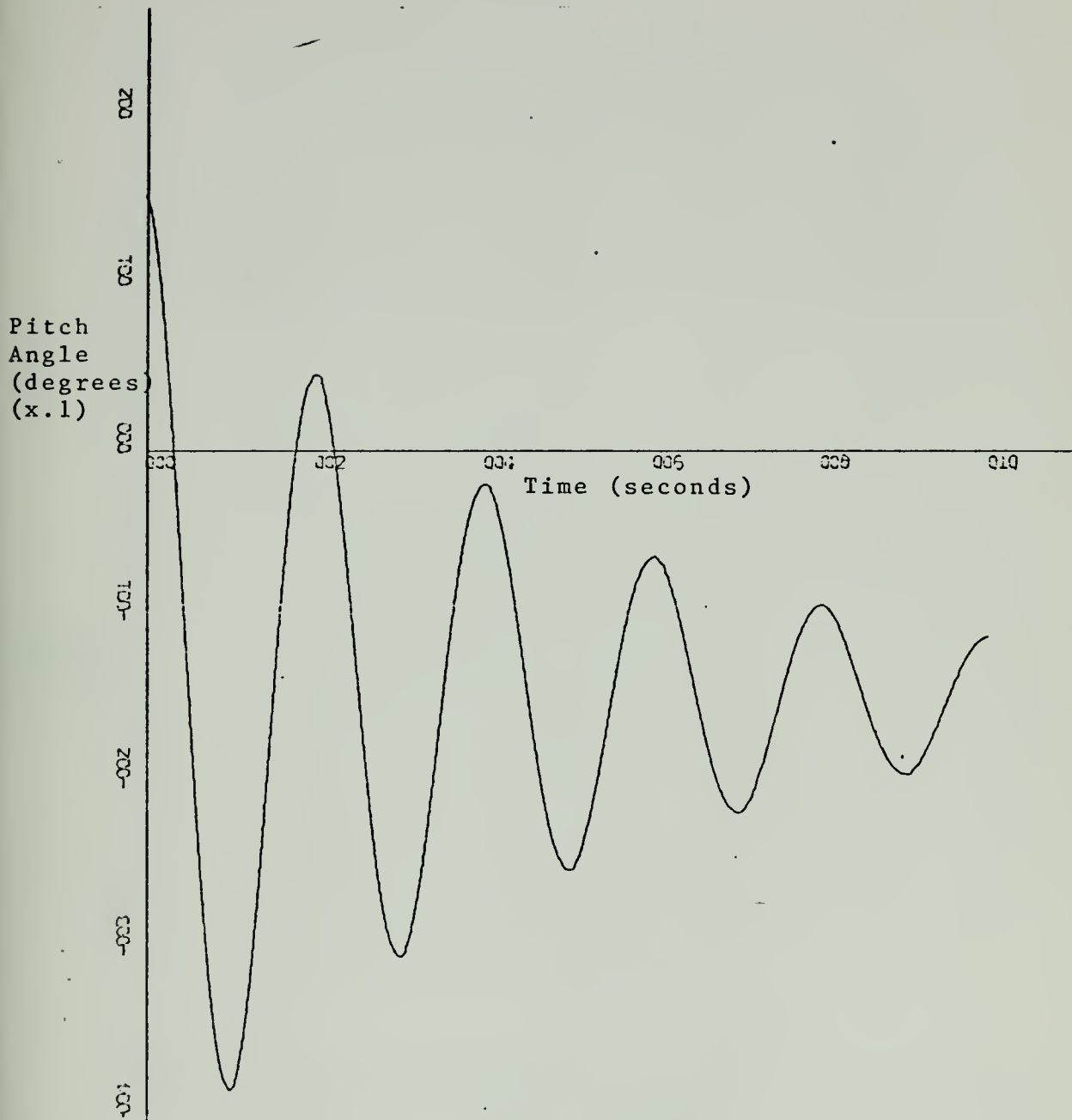


FIGURE 36

COMPUTER SIMULATION 3 DEGREE PITCH STEP RESPONSE, 19.45 KNOTS  
ORIGINAL XR-3 PITCH VERSES TIME



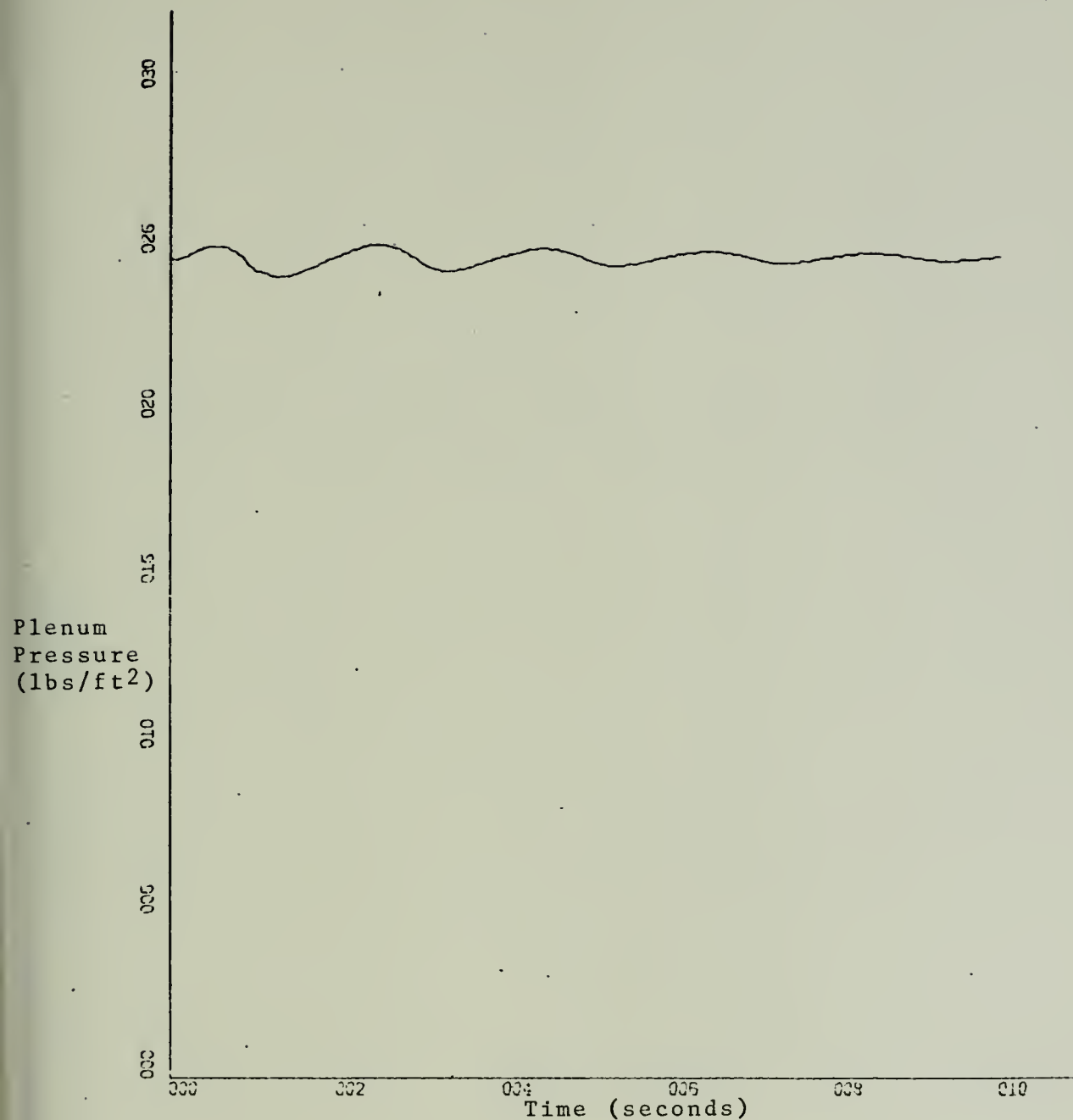


FIGURE 37

COMPUTER SIMULATION 3 DEGREE PITCH STEP RESPONSE, 19.45 KNOTS  
ORIGINAL XR-3 PLENUM PRESSURE VERSES TIME



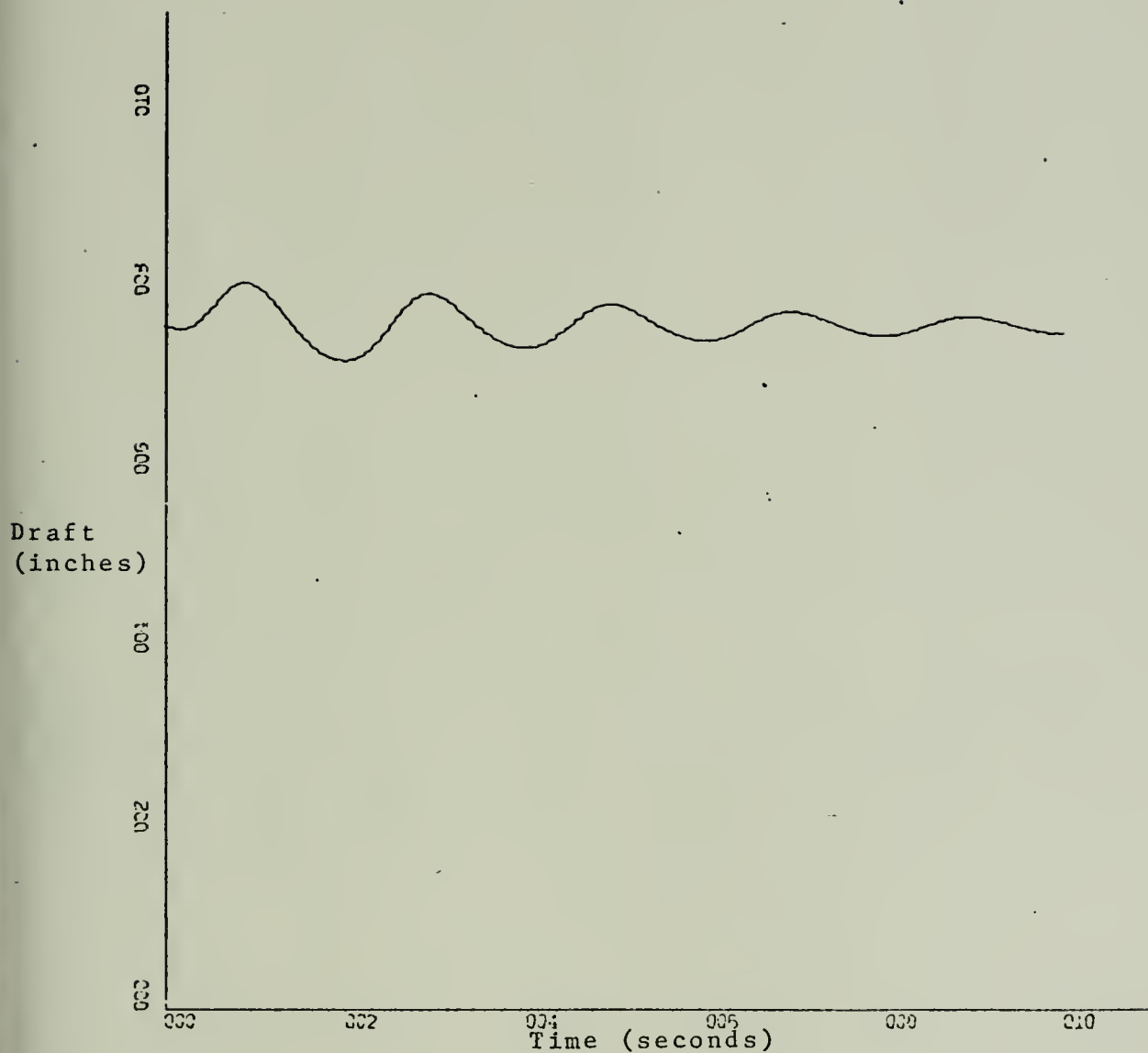


FIGURE 38  
COMPUTER SIMULATION 3 DEGREE PITCH STEP RESPONSE, 19.45 KNOTS  
ORIGINAL XR-3 DRAFT AT C.G. VERSES TIME





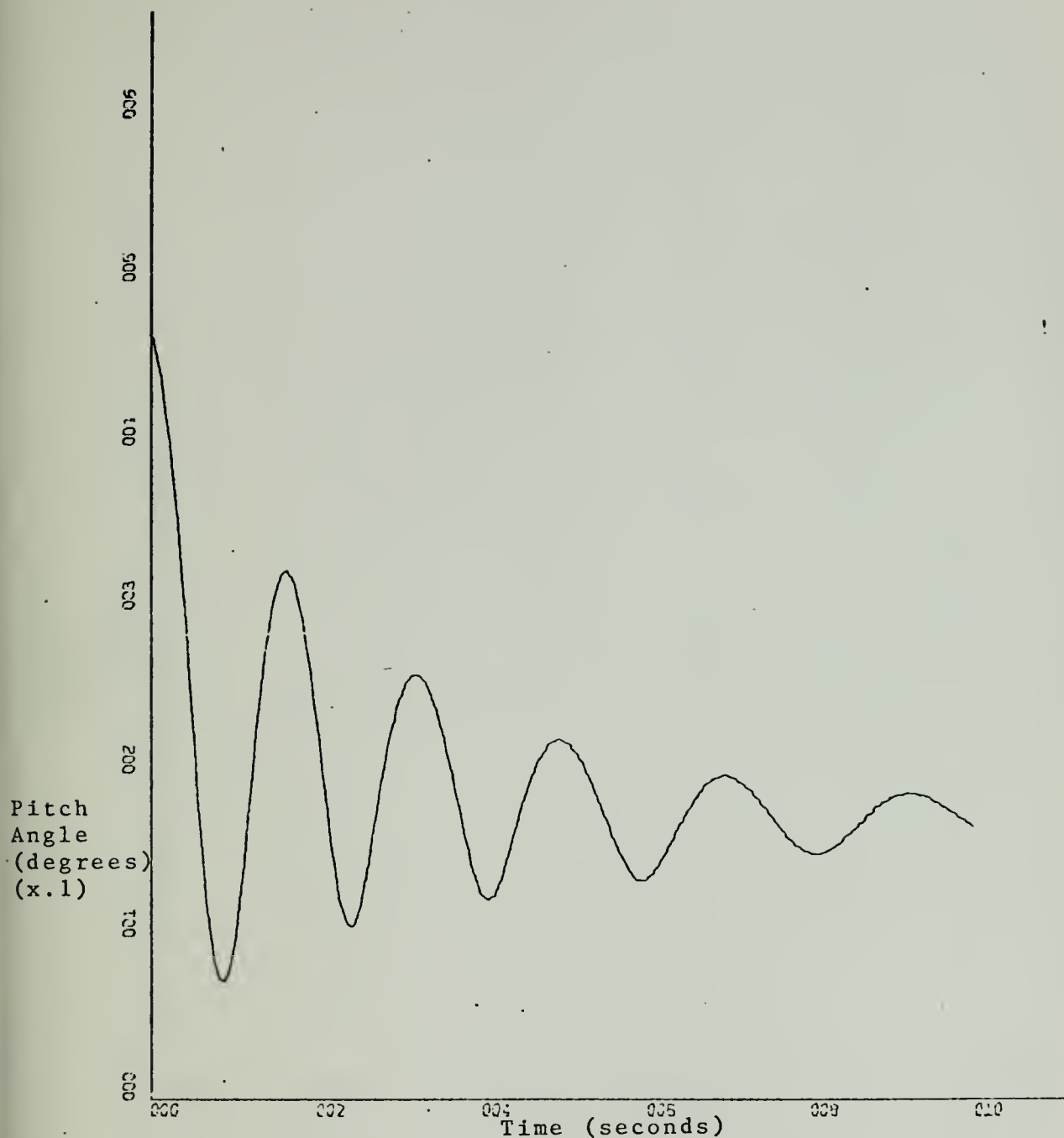


FIGURE 39  
COMPUTER SIMULATION 3 DEGREE PITCH STEP RESPONSE, 19.45 KNOTS  
NEW XR-3 PITCH VERSES TIME



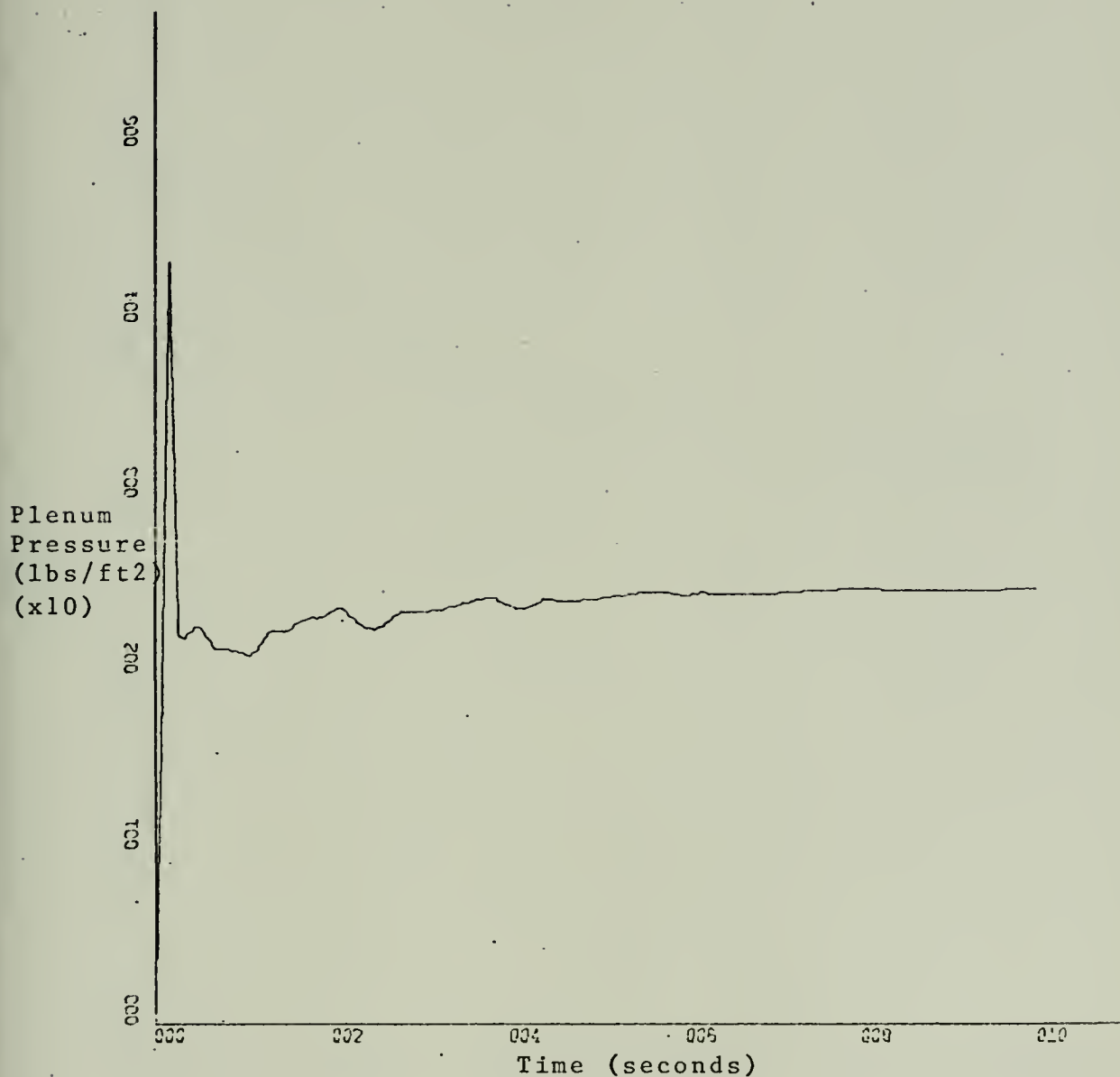


FIGURE 40

COMPUTER SIMULATION 3 DEGREE PITCH STEP RESPONSE, 19.45 KNOTS  
NEW XR-3 PLENUM PRESSURE VERSES TIME.



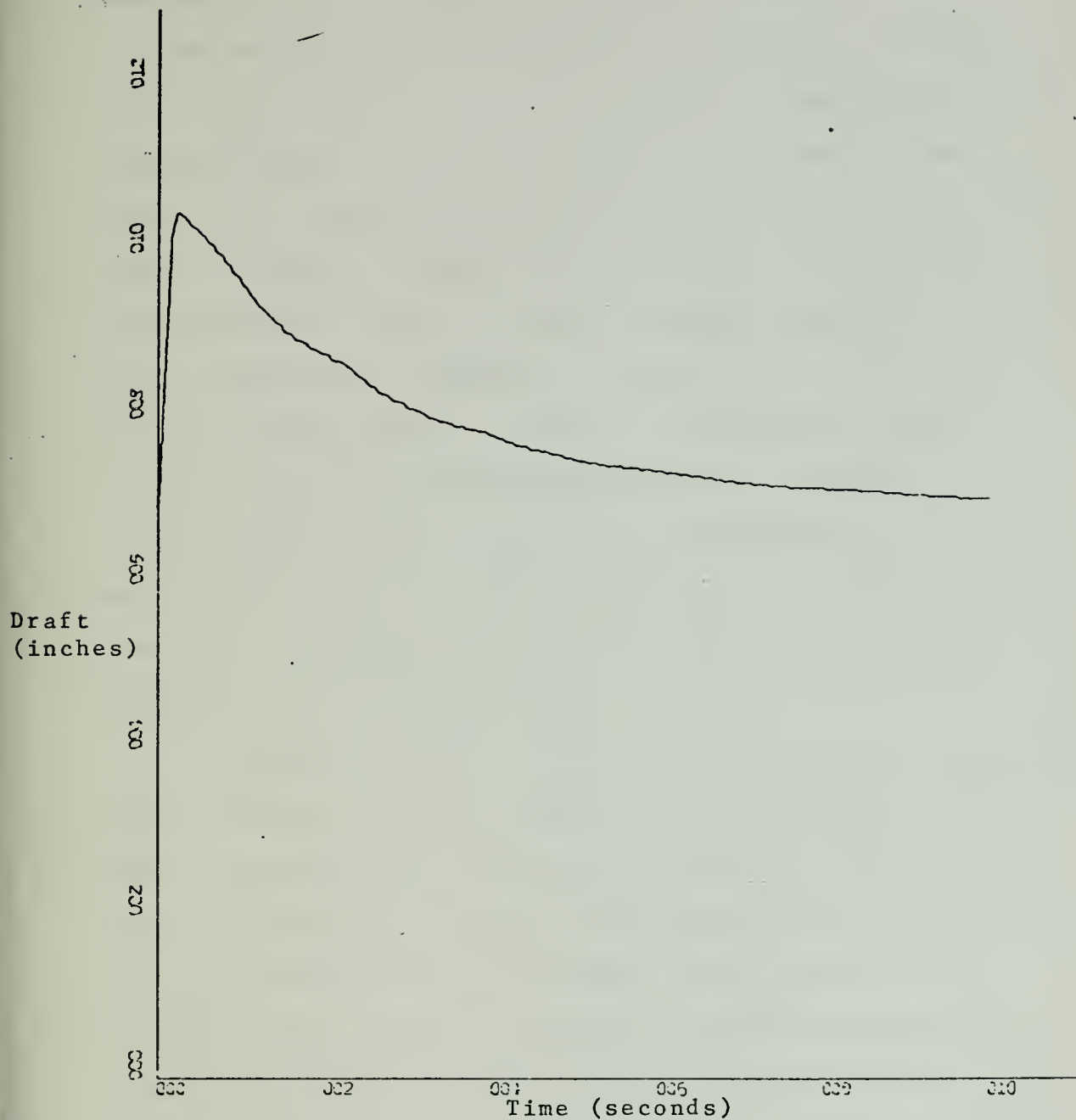


FIGURE 41  
COMPUTER SIMULATION 3 DEGREE PITCH STEP RESPONSE, 19.45 KNOTS  
NEW XR-3 DRAFT AT C.G. VERSES TIME



of the bow and stern seal models changes to a frequency of .42 Hz at the end of ten seconds. The time constant has lengthened to 4.3 seconds in the same period.

The behavior of the old model is different. Because of the high capacity of the fan maps the damping effect of plenum pressure is minimal. The draft movement shown in Figure 38 is therefore highly underdamped whereas the draft motion for the new model did not display any oscillatory tendencies (see Figure 41) and displayed exponential decay type response when returning to steady state conditions. In pitch motion shown in Figure 36 the original model displays a first overshoot magnitude of 78 percent of original offset. The frequency of oscillation is .5 Hz and the decay time constant is 4.78 seconds. Both the time constant and pitch oscillation frequency remain constant throughout the 10 second simulation.

To further evaluate the differences between the original and new models a second simulation run was made at 19.45 knots. This run was in ahead sea state 2 irregular seas. Figures 42 and 43 show that the plenum pressure fluctuations in the new model were 600 percent greater than in the original model. Whereas the plenum pressure varied from 5 to about 45 PSF in the new model the pressure only varied from about 21 to 27 PSF in the original. Draft fluctuations were about 300 percent greater in the new model than in the original (see Figures 44 and 45). Pitch angle fluctuations were comparable in both models (Figures 46 and 47).





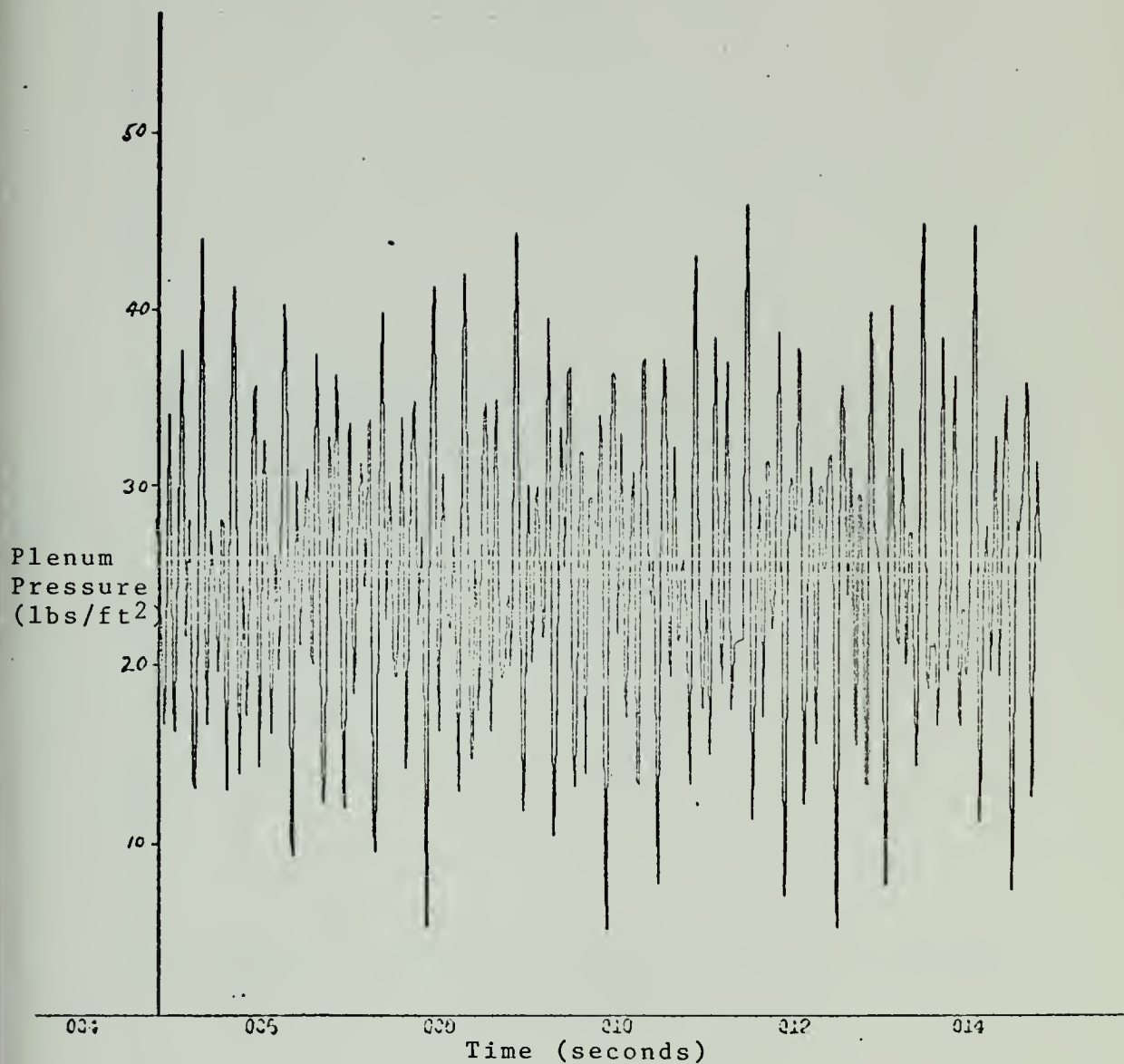


FIGURE 42

COMPUTER SIMULATION PLENUM PRESSURE VERSES TIME, 19.45 KNOTS  
NEW XR-3, SEA STATE 2



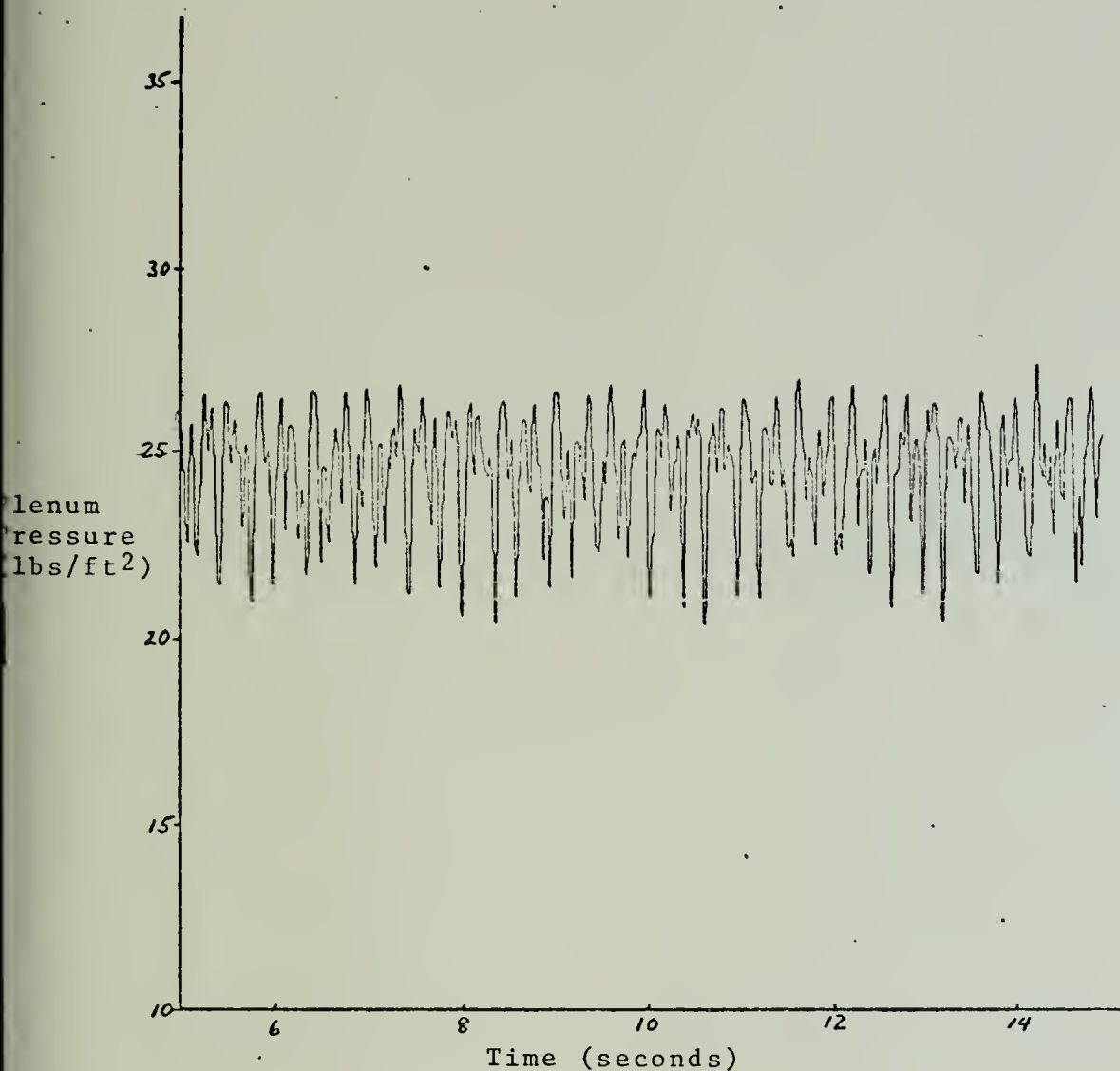


FIGURE 43

COMPUTER SIMULATION PLENUM PRESSURE VERSES TIME, 19.45 KNOTS  
ORIGINAL XR-3, SEA STATE 2



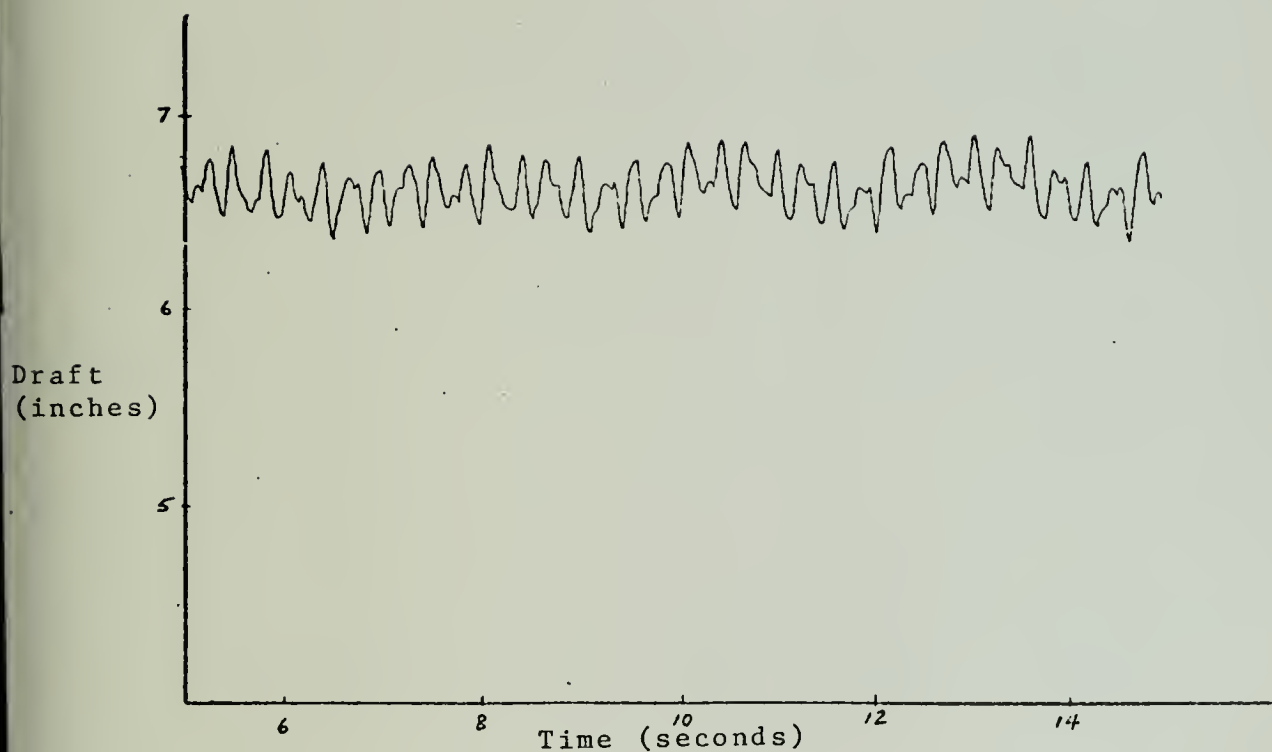


FIGURE 44  
COMPUTER SIMULATION DRAFT AT C.G. VERSES TIME, 19.45 KNOTS  
NEW XR-3, SEA STATE 2



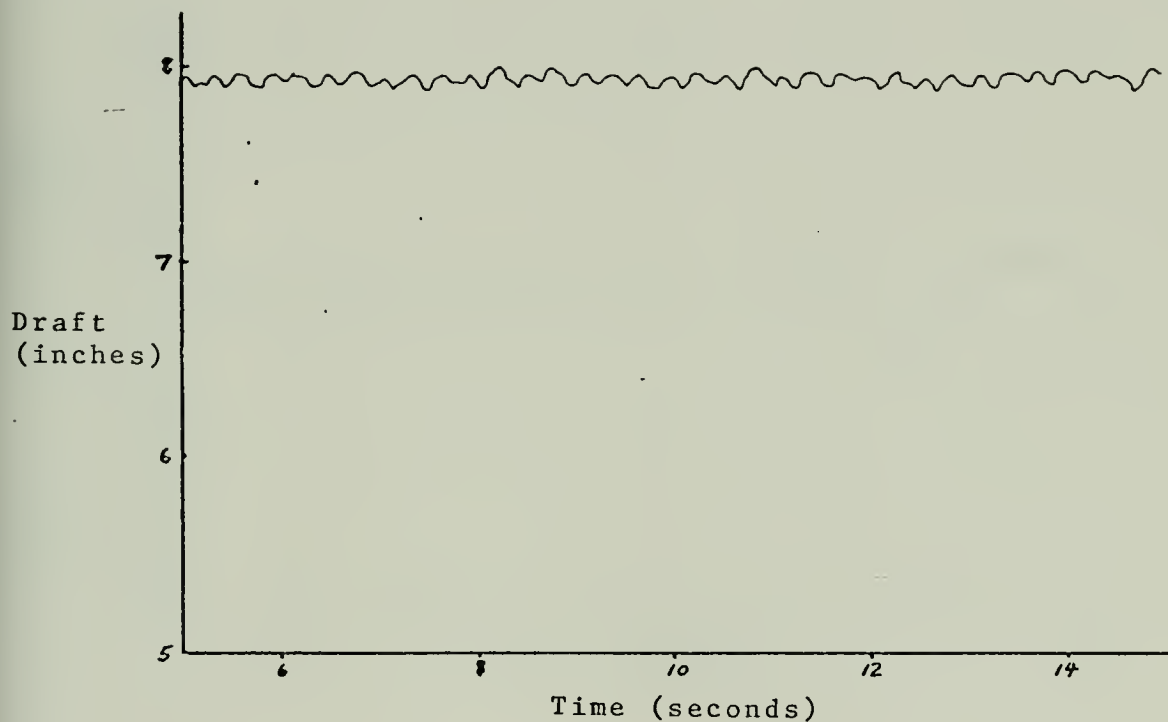


FIGURE 45

COMPUTER SIMULATION DRAFT AT C.G. VERSES TIME, 19.45 KNOTS  
ORIGINAL XR-3, SEA STATE 2





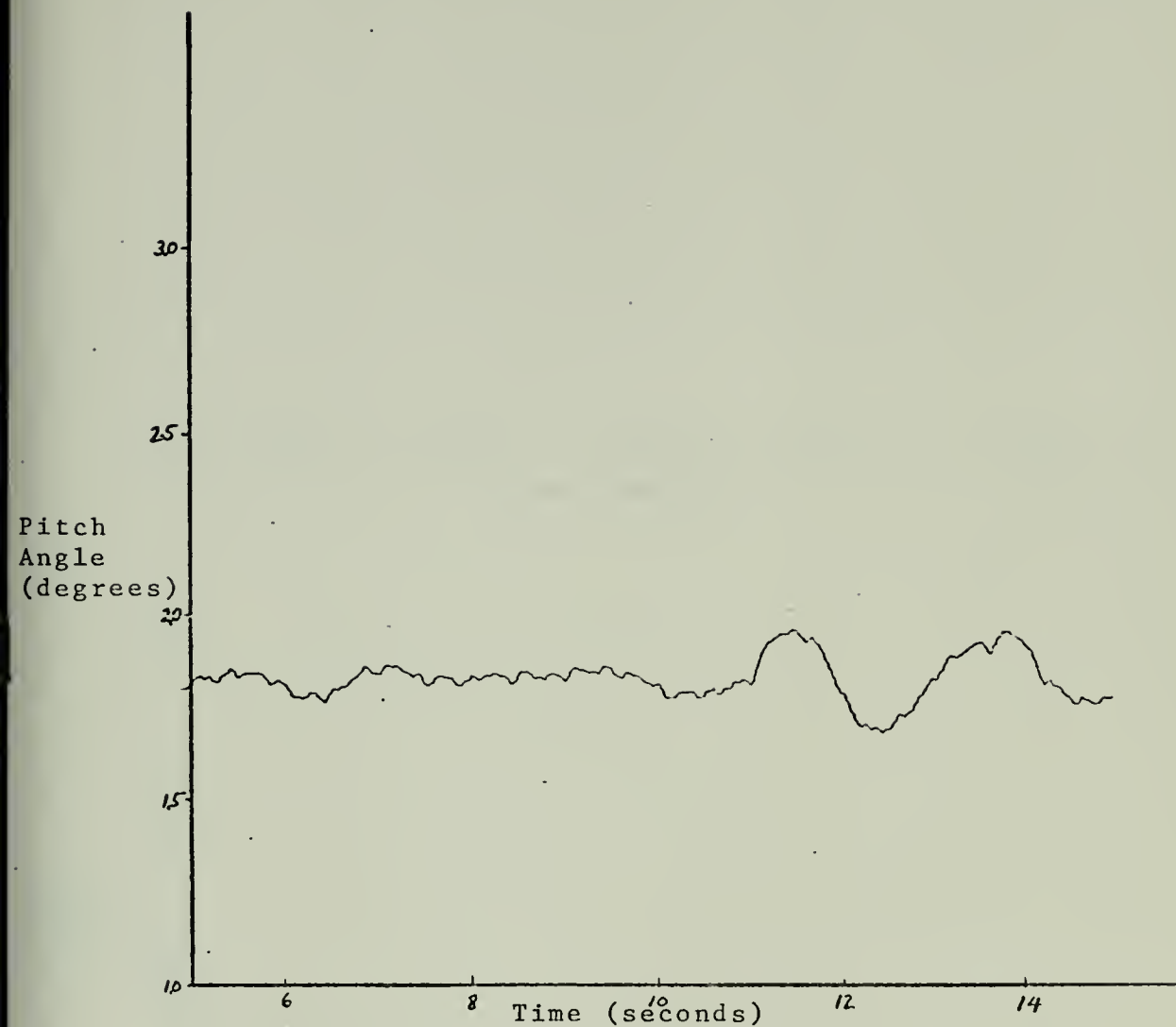


FIGURE 46

COMPUTER SIMULATION PITCH ANGLE VERSES TIME, 19.45 KNOTS  
NEW XR-3, SEA STATE 2



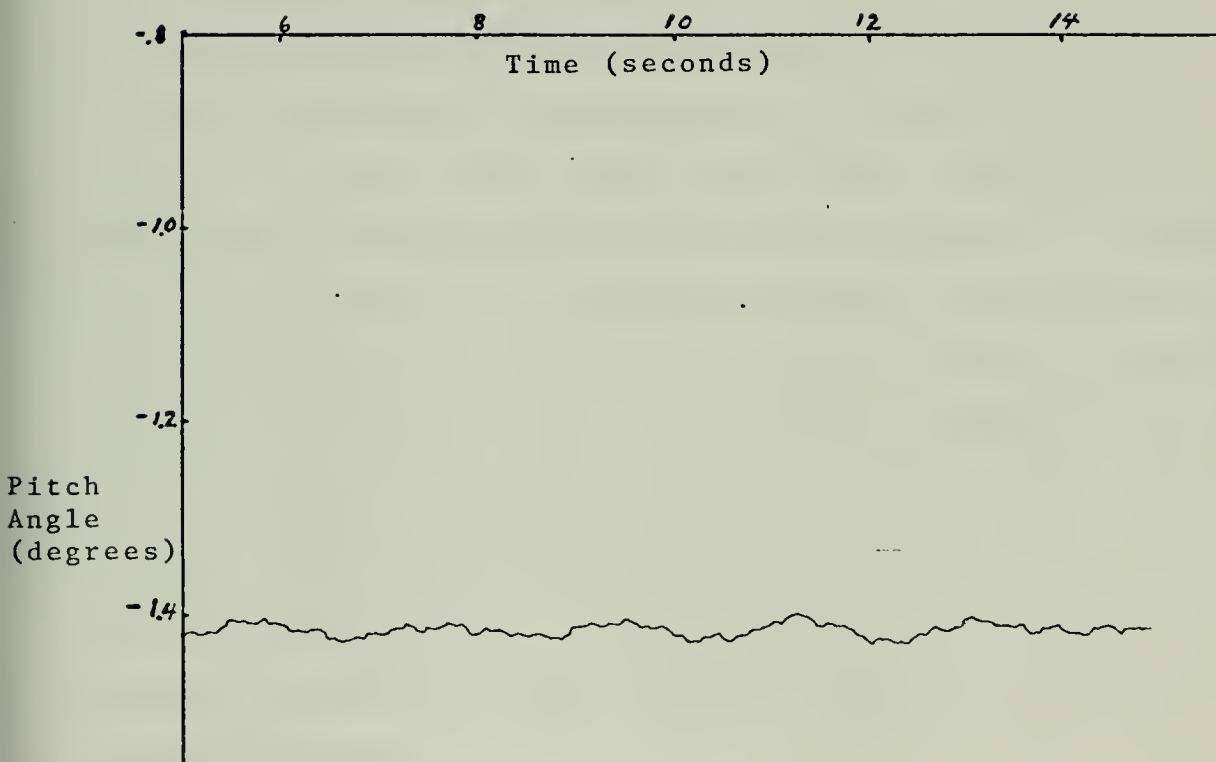


FIGURE 47

COMPUTER SIMULATION PITCH ANGLE VERSES TIME, 19.45 KNOTS  
ORIGINAL XR-3, SEA STATE 2



## V. CONCLUSIONS AND RECOMMENDATIONS

Making accurate measurements from the collected data was extremely difficult because of the high relative level of steady state oscillation present in both the pitch and roll motion. Signal noise coupled with the fact that the decay time constants and the periods of the oscillations were of the same general magnitude made accurate measurement of the decay time constants practically impossible.

Although accurate measurement of the time constants was not possible general observations could be made. It was clearly evident that the pitch and roll transients induced in the XR-3 test craft decayed very rapidly and not with the highly underdamped characteristics shown by the computer simulation models. The measured tape data confirmed the observations made aboard the XR-3 while conducting these runs that the craft come to steady state conditions with only one or two overshoots after the forcing action had ceased. Roll motion transients were normally completed in less than two cycles. Both the longitudinal and athwartships stability were highly speed dependent gaining stability as speed increased.

These observations were not based solely on "feel" but were made by sighting across the deck of the XR-3 and observing the motion of the deck edge relative to the shore line.



Simulation runs have shown that for large perturbations the transient response of the new model is quite different from the original. Since it was not possible to excite such large perturbations in the actual test craft it remains to be verified that the new bow and stern seal models more accurately predict the forces generated by the actual seals than does the original seal model.

The new seal fan maps are more accurate than the original since they are based on actual verified manufacturer's data. Leakage areas are now proportional to those of the actual craft.

The fact that the present computer models of the XR-3 both old and new do not appear to accurately represent the actual transient behavior of the XR-3 in pitch and roll opens many areas which should be investigated for possible errors. As both the pitch and roll transients appear to be in error the sidewall subroutine becomes a prime area of investigation as it contributes major components to both the roll and pitch force moments.

Figure 48 shows one area which should be explored and that is the area of hydrodynamic lift of the sidewalls. Figure 48 is a simplified drawing of the underside of the XR-3. The flat sections on the bottom of each sidewall are cross-hatched for clarity. At high velocity (20-25 knots) these areas become effective planing surfaces. In this program the lift of the sidewall sections due to planing does not appear to take





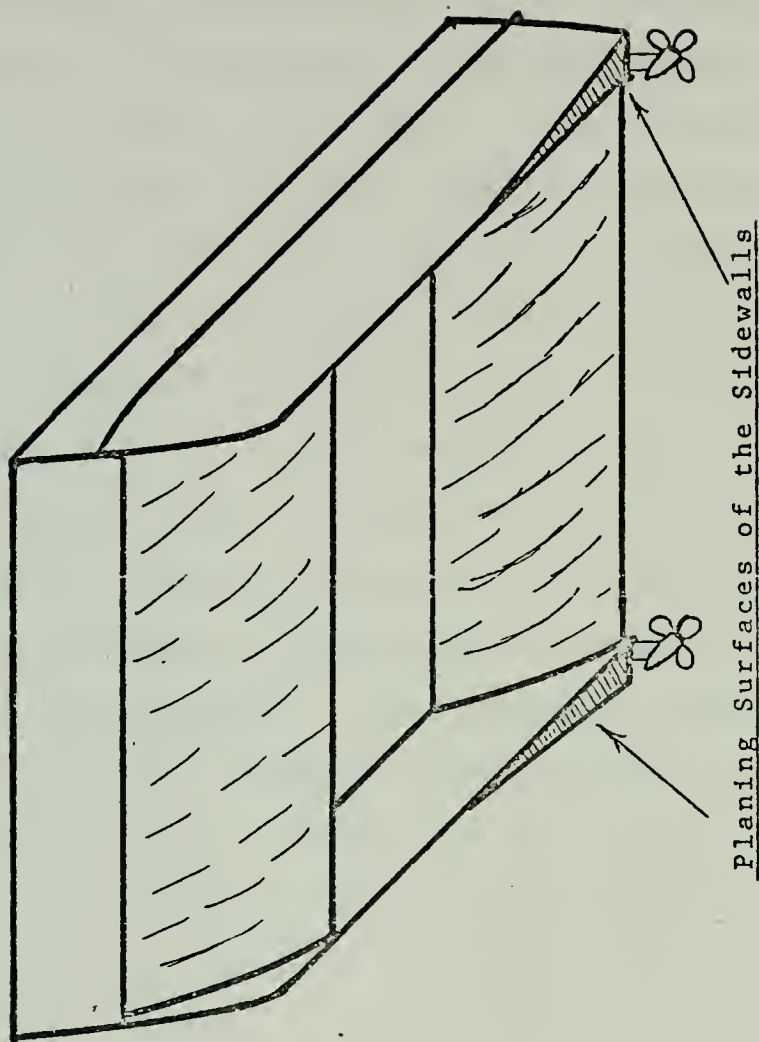


FIGURE 48

BOTTOM VIEW OF THE XR-3 SHOWING PLANING AREAS AT THE REAR



into account the underwater body shape. This shape changes radically from bow to stern. Whether or not this shape has significant effect on roll and pitch transient behavior is not known but should be investigated. Another aspect of the sidewall modeling which should be investigated is the inclusion of forces due to the displacement of water per unit of time. A term such as this would not only have terms based on draft and pitch angle but would also include terms which took into account the rate of change of displacement and the rate of change of the pitch angle. The addition of first derivative terms such as these would have a definite effect on the transient behavior of the sidewalls.

A third area of study concerning the sidewalls is the effect of sidewall deadrise on turning performance. Modeling of the deadrise forces would be incorporated in the cross-flow force modeling. This deadrise could have significant effect on the outboard sidewall during a turn determining whether it has a tendency to rise and ride over the water as the craft skids or dig in and cause the craft to undergo violent roll motion as reported in Ref. 6.

Another area of study which needs investigation is the effect of plenum pressure on the transient response (of the computer model). If it can be shown that the computer model as presently configured can be made to duplicate actual measured craft transient motion by just adjusting the plenum pressure, further modifications of the program may be unnecessary. Further transient motion studies are



needed where both the plenum pressure and the seal pressures are included in the recorded data. Because of the stochastic nature of the actual measured data many duplicate runs will be needed to arrive at accurate averages of the test craft's oscillation frequencies and the decay time constants. These averages should then be used in comparing the actual craft with the computer model.

As can be seen in the recorded data presented herein a fruitful area of study would be in reducing the signal noise on the recorded data. This could be in the recording phase or processing phase of the data. Thorough tests under controlled conditions need to be made of the actual transfer characteristics of the different sensors installed in the test craft.

Earlier in this report it was mentioned that there existed steady state roll and pitch oscillations while the boat was traveling straight on calm water. These oscillations could exist and could be the result of the craft being in some limit cycle type of motion because of the inherent nonlinearity of vehicles operating in fluid mediums. On the other hand, it could be the result of instrumentation for example if the vertical seeking gyro from which all roll and pitch motions are derived was precessing about the true vertical then it could impose a sinusoidal oscillation signal on both the pitch and roll sensors that would show up in the recorded data.



In conclusion it must be stated that there are still many areas in this subject of sidewall modeling of the XR-3 which should and need to be explored before the XR-3 model as originally stated in Ref. 3 and modified herein can be accepted as a reasonably accurate representation of the actual XR-3 test craft. Further investigation into the data collection and processing is also needed to refine the processed data to the point where it is accurate enough for dynamic studies.





## APPENDIX A

### LISTING OF BOWSEAL SUBROUTINE 'BOWSL'

The entering arguments needed for the new bow seal routine are the same as presented in Ref. 3 for the original bow seal except that instead of entering the angle between the leading edge and craft vertical in columns 46-55, the length of the rear cables is entered (in feet). An additional card is needed to enter the length of the middle support cables. The new data card should be entered as shown below.

<u>CARD</u>	<u>COLUMNS</u>	<u>FORMAT</u>	<u>ENTRY</u>
1	1- 5	I	00601 - control tag
	6-15	F	X coordinate of seal hinge (ft) forward of transom
	16-25	F	Seal leakage orifice coefficient
	26-35	F	Pressure differential between bow seal and plenum chamber (PSF)
	36-45	F	Z coordinate of seal hinge (ft) above keel
	46-55		Length of rear support cable (ft) (1.875 is full down)
	56-65		Length of the seal leading edge (ft)
	66-75		Base leakage area (ft <sup>2</sup> ) Nominal .08 ft <sup>2</sup> )
2	1- 5		00602 - control tag
	6-15		Length of middle support cable (ft) (1.1875 is full down)



```

SUBROUTINE BOWSL
INTEGER ON
COMMON /AIR/ PINF,RHOINF,GAM
COMMON /CONST/ PI,RAD,UO
COMMON /FORBS/ FX,FY,FZ,FK,FM,FN,QL
COMMON /GEOM/ WIDTH,XL,XX(4,11),YY(4,11),YY(4,11),NSTA(4),AB,VOLNOM,DELS(4,BSL
110),XCP,ZCP
COMMON /GEOMBS/ DETABX(11),DETABT(11),ARM1B(10),ARM2B(10),DFBS(10)BSL
1,TSKIB(10)BSL
COMMON /LEAKER/ ALEAK,BLEAK,CFSS,CFBSBSL
COMMON /MASSES/ AM,AIXX,AIYY,AIZZ,AIMAX,G,WEIGHT,RHO,NMASS,AMBSL
11(201),XI(201),YI(201),ZI(201),XS,ZS,HRHOBSL
COMMON /PRINT/ ON,IACCEL,IVEL,ITRAJ,ISIDWL,IBOWSL,ISTNSL,IWAVES,IBSL
1RUD,IPROP,IAEROD,IRHSBSL
COMMON /SLOPE/ WATSLP,XPMV,XLXPMV,PWVHT,XPMVXSBSL
COMMON /SOFTBS/ XBF,PBS,SINBS,COSBS,XBS,ZBS,DELYBS,DPBS,ELMAXB,YAVBSL
1GB(10),CENCABBSL
COMMON /WAVE/ ETA(4,11),AW(10),OMEGA(10),DVOLW,NWAVE,BETA,FXWAV,FYBSL
1WAV,FZWAV,FKWAV,FMWAV,FNWAV,ZBAR,PHIBAR,THEBAR,TC,COSBET,SINBET,PBBSL
2BARBSL
DIMENSION ELSKID(11),WETLEN(11),BWSL(6,24),GAP(11),ELSKI(11),BSL
1DPET(11),WTAB(6),ZTAB(6)BSL
DATA NPTS,IBS/6,0/BSL
DATA WIAB/0,0,3,75,5,42,6,67,7,5,8,42/BSL
DATA ZTAB/3,75,4,00,4,42,4,83,5,25,5,67/BSL
DATA ENU,UNSKI,CLSKI,HIGHT/1,28E-05,0,0,1,5708,1,875/BSL
DATA BWSL/0,0,3,8,6,9,9,12,3,15,0,0,0,4,1,7,3,10,5,13,2,15,7,0,0BSL
1,4,3,7,7,11,0,13,7,16,7,0,0,4,7,8,2,11,5,14,5,17,4,0,0,5,2,8,9,12,BSL
24,15,4,18,3,0,0,5,5,9,6,13,3,16,1,19,6,0,0,5,8,9,9,13,8,17,1,20,6,BSL
30,0,6,1,10,6,14,7,18,4,21,9,0,0,6,4,11,3,15,3,19,3,23,3,0,0,6,6,11BSL
4,7,16,4,20,5,24,5,0,0,6,9,12,3,17,6,22,1,25,7,0,0,7,2,13,5,19,6,24BSL
5,1,28,3,0,0,8,2,15,3,21,7,26,3,31,3,0,0,9,6,17,5,24,2,29,7,34,6,0,BSL
60,11,9,20,0,26,7,32,3,38,0,0,0,14,0,22,5,30,0,35,8,41,0,0,0,17,5,2BSL
75,5,32,5,39,7,44,5,0,0,21,0,30,0,37,4,42,0,47,0,0,0,24,6,33,7,41,0BSL
8,45,0,48,7,0,0,29,4,38,5,45,0,48,7,0,0,33,0,45,0,48,7,48,7,48BSL
9,7,0,0,40,0,48,7,48,7,48,7,48,7,48,7,48,7,48,7,48,7,48,7,48,7,48BSL
$8,7,48,7,48,7,48,7,48,7,48,7,48,7,48,7,48,7,48,7,48,7,48,7,48BSL
EQUIVALENCE (VAL(1),TIME), (VAL(2),U), (VAL(3),V), (VAL(4),W), (VABSL
1L(5),P), (VAL(6),Q), (VAL(7),R), (VAL(8),PHI), (VAL(9),THETA), (VABSL
2L(10),Z), (VAL(11),BMASS), (VAL(21),X), (VAL(22),Y), (VAL(23),PSI)BSL
3, (VAL(24),PB)BSL
DO 1 J=1,11
GAP(J) = 0.0
ELSKI(J) = 0.0
WETLEN(J) = 0.0

```

C



```

C
1  ELISKID(J) = 0.0
   CONTINUE
   ALBS = 0.0
   FX = 0.0
   FZ = 0.0
   FK = 0.0
   FM = 0.0
   FN = 0.0
   DELPBG = PBS-PB
   IF (DELPBG.LT.0.0) DELPBG=0.0
   PBAR = PB-PINF
   DELP = PBAR
   IF (DELP.LT.0.0) DELP=0.0
   ARGO = ELMAXB/CORLEN
   ANGO = ARSIN(ARGO)
   X1 = XBS+ZBS*THETA-CORLEN*COS(ANGO)
   Z1 = -Z-ZBS+XBS*THETA-ELMAXB*COS(THETA)
   DPHTFT = (5.5/(1.+(U/25.)))*2.0/12.0
   IF (CENCAB.GT.1.1875) CENCAB=1.1875
   N = NSTA(3)

C
DO 3 K=1,N
  DPFT(K) = DPHTFT
  ELSKI(K) = (ETA(3,K)-DETABX(K)*(XX(3,K)-X1)-Z1)+YY(3,K)*PHI+XLXPWVB
1*WATSLP
  IF (ELSKI(K).GT.HINGHT) ELSKI(K)=HINGHT
  IF ((HINGHT-ELSKI(K)+DPFT(K)).GE.ELMAXB) DPFT(K)=ELMAXB-HINGHT+EL
1KI(K)
  IF (DPFT(K).LT.0.0) DPFT(K)=0.0
  ELSKID(K) = (ELSKI(K)-DPFT(K))*12.0
  IF ((HINGHT-ELSKID(K)/12.0).GE.ELMAXB) ELSKID(K)=(HINGHT-ELMAXB)*
12.0
  DPIN = DPFT(K)*12.0
  MM1 = DPIN
  MM1 = MM1+1
  MM2 = MM1+1
  DINC = DPIN-MM
  GAP(K) = -ELSKI(K)+(HINGHT-ELMAXB)
  IF (GAP(K).LT.0.0) GAP(K)=0.0
  IF (ELSKID(K).GE.0.) GO TO 2
  WETLEN(K) = ELSKI(K)
  GO TO 3
2  MM3 = ELSKID(K)
  MM4 = MM3+1
  MM5 = MM4+1
  DLINC = ELSKID(K)-MM3
  BWSL1 = BWSL(MM1,MM4)

```



```

BWSL2 = BWSL(MM1,MM5)
BWSL3 = BWSL(MM2,MM4)
BWSL4 = BWSL(MM2,MM5)
BWSLA1 = (BWSL2-BWSL1)*DLINC+BWSL1
BWSLA2 = (BWSL4-BWSL3)*DLINC+BWSL3
WETLEN(K) = ((BWSLA2-BWSLA1)*DINC+BWSLA1)/12.0
3 CONTINUE
C
C
N = NSTA(3)-1
DO 10 J=1,N
WETLAV = (WETLEN(J+1)+WETLEN(J))/2.0
IF (WETLAV.LE.0.001) GO TO 8
DPFTAV = (DPFT(J+1)+DPFT(J))/2.0
ELSKIA = (ELSKI(J+1)+ELSKI(J))/2.0
ELSKDA = (ELSKID(J+1)+ELSKID(J))/24.0
SEALHT = HINGHT-ELSKDA
DIFF = 2.0*CENCAB-(SEALHT+0.5)
IF (DIFF.GT.0.5) DIFF=0.5
ARM1B(J) = X1+WETLAV/2.0
ARM2B(J) = ZS-ELSKIA+DPFTAV/2.0
IF (DIFF.GE.0.25) GO TO 4
DFBS(J) = -DELP*DELYBS*WETLAV
GO TO 7
4 FORLEN = XBF-WETLAV
IF (FORLEN.EQ.0.0) GO TO 5
ARGW = (HINGHT-ELSKIA)/FORLEN
IF (ARGW.GT.1.0) ARGW=1.0
ANGW = ARSIN(ARGW)
FORCGS = COS(ANGW)
GO TO 6
5 FORCOS = 0.0
6 DFBS(J) = -DELP*DELYBS*WETLAV-DELP*FORLEN*DELYBS*FORCOS*((FORLEN*0.5*FORCOS)/(FORLEN*FORCOS+WETLAV/2.0))*((DIFF-0.25)*4.0)
7 RESKI = 0.5*RHO*U*WETLAV*DELYBS
CDTSKI = U*WETLAV/ENU
CDTSKI = 0.427/(ALOG10(RESKI)-0.407)**2.64
TSKIB(J) = -ARG*CDTSKI
GO TO 9
8 DFBS(J) = 0.0
9 TSKIB(J) = 0.0
CONTINUE
FX = FX+DFBS(J)
FZ = FZ+DFBS(J)
FK = FK+DFBS(J)*YAVGB(J)
FM = FM-DFBS(J)*ARM1B(J)+TSKIB(J)*ARM2B(J)
FN = FN-TSKIB(J)*YAVGB(J)
ALBS = ALBS+(GAP(J)+GAP(J+1))*DELYBS/2.0

```





C	10	CONTINUE	BSL	1450
		ALBS = ALBS+BLEAK	BSL	1460
		SQFAC = SQRT(2.*ABS(PBAR)/RHOINF)	BSL	1470
		QL = CFBS*ALBS*SQFAC*SIGN(1.,PBAR)	BSL	1480
		IF (IBOWSL.NE.ON) RETURN	BSL	1490
		WRITE (6,11) GAP,WETLEN,FX,FY,FZ,FK,FM,FN	BSL	1500
		RETURN	BSL	1510
			BSL	1520
C	11	FORMAT (//10X,8HBOW SEAL/26H GAP (FT.) (PORT TO STBD.)/11F10.5/28HBOWSL	BSL	1530
		1 WETLEN(FT.) {PORT TO STBD.)/11F10.5/10X,23HBOWSL FX,FY,FZ,FK,FM,FN,FBOWSL	BSL	1540
		2N/6E15.4)	BSL	1550
		END	BSL	1560
			BSL	1570



## APPENDIX B

### LISTING OF STERN SEAL SUBROUTINE 'STNSL'

The entries for this routine are the same as the original stern seal except that in columns 46-55 the rear support cable length is entered instead of the seal angle.

Block 5 entries are as follows:

<u>CARD</u>	<u>COLUMNS</u>	<u>FORMAT</u>	<u>ENTRY</u>
1	1- 5	I	00500 - control tag
	6-15	F	X coordinate of seal hinge, (ft) forward of transom
	16-25	F	Z coordinate of seal hinge above keel (ft)
	26-35	F	Base leakage area (ft <sup>2</sup> ) 3.79 nominal
	36-45	F	Seal leakage orifice coefficient
	46-55	F	Length of rear support cable (ft) 1.875 is full down
	56-65	F	Pressure differential between stern seal and plenum chamber (PSF)
	66-75	F	Length of the leading edge of the seal (ft)



## LISTING OF STERN SEAL SUBROUTINE STNSL

121









S	490
S	500
S	510
S	520
S	530
S	540
S	550
S	560
S	570
S	580
S	590
S	600
S	610
S	620
S	630
S	640
S	650
S	660
S	670
S	680
S	690
S	700
S	710
S	720
S	730
S	740
S	750
S	760
S	770
S	780
S	790
S	800
S	810
S	820
S	830
S	840
S	850
S	860
S	870
S	880
S	890
S	900
S	910
S	920
S	930
S	940
S	950
S	960



# APPENDIX C

## LISTING OF FAN SUBROUTINE 'FAN'

The entries for the fan subroutine remain the same. The nominal fan RPM is 8000 RPM vice 2615 RPM. Printed below are copies of the appropriate entries for the bow seal, stern seal and main plenum fans.

01901	2.0	8000.0	19.0	5.203	1.0	10.406	15.609	18.211	20.812
-10.406	-5.203	0.0	31.218	33.820	36.421	41.624	46.827		
23.414	26.015	28.617							
52.030	57.233	62.436	19.60	18.367	17.133	16.467	15.10		
22.7	22.067	20.67	6.40	5.20	4.33	2.60	.983		
12.20	10.00	7.80							
-.020	-1.06	-2.03							
01902	2.0	8000.0	19.0	5.203	1.0	10.406	15.609	18.211	20.812
-10.406	-5.203	0.0	31.218	33.820	36.421	41.624	46.827		
23.414	26.015	28.617							
52.030	57.233	62.436	19.60	18.367	17.133	16.467	15.10		
22.7	22.067	20.67	6.40	5.20	4.33	2.60	.983		
12.20	10.00	7.80							
-.020	-1.06	-2.03							
01903	1.0	8000.0	19.0	5.203	1.0	10.406	15.609	18.211	20.812
-10.406	-5.203	0.0	31.218	33.920	36.421	41.624	46.827		
23.414	26.015	28.617							
52.030	57.233	62.436	21.83	20.61	19.33	18.85	17.73		
25.70	24.33	23.167	8.033	6.331	5.073	3.035	1.60		
16.40	12.60	10.367							
0.00	-1.06	-2.03							



# APPENDIX C

## LISTING OF FAN SUBROUTINE FAN

```

SUBROUTINE FAN
  INTEGER ON
  COMMON /AIR/ PINF, RHOINF, GAM
  COMMON /FANMAP/ QIN, QBFAN(25), QMFAN(25), QSFAN(25), ENBFAN, ENMFAN, ENFAN
  1 SFAN, BRPM, EMRPM, SRPM, NPTSB, NPTSS, PBFAN(25), PMFAN(25), PSFAN(25)
  25), TMEB(25), DELB(25), NB, TMES(25), DELS(25), NS
  COMMON /PRIINI/ ON, IACCEL, IVEL, ITRAJ, ISIDL, IBOWSL, ISTNSL, IWAVES, IFAN
  1 RUD, IPROP, IAEROD, IRHS
  COMMON /SOFTBS/ XBF, PBS, SINBS, COSBS, XBS, ZBS, DELYBS, DPBS, ELMAXB, YAVFAN
  1 GB(10)
  COMMON /SOFTSS/ XLF, PSS, SINTH, COSTH, XSS, ZSS, DELYSS, DPSS, ELMAXS, YAVFAN
  1 GS(10)
  COMMON /VARBLE/ VAL(40)
  DIMENSION QB(1), QM(1), QS(1), PBOW(1), PM(1), PS(1), HP(8)
  EQUIVALENCE (VAL(1), TIME), (VAL(2), U), (VAL(3), V), (VAL(4), W), (VAFAN
  1 L(5), P), (VAL(6), Q), (VAL(7), R), (VAL(8), PHI), (VAL(9), THETA), (VAFAN
  2 L(10), Z), (VAL(11), BMASS), (VAL(21), X), (VAL(22), Y), (VAL(23), PSI)
  3, (VAL(24), PB)
  EQUIVALENCE (VAL(18), FANPWR)
  EQUIVALENCE (QB(1), QBFAN(1), QM(1), QMFAN(1), QM(1)), (QSFAN(1), QS(1)),
  1 (PBFAN(1), P6QW(1)), (PMFAN(1), PM(1)), (PSFAN(1), PS(1))
  DATA HP/2.9, 2.3, 1.95, 1.77, 1.85, 2.05, 1.93, 1.62/
  BRAT = 8000/BRPM
  EMRAT = 8000/EMRPM
  SRAT = 8000/SRPM
  TL = VAL(1)
  IF (NB.EQ.0.0) GO TO 1
  DPBS = FGI(TL, NB, TMEB, DELB, ILB)
  PBS = PB+DPBS
  1 IF (NS.EQ.0.0) GO TO 2
  DPSS = FGI(TL, NS, TMES, DELS, ILS)
  PSS = PB+DPSS
  2 CONTINUE
  PB1 = PBS-PINF
  PB2 = PB-PINF
  PB3 = PSS-PINF
  PBARB = PB1*BRAT**2
  PBARM = PB2*EMRAT**2
  PBARS = PB3*SRAT**2
  QBOW = ENBFAN*FGI(PBARB, NPTSB, PBOW, QB, IB)/BRAT
  QMAIN = ENMFAN*FGI(PBARM, NPTSM, PM, QM, IM)/EMRAT
  QSTN = ENSFAN*FGI(PBARS, NPTSS, PS, QS, IS)/SRAT
  QIN = QBOW+QMAIN+QSTN
  MB1 = (QBOW/ENBFAN+5.0)/5.0
  MB2 = MB1+1
  MB3 = MB2+1
  BINCP = ((QBOW/ENBFAN+5.0)-MB1*5.0)/5.0
  BFANHP = ((HP(MB3)-HP(MB2))*BINCP+HP(MB2))*ENBFAN*(1./BRAT)**3.0

```



```

MS1 = (QSTN/ENSFAN+5.0)/5.0
MS2 = MS1+1
MS3 = MS2+1
STINC = ((QSTN/ENSFAN+5.0)-MS1*5.0)/5.0
SFANHP = ((HP(MS3))-HP(MS2))*STINC+HP(MS2))*ENSFAN*(1./SRAT)**3.0
MM1 = (QMAIN/ENMFAN+5.0)/5.0
MM2 = MM1+1
MM3 = MM2+1
PLINC = ((QMAIN/ENMFAN+5.0)-MM1*5.0)/5.0
PFANHP = ((HP(MM3))-HP(MM2))*PLINC+HP(MM2))*ENMFAN*(1./EMRAT)**3.0
REL PWR = PFANHP+8*FANHP+SFANHP
FANPWR = (QBW*PB1+QMAIN*PB2+QSTN*PB3)/550.
FANEFF = FANPWR/REL PWR
IF (IRHS.NE.ON) RETURN
WRITE (6,3) QBOW,QMAIN,QSTN,PBARB,PBARM,PBARS,REL PWR,FANPWR,FANEFF
RETURN
3 FORMAT (//4H FAN/32H Q - BWOW,MAIN,STERN (CU FT /SEC)3F12.1/28H DEL
1P - BWOW,MAIN,STERN (PSF)3F11.2/60H ACTUAL FAN POWER REQUIRED(HP),
2 IDEAL FAN POWER, EFFICIENCY 3F12.4)
END

```

C

```

FAN 490
FAN 500
FAN 510
FAN 520
FAN 530
FAN 540
FAN 550
FAN 560
FAN 570
FAN 580
FAN 590
FAN 600
FAN 610
FAN 620
FAN 630
FAN 640
FAN 650
FAN 660
FAN 670
FAN 680
FAN 690

```





## APPENDIX D

### LISTING OF INITIAL CONDITION SUBROUTINE 'INCON'

The INCON subroutine was modified to permit it to calculate the wave components of the various sea states if desired instead of having to enter each component individually.

Block 11 options 1 and 2 remain identical. New options 3 and 4 have been added and are entered as follows:

#### BLOCK 11 - OPTION TAG 3

<u>CARD</u>	<u>COLUMNS</u>	<u>FORMAT</u>	<u>ENTRY</u>
1	1- 5	I	01103 control and option tag
	6-15	F	Number of wave components maximum of 10
	16-25	F	Initial wave heading (deg) (180 deg = ahead waves)
	26-35	F	Average height of 1/3 highest waves (ft)
	36-45	F	Shortest significant period (sec)
	46-55	F	Longest significant period (sec)

#### BLOCK 11 - OPTION TAG 4

<u>CARD</u>	<u>COLUMNS</u>	<u>FORMAT</u>	<u>ENTRY</u>
1	1- 5	I	01104 control and option tag
	6-15	F	Number of wave components maximum of 10
	16-25	F	Initial wave heading (deg) (180 deg = ahead waves)
	26-35	F	Average height of 1/3 highest waves (ft)



<u>CARD</u>	<u>COLUMNS</u>	<u>FORMAT</u>	<u>ENTRY</u>
1	36-45	F	Lowest significant frequency (Hz)
	46-55	F	Highest significant frequency (Hz)



# APPENDIX D

## LISTING OF INITIAL CONDITION SUBROUTINE INCON

```

SUBROUTINE INCON (TIME)
REAL*8 TICRD
INTEGER ON
COMMON /AIR/ PINF,RHOINF,GAM
COMMON /AXIS/NXYS(26)
COMMON /BMCO / IMM,IMNX,IMNY,IBMFIL,BTIME,IMT,XMI(10),YMI(7),IX,IY
COMMON /COLUMN/ IVERT,ILATRL
COMMON /CONST/ PI,RAD,UO
COMMON /CNTRL/CONTW,CONTH,QMULT,LOUVER,ACONTZ,ACONTW,ZEQUIL
1,THEQL,ACBASE
COMMON /CURVE/NCURV(10)
COMMON /ENGINE/NPS,NPP,THSIS(25),THSTP(25),XP,YP,ZP,STHS,STHP,
ATIP(25),TIS(25)
COMMON /EQNCO/ NEQS,TOL(20),JQQ
COMMON /FAIR/ RHOA,XLAERO
COMMON /FANMAP/QIN,QBFAN(25),QMFAN(25),QSFAN(25),ENBFAN,ENMFAN,
1 ENSFAN,BRPM,EMRPM,NPTSM,NPTSB,NPTSM,NPTSS
2,PBFAN(25),PMFAN(25),PSFAN(25),TMEB(25),DELB(25),NB,TMES(25),
3DETS(25),NS
COMMON /FROUDE / FN,FNCRIT
COMMON /G8OW/ XBOW
COMMON /GEOM/ WIDTH,XL,XX(4,11),YY(4,11),NSTA(4),AB,VOLNOM
1,DELS(4,10),XCP,ZCP
COMMON /GEOMSW/ XAVG(10),DS
COMMON /GRAF/NGRAF,NDRW
COMMON /HEADG/TICRD(6)
COMMON /PWAVE/ FNCON,PWVCON
COMMON /LEAKER/ALFAK,BLEAK,CFSS,CFBS
COMMON /MASSES/ AM,AIXX,AIYY,AIZZ,AIMAX,G,WEIGHT,RHO,NMASS,
AM1(201),XI(201),YI(201),ZI(201),XS,ZS,HRHO
COMMON /MATRIX/ A(6,6)
COMMON /OPTION/ I3DOF,ISRGE,ITRIM,IDIA
COMMON /PLENUM/XLBW,XBBW,ABW,BUBHGT
COMMON /PLVCQQ/NVI,NVD,NLI,NLD
COMMON /PRIME/ STIME,FTIME,DELT,DELPNT,TPRINT
COMMON /PRFTIN/ON,IACCEL,IVEL,ITRAJ,ISLOWL,IBOWSL,I STNSL,IWAVES,
-IRUD,IPROP,IAEROD,IRHS
COMMON /ROLL/ PHIMAX,TROLL
COMMON /RUDDR/ NPR,DELRUD(25),XR,YR,ZR,IRDS,TL,RSPAN,RAREA,RASPR,
ARCLB,RTC,RUDANG,TIR(25)
COMMON /RISER/ AMPTC
COMMON /SOFTBS/XBF,PBS,SINBS,COSBS,XBS,ZBS,DELYBS,DPBS,ELMAXB,YAVG
1B(10),CENCAB
COMMON /SOFTSS/ XLF,PSS,SINTH,COSTH,XSS,ZSS,DELYSS,DPSS
1,ELMAXS,YAVGS(10)
COMMON /SIDE/FXSW,FYSW,FZSW,FKSW,FMSW,FNSW,ALSW,YSW,XLSW,CFSW,CDSW
1,VAREA,VCHORD,VSPAN,VANGLE,VCOS,VX,VY,VZ,AVBMSW,DELX,VTC
COMMON/SLOPE/WATSLP,XPNV,XLXPNV,PWHT,XPNVXS

```



```

COMMON /STABLE/ S(4), I, STAB
COMMON /STSLR/ CPHI, CPHID
COMMON /SUM/ ISUM1(8), ISUM2(8)
COMMON /VALOLD/ YOLD(20)
COMMON /VARBLE/ VAL(40)
COMMON /WAVE/ ETA(4,11), AW(10), OMEGA(10), DVOLW, NWAVE, BETA,
1 FXWAV, FYWAV, FZWAV, FMWAV, FNWAV
2 ZBAR, PHIBAR, THEBAR, TC, COSBET, SINBET, PBBAR
COMMON /WAVEF/WAVLEN(10), QMEGAE(10), WAVSLP(10), ENCPER(10)
COMMON /WAVTAB/ NAL,DAL,SAL,NDS,DDS,SDS,NTH,OTH,STH,NBB,DBB,SBB,
1 AC1(20,5,7), AC2(20,5,7), AC3(20,5,7), AC4(20,5,7),
2 AC5(20,5,7), AC6(20,5,7), AC7(20,5,7),
3 AC8(20,5,7), AC9(20,5,7),
4 AS1(20,5,7), AS2(20,5,7), AS3(20,5,7), AS4(20,5,7),
5 AS5(20,5,7), AS6(20,5,7), AS7(20,5,7),
6 AS8(20,5,7), AS9(20,5,7), AS10(20,5,7),
7 AS11(20,5,7), AS12(20,5,7), AS13(20,5,7),
8 AS14(20,5,7), AS15(20,5,7), AS16(20,5,7),
9 AS17(20,5,7), AS18(20,5,7), AS19(20,5,7),
10 AS20(20,5,7), AS21(20,5,7), AS22(20,5,7), AS23(20,5,7),
11 AS24(20,5,7), AS25(20,5,7), AS26(20,5,7), AS27(20,5,7),
12 AS28(20,5,7), AS29(20,5,7), AS30(20,5,7), AS31(20,5,7),
13 AS32(20,5,7), AS33(20,5,7), AS34(20,5,7), AS35(20,5,7),
14 AS36(20,5,7), AS37(20,5,7), AS38(20,5,7), AS39(20,5,7),
15 AS40(20,5,7), AS41(20,5,7), AS42(20,5,7), AS43(20,5,7),
16 AS44(20,5,7), AS45(20,5,7), AS46(20,5,7), AS47(20,5,7),
17 AS48(20,5,7), AS49(20,5,7), AS50(20,5,7), AS51(20,5,7),
18 AS52(20,5,7), AS53(20,5,7), AS54(20,5,7), AS55(20,5,7),
19 AS56(20,5,7), AS57(20,5,7), AS58(20,5,7), AS59(20,5,7),
20 AS60(20,5,7), AS61(20,5,7), AS62(20,5,7), AS63(20,5,7),
21 AS64(20,5,7), AS65(20,5,7), AS66(20,5,7), AS67(20,5,7),
22 AS68(20,5,7), AS69(20,5,7), AS70(20,5,7), AS71(20,5,7),
23 AS72(20,5,7), AS73(20,5,7), AS74(20,5,7), AS75(20,5,7),
24 AS76(20,5,7), AS77(20,5,7), AS78(20,5,7), AS79(20,5,7),
25 AS80(20,5,7), AS81(20,5,7), AS82(20,5,7), AS83(20,5,7),
26 AS84(20,5,7), AS85(20,5,7), AS86(20,5,7), AS87(20,5,7),
27 AS88(20,5,7), AS89(20,5,7), AS90(20,5,7), AS91(20,5,7),
28 AS92(20,5,7), AS93(20,5,7), AS94(20,5,7), AS95(20,5,7),
29 AS96(20,5,7), AS97(20,5,7), AS98(20,5,7), AS99(20,5,7),
30 AS100(20,5,7), AS101(20,5,7), AS102(20,5,7), AS103(20,5,7),
31 AS104(20,5,7), AS105(20,5,7), AS106(20,5,7), AS107(20,5,7),
32 AS108(20,5,7), AS109(20,5,7), AS110(20,5,7), AS111(20,5,7),
33 AS112(20,5,7), AS113(20,5,7), AS114(20,5,7), AS115(20,5,7),
34 AS116(20,5,7), AS117(20,5,7), AS118(20,5,7), AS119(20,5,7),
35 AS120(20,5,7), AS121(20,5,7), AS122(20,5,7), AS123(20,5,7),
36 AS124(20,5,7), AS125(20,5,7), AS126(20,5,7), AS127(20,5,7),
37 AS128(20,5,7), AS129(20,5,7), AS130(20,5,7), AS131(20,5,7),
38 AS132(20,5,7), AS133(20,5,7), AS134(20,5,7), AS135(20,5,7),
39 AS136(20,5,7), AS137(20,5,7), AS138(20,5,7), AS139(20,5,7),
40 AS140(20,5,7), AS141(20,5,7), AS142(20,5,7), AS143(20,5,7),
41 AS144(20,5,7), AS145(20,5,7), AS146(20,5,7), AS147(20,5,7),
42 AS148(20,5,7), AS149(20,5,7), AS150(20,5,7), AS151(20,5,7),
43 AS152(20,5,7), AS153(20,5,7), AS154(20,5,7), AS155(20,5,7),
44 AS156(20,5,7), AS157(20,5,7), AS158(20,5,7), AS159(20,5,7),
45 AS160(20,5,7), AS161(20,5,7), AS162(20,5,7), AS163(20,5,7),
46 AS164(20,5,7), AS165(20,5,7), AS166(20,5,7), AS167(20,5,7),
47 AS168(20,5,7), AS169(20,5,7), AS170(20,5,7), AS171(20,5,7),
48 AS172(20,5,7), AS173(20,5,7), AS174(20,5,7), AS175(20,5,7),
49 AS176(20,5,7), AS177(20,5,7), AS178(20,5,7), AS179(20,5,7),
50 AS180(20,5,7), AS181(20,5,7), AS182(20,5,7), AS183(20,5,7),
51 AS184(20,5,7), AS185(20,5,7), AS186(20,5,7), AS187(20,5,7),
52 AS188(20,5,7), AS189(20,5,7), AS190(20,5,7), AS191(20,5,7),
53 AS192(20,5,7), AS193(20,5,7), AS194(20,5,7), AS195(20,5,7),
54 AS196(20,5,7), AS197(20,5,7), AS198(20,5,7), AS199(20,5,7),
55 AS200(20,5,7), AS201(20,5,7), AS202(20,5,7), AS203(20,5,7),
56 AS204(20,5,7), AS205(20,5,7), AS206(20,5,7), AS207(20,5,7),
57 AS208(20,5,7), AS209(20,5,7), AS210(20,5,7), AS211(20,5,7),
58 AS212(20,5,7), AS213(20,5,7), AS214(20,5,7), AS215(20,5,7),
59 AS216(20,5,7), AS217(20,5,7), AS218(20,5,7), AS219(20,5,7),
60 AS220(20,5,7), AS221(20,5,7), AS222(20,5,7), AS223(20,5,7),
61 AS224(20,5,7), AS225(20,5,7), AS226(20,5,7), AS227(20,5,7),
62 AS228(20,5,7), AS229(20,5,7), AS230(20,5,7), AS231(20,5,7),
63 AS232(20,5,7), AS233(20,5,7), AS234(20,5,7), AS235(20,5,7),
64 AS236(20,5,7), AS237(20,5,7), AS238(20,5,7), AS239(20,5,7),
65 AS240(20,5,7), AS241(20,5,7), AS242(20,5,7), AS243(20,5,7),
66 AS244(20,5,7), AS245(20,5,7), AS246(20,5,7), AS247(20,5,7),
67 AS248(20,5,7), AS249(20,5,7), AS250(20,5,7), AS251(20,5,7),
68 AS252(20,5,7), AS253(20,5,7), AS254(20,5,7), AS255(20,5,7),
69 AS256(20,5,7), AS257(20,5,7), AS258(20,5,7), AS259(20,5,7),
70 AS260(20,5,7), AS261(20,5,7), AS262(20,5,7), AS263(20,5,7),
71 AS264(20,5,7), AS265(20,5,7), AS266(20,5,7), AS267(20,5,7),
72 AS268(20,5,7), AS269(20,5,7), AS270(20,5,7), AS271(20,5,7),
73 AS272(20,5,7), AS273(20,5,7), AS274(20,5,7), AS275(20,5,7),
74 AS276(20,5,7), AS277(20,5,7), AS278(20,5,7), AS279(20,5,7),
75 AS280(20,5,7), AS281(20,5,7), AS282(20,5,7), AS283(20,5,7),
76 AS284(20,5,7), AS285(20,5,7), AS286(20,5,7), AS287(20,5,7),
77 AS288(20,5,7), AS289(20,5,7), AS290(20,5,7), AS291(20,5,7),
78 AS292(20,5,7), AS293(20,5,7), AS294(20,5,7), AS295(20,5,7),
79 AS296(20,5,7), AS297(20,5,7), AS298(20,5,7), AS299(20,5,7),
80 AS300(20,5,7), AS301(20,5,7), AS302(20,5,7), AS303(20,5,7),
81 AS304(20,5,7), AS305(20,5,7), AS306(20,5,7), AS307(20,5,7),
82 AS308(20,5,7), AS309(20,5,7), AS310(20,5,7), AS311(20,5,7),
83 AS312(20,5,7), AS313(20,5,7), AS314(20,5,7), AS315(20,5,7),
84 AS316(20,5,7), AS317(20,5,7), AS318(20,5,7), AS319(20,5,7),
85 AS320(20,5,7), AS321(20,5,7), AS322(20,5,7), AS323(20,5,7),
86 AS324(20,5,7), AS325(20,5,7), AS326(20,5,7), AS327(20,5,7),
87 AS328(20,5,7), AS329(20,5,7), AS330(20,5,7), AS331(20,5,7),
88 AS332(20,5,7), AS333(20,5,7), AS334(20,5,7), AS335(20,5,7),
89 AS336(20,5,7), AS337(20,5,7), AS338(20,5,7), AS339(20,5,7),
90 AS340(20,5,7), AS341(20,5,7), AS342(20,5,7), AS343(20,5,7),
91 AS344(20,5,7), AS345(20,5,7), AS346(20,5,7), AS347(20,5,7),
92 AS348(20,5,7), AS349(20,5,7), AS350(20,5,7), AS351(20,5,7),
93 AS352(20,5,7), AS353(20,5,7), AS354(20,5,7), AS355(20,5,7),
94 AS356(20,5,7), AS357(20,5,7), AS358(20,5,7), AS359(20,5,7),
95 AS360(20,5,7), AS361(20,5,7), AS362(20,5,7), AS363(20,5,7),
96 AS364(20,5,7), AS365(20,5,7), AS366(20,5,7), AS367(20,5,7),
97 AS368(20,5,7), AS369(20,5,7), AS370(20,5,7), AS371(20,5,7),
98 AS372(20,5,7), AS373(20,5,7), AS374(20,5,7), AS375(20,5,7),
99 AS376(20,5,7), AS377(20,5,7), AS378(20,5,7), AS379(20,5,7),
100 AS380(20,5,7), AS381(20,5,7), AS382(20,5,7), AS383(20,5,7),
101 AS384(20,5,7), AS385(20,5,7), AS386(20,5,7), AS387(20,5,7),
102 AS388(20,5,7), AS389(20,5,7), AS390(20,5,7), AS391(20,5,7),
103 AS392(20,5,7), AS393(20,5,7), AS394(20,5,7), AS395(20,5,7),
104 AS396(20,5,7), AS397(20,5,7), AS398(20,5,7), AS399(20,5,7),
105 AS400(20,5,7), AS401(20,5,7), AS402(20,5,7), AS403(20,5,7),
106 AS404(20,5,7), AS405(20,5,7), AS406(20,5,7), AS407(20,5,7),
107 AS408(20,5,7), AS409(20,5,7), AS410(20,5,7), AS411(20,5,7),
108 AS412(20,5,7), AS413(20,5,7), AS414(20,5,7), AS415(20,5,7),
109 AS416(20,5,7), AS417(20,5,7), AS418(20,5,7), AS419(20,5,7),
110 AS420(20,5,7), AS421(20,5,7), AS422(20,5,7), AS423(20,5,7),
111 AS424(20,5,7), AS425(20,5,7), AS426(20,5,7), AS427(20,5,7),
112 AS428(20,5,7), AS429(20,5,7), AS430(20,5,7), AS431(20,5,7),
113 AS432(20,5,7), AS433(20,5,7), AS434(20,5,7), AS435(20,5,7),
114 AS436(20,5,7), AS437(20,5,7), AS438(20,5,7), AS439(20,5,7),
115 AS440(20,5,7), AS441(20,5,7), AS442(20,5,7), AS443(20,5,7),
116 AS444(20,5,7), AS445(20,5,7), AS446(20,5,7), AS447(20,5,7),
117 AS448(20,5,7), AS449(20,5,7), AS450(20,5,7), AS451(20,5,7),
118 AS452(20,5,7), AS453(20,5,7), AS454(20,5,7), AS455(20,5,7),
119 AS456(20,5,7), AS457(20,5,7), AS458(20,5,7), AS459(20,5,7),
120 AS460(20,5,7), AS461(20,5,7), AS462(20,5,7), AS463(20,5,7),
121 AS464(20,5,7), AS465(20,5,7), AS466(20,5,7), AS467(20,5,7),
122 AS468(20,5,7), AS469(20,5,7), AS470(20,5,7), AS471(20,5,7),
123 AS472(20,5,7), AS473(20,5,7), AS474(20,5,7), AS475(20,5,7),
124 AS476(20,5,7), AS477(20,5,7), AS478(20,5,7), AS479(20,5,7),
125 AS480(20,5,7), AS481(20,5,7), AS482(20,5,7), AS483(20,5,7),
126 AS484(20,5,7), AS485(20,5,7), AS486(20,5,7), AS487(20,5,7),
127 AS488(20,5,7), AS489(20,5,7), AS490(20,5,7), AS491(20,5,7),
128 AS492(20,5,7), AS493(20,5,7), AS494(20,5,7), AS495(20,5,7),
129 AS496(20,5,7), AS497(20,5,7), AS498(20,5,7), AS499(20,5,7),
130 AS500(20,5,7), AS501(20,5,7), AS502(20,5,7), AS503(20,5,7),
131 AS504(20,5,7), AS505(20,5,7), AS506(20,5,7), AS507(20,5,7),
132 AS508(20,5,7), AS509(20,5,7), AS510(20,5,7), AS511(20,5,7),
133 AS512(20,5,7), AS513(20,5,7), AS514(20,5,7), AS515(20,5,7),
134 AS516(20,5,7), AS517(20,5,7), AS518(20,5,7), AS519(20,5,7),
135 AS520(20,5,7), AS521(20,5,7), AS522(20,5,7), AS523(20,5,7),
136 AS524(20,5,7), AS525(20,5,7), AS526(20,5,7), AS527(20,5,7),
137 AS528(20,5,7), AS529(20,5,7), AS530(20,5,7), AS531(20,5,7),
138 AS532(20,5,7), AS533(20,5,7), AS534(20,5,7), AS535(20,5,7),
139 AS536(20,5,7), AS537(20,5,7), AS538(20,5,7), AS539(20,5,7),
140 AS540(20,5,7), AS541(20,5,7), AS542(20,5,7), AS543(20,5,7),
141 AS544(20,5,7), AS545(20,5,7), AS546(20,5,7), AS547(20,5,7),
142 AS548(20,5,7), AS549(20,5,7), AS550(20,5,7), AS551(20,5,7),
143 AS552(20,5,7), AS553(20,5,7), AS554(20,5,7), AS555(20,5,7),
144 AS556(20,5,7), AS557(20,5,7), AS558(20,5,7), AS559(20,5,7),
145 AS560(20,5,7), AS561(20,5,7), AS562(20,5,7), AS563(20,5,7),
146 AS564(20,5,7), AS565(20,5,7), AS566(20,5,7), AS567(20,5,7),
147 AS568(20,5,7), AS569(20,5,7), AS570(20,5,7), AS571(20,5,7),
148 AS572(20,5,7), AS573(20,5,7), AS574(20,5,7), AS575(20,5,7),
149 AS576(20,5,7), AS577(20,5,7), AS578(20,5,7), AS579(20,5,7),
150 AS580(20,5,7), AS581(20,5,7), AS582(20,5,7), AS583(20,5,7),
151 AS584(20,5,7), AS585(20,5,7), AS586(20,5,7), AS587(20,5,7),
152 AS588(20,5,7), AS589(20,5,7), AS590(20,5,7), AS591(20,5,7),
153 AS592(20,5,7), AS593(20,5,7), AS594(20,5,7), AS595(20,5,7),
154 AS596(20,5,7), AS597(20,5,7), AS598(20,5,7), AS599(20,5,7),
155 AS600(20,5,7), AS601(20,5,7), AS602(20,5,7), AS603(20,5,7),
156 AS604(20,5,7), AS605(20,5,7), AS606(20,5,7), AS607(20,5,7),
157 AS608(20,5,7), AS609(20,5,7), AS610(20,5,7), AS611(20,5,7),
158 AS612(20,5,7), AS613(20,5,7), AS614(20,5,7), AS615(20,5,7),
159 AS616(20,5,7), AS617(20,5,7), AS618(20,5,7), AS619(20,5,7),
160 AS620(20,5,7), AS621(20,5,7), AS622(20,5,7), AS623(20,5,7),
161 AS624(20,5,7), AS625(20,5,7), AS626(20,5,7), AS627(20,5,7),
162 AS628(20,5,7), AS629(20,5,7), AS630(20,5,7), AS631(20,5,7),
163 AS632(20,5,7), AS633(20,5,7), AS634(20,5,7), AS635(20,5,7),
164 AS636(20,5,7), AS637(20,5,7), AS638(20,5,7), AS639(20,5,7),
165 AS640(20,5,7), AS641(20,5,7), AS642(20,5,7), AS643(20,5,7),
166 AS644(20,5,7), AS645(20,5,7), AS646(20,5,7), AS647(20,5,7),
167 AS648(20,5,7), AS649(20,5,7), AS650(20,5,7), AS651(20,5,7),
168 AS652(20,5,7), AS653(20,5,7), AS654(20,5,7), AS655(20,5,7),
169 AS656(20,5,7), AS657(20,5,7), AS658(20,5,7), AS659(20,5,7),
170 AS660(20,5,7), AS661(20,5,7), AS662(20,5,7), AS663(20,5,7),
171 AS664(20,5,7), AS665(20,5,7), AS666(20,5,7), AS667(20,5,7),
172 AS668(20,5,7), AS669(20,5,7), AS670(20,5,7), AS671(20,5,7),
173 AS672(20,5,7), AS673(20,5,7), AS674(20,5,7), AS675(20,5,7),
174 AS676(20,5,7), AS677(20,5,7), AS678(20,5,7), AS679(20,5,7),
175 AS680(20,5,7), AS681(20,5,7), AS682(20,5,7), AS683(20,5,7),
176 AS684(20,5,7), AS685(20,5,7), AS686(20,5,7), AS687(20,5,7),
177 AS688(20,5,7), AS689(20,5,7), AS690(20,5,7), AS691(20,5,7),
178 AS692(20,5,7), AS693(20,5,7), AS694(20,5,7), AS695(20,5,7),
179 AS696(20,5,7), AS697(20,5,7), AS698(20,5,7), AS699(20,5,7),
180 AS700(20,5,7), AS701(20,5,7), AS702(20,5,7), AS703(20,5,7),
181 AS704(20,5,7), AS705(20,5,7), AS706(20,5,7), AS707(20,5,7),
182 AS708(20,5,7), AS709(20,5,7), AS710(20,5,7), AS711(20,5,7),
183 AS712(20,5,7), AS713(20,5,7), AS714(20,5,7), AS715(20,5,7),
184 AS716(20,5,7), AS717(20,5,7), AS718(20,5,7), AS719(20,5,7),
185 AS720(20,5,7), AS721(20,5,7), AS722(20,5,7), AS723(20,5,7),
186 AS724(20,5,7), AS725(20,5,7), AS726(20,5,7), AS727(20,5,7),
187 AS728(20,5,7), AS729(20,5,7), AS730(20,5,7), AS731(20,5,7),
188 AS732(20,5,7), AS733(20,5,7), AS734(20,5,7), AS735(20,5,7),
189 AS736(20,5,7), AS737(20,5,7), AS738(20,5,7), AS739(20,5,7),
190 AS740(20,5,7), AS741(20,5,7), AS742(20,5,7), AS743(20,5,7),
191 AS744(20,5,7), AS745(20,5,7), AS746(20,5,7), AS747(20,5,7),
192 AS748(20,5,7), AS749(20,5,7), AS750(20,5,7), AS751(20,5,7),
193 AS752(20,5,7), AS753(20,5,7), AS754(20,5,7), AS755(20,5,7),
194 AS756(20,5,7), AS757(20,5,7), AS758(20,5,7), AS759(20,5,7),
195 AS760(20,5,7), AS761(20,5,7), AS762(20,5,7), AS763(20,5,7),
196 AS764(20,5,7), AS765(20,5,7), AS766(20,5,7), AS767(20,5,7),
197 AS768(20,5,7), AS769(20,5,7), AS770(20,5,7), AS771(20,5,7),
198 AS772(20,5,7), AS773(20,5,7), AS774(20,5,7), AS775(20,5,7),
199 AS776(20,5,7), AS777(20,5,7), AS778(20,5,7), AS779(20,5,7),
200 AS780(20,5,7), AS781(20,5,7), AS782(20,5,7), AS783(20,5,7),
201 AS784(20,5,7), AS785(20,5,7), AS786(20,5,7), AS787(20,5,7),
202 AS788(20,5,7), AS789(20,5,7), AS790(20,5,7), AS791(20,5,7),
203 AS792(20,5,7), AS793(20,5,7), AS794(20,5,7), AS795(20,5,7),
204 AS796(20,5,7), AS797(20,5,7), AS798(20,5,7), AS799(20,5,7),
205 AS800(20,5,7), AS801(20,5,7), AS802(20,5,7), AS803(20,5,7),
206 AS804(20,5,7), AS805(20,5,7), AS806(20,5,7), AS807(20,5,7),
207 AS808(20,5,7), AS809(20,5,7), AS810(20,5,7), AS811(20,5,7),
208 AS812(20,5,7), AS813(20,5,7), AS814(20,5,7), AS815(20,5,7),
209 AS816(20,5,7), AS817(20,5,7), AS818(20,5,7), AS819(20,5,7),
210 AS820(20,5,7), AS821(20,5,7), AS822(20,5,7), AS823(20,5,7),
211 AS824(20,5,7), AS825(20,5,7), AS826(20,5,7), AS827(20,5,7),
212 AS828(20,5,7), AS829(20,5,7), AS830(20,5,7), AS831(20,5,7),
213 AS832(20,5,7), AS833(20,5,7), AS834(20,5,7), AS835(20,5,7),
214 AS836(20,5,7), AS837(20,5,7), AS838(20,5,7), AS839(20,5,7),
215 AS840(20,5,7), AS841(20,5,7), AS842(20,5,7), AS843(20,5,7),
216 AS844(20,5,7), AS845(20,5,7), AS846(20,5,7), AS847(20,5,7),
217 AS848(20,5,7), AS849(20,5,7), AS850(20,5,7), AS851(20,5,7),
218 AS852(20,5,7), AS853(20,5,7), AS854(20,5,7), AS855(20,5,7),
219 AS856(20,5,7), AS857(20,5,7), AS858(20,5,7), AS859(20,5,7),
220 AS860(20,5,7), AS861(20,5,7), AS862(20,5,7), AS863(20,5,7),
221 AS864(20,5,7), AS865(20,5,7), AS866(20,5,7), AS867(20,5,7),
222 AS868(20,5,7), AS869(20,5,7), AS870(20,5,7), AS871(20,5,7),
223 AS872(20,5,7), AS873(20,5,7), AS874(20,5,7), AS875(20,5,7),
224 AS876(20,5,7), AS877(20,5,7), AS878(20,5,7), AS879(20,5,7),
225 AS880(20,5,7), AS881(20,5,7), AS882(20,5,7), AS883(20,5,7),
226 AS884(20,5,7), AS885(20,5,7), AS886(20,5,7), AS887(20,5,7),
227 AS888(20,5,7), AS889(20,5,7), AS890(20,5,7), AS891(20,5,7),
228 AS892(20,5,7), AS893(20,5,7), AS894(20,5,7), AS895(20,5,7),
229 AS896(20,5,7), AS897(20,5,7), AS898(20,5,7), AS899(20,5,7),
230 AS900(20,5,7), AS901(20,5,7), AS902(20,5,7), AS903(20,5,7),
231 AS904(20,5,7), AS905(20,5,7), AS906(20,5,7), AS907(20,5,7),
232 AS908(20,5,7), AS909(20,5,7), AS910(20,5,7), AS911(20,5,7),
233 AS912(20,5,7), AS913(20,5,7), AS914(20,5,7), AS915(20,5,7),
234 AS916(20,5,7), AS917(20,5,7), AS918(20,5,7), AS919(20,5,7),
235 AS920(20,5,7), AS921(20,5,7), AS922(20,5,7), AS923(20,5,7),
236 AS924(20,5,7), AS925(20,5,7), AS926(20,5,7), AS927(20,5,7),
237 AS928(20,5,7), AS929(20,5,7), AS930(20,5,7), AS931(20,5,7),
238 AS932(20,5,7), AS933(20,5,7), AS934(20,5,7), AS935(20,5,7),
239 AS936(20,5,7), AS937(20,5,7), AS938(20,5,7), AS939(20,5,7),
240 AS940(20,5,7), AS941(20,5,7), AS942(20,5,7), AS
```





```

11400,1500,1600,1700,1800,1900,2000,2100,2200),ISYS
C
PROGRAM CONTROL PARAMETERS
100 CONTINUE
101 GOTO (101,102,103,104,105),IOPT
CONTINUE
STIME=TEMP(1)
FTIME=TEMP(2)
DELO=TEMP(3)
DELPNT=TEMP(4)
TPRINO=TEMP(5)
IF (TPRINO.LT.STIME+DELPNT) TPRINO = STIME+DELPNT
IF (DELO.GT.DELPNT) DELO=DELPNT
IF (DELO.EQ.0.0) GO TO 140
GOTO 10
2000 READ(5,3003) NCURV
3003 FORMAT(10I1)
GO TO 10
2100 READ(5,2210) ISUM1
2210 READ(5,2210) ISUM2
FORMAT(8I2)
GO TO 10
102 READ (5,191) IACCEL,IVEL,ITRAJ,ISIDWL,IBOWSL,ISTNSL,IWAVES,IRUD,
1 IPROP,IAEROD,IRHS
GO TO 10
103 READ (5,175) NEQS,JQQ,(TOL(J),J=1,NEQS)
GO TO 10
104 READ(5,191) IVERT,ILATRL,NVD,NVI,NLD,NLI
GO TO 10
105 CONTINUE
I3DOF=TEMP(1)
ISRGE=TEMP(2)
ITRIM=TEMP(3)
IDIA=TEMP(4)
GO TO 10
140 WRITE(6,195)
STOP

C MASS DISTRIBUTION
200 G=32.17
RHO=1.99
HRHO=RHO/2.
GO TO (210,220,230), IOPT
210 IMM = 0
WEIGHT = TEMP(1)
AM = WEIGHT/G
XS = TEMP(2)
ZS = TEMP(3)

```



```

C      212      AIXX = TEMP(4)
C      211      AIYY = TEMP(5)
C      213      AIZZ = TEMP(6)
C      214      AIXZ = TEMP(7)
C      215      INERTIA MATRIX OPERATIONS
C      216      DO 211 I=1,6
C      217      DO 211 N=1,6
C      218      A(I,N) = 0.0
C      219      DO 213 N=1,3
C      220      A(N,N)=AM
C      221      A(4,4)=AIXX
C      222      A(5,5)=AIYY
C      223      A(6,6)=AIZZ
C      224      A(4,6)=-AIXZ
C      225      A(6,4)=-AIXZ
C      226      A(6,4)=AMAXI(AM,AIXX,AIYY,AIZZ,ABS(AIXZ))
C      227      DO 214 I=1,6
C      228      DO 214 J=1,6
C      229      A(I,J)=A(I,J)/AIMAX
C      230      CALL DMINV (A,6,D)
C      231      DO 215 I=1,6
C      232      DO 215 J=1,6
C      233      A(I,J)=A(I,J)/AIMAX
C      234      IF (D.NE.0.0) GO TO 10
C      235      WRITE (6,216)
C      236      STOP
C      237      WEIGHT DISTRIBUTION - ASSUME TRANSVERSE (PORT/STBD) SYMMETRY
C      238      READ X INPUT DIST. FWD. OF (SIDEWALL) TRANSOM
C      239      Y INPUT DIST. TO STARBOARD
C      240      I = 1
C      241      Z INPUT DIST. UP FROM KEEL-LINE
C      242      READ (5,192) AMI(I),XI(I),YI(I),ZI(I)
C      243      IF (AMI(I).LT.0.0) GO TO 224
C      244      I = I+1
C      245      IF (I.GT.201) GO TO 70
C      246      GO TO 222
C      247      NMASS = 1-1
C      248      SUM = 0.0
C      249      SUZ = 0.0
C      250      SUZ = 0.0
C      251      DO 225 I=1,NMASS
C      252      AMI(I) = AMI(I)/G
C      253      SUM = SUM+AMI(I)
C      254      SUZ = SUM+AMI(I)*XI(I)
C      255      SUZ = SUZ+AMI(I)*ZI(I)
C      256      AM = SUM#2.0
C      257      WEIGHT = AM*G
C      258      ZS = SUZ/SUM

```



XS	=	SUX/SUM	INC	1930
SUM	=	0.0	INC	1940
SUX	=	0.0	INC	1950
SUY	=	0.0	INC	1960
SUZ	=	0.0	INC	1970
DO 226	I=1,NMASS		INC	1980
XI(I)	= XI(I)-XS		INC	1990
ZI(I)	= -ZI(I)+ZS		INC	2000
AMK	= AMI(I)*2.0		INC	2010
SUX	= SUX+AMK*XI(I)*XI(I)		INC	2020
SUY	= SUY+AMK*YI(I)*YI(I)		INC	2030
SUZ	= SUZ+AMK*ZI(I)*ZI(I)		INC	2040
SUM	= SUM+AMK*XI(I)*ZI(I)		INC	2050
226	AIXX = SUY+SUZ		INC	2060
	AIYY = SUX+SUZ		INC	2070
	AIZZ = SUX+SUY		INC	2080
	AIXZ = SUM		INC	2090
	GO TO 212		INC	2100
230	GO TO 10		INC	2110
			INC	2120
			INC	2130
			INC	2140
			INC	2150
			INC	2160
			INC	2170
			INC	2180
			INC	2190
			INC	2200
			INC	2210
			INC	2220
			INC	2230
			INC	2240
			INC	2250
			INC	2260
			INC	2270
			INC	2280
			INC	2290
			INC	2300
			INC	2310
			INC	2320
			INC	2330
			INC	2340
			INC	2350
			INC	2360
			INC	2370
			INC	2380
			INC	2390
			INC	2400

XX AND YY TABLES		
CONTINUE		
NSIA(1) = TEMP(1)		
NSTA(2) = TEMP(2)		
NSTA(3) = TEMP(3)		
NSTA(4) = TEMP(4)		
XLTOT=TEMP(5)		
GOTO 10		

SIDEWALL (INCLUDING APPENDAGES)		
CONTINUE		
GOTO (401,402),IOPT		
YSW=TEMP(1)		
XLSSW=TEMP(2)		
CFSW=TEMP(3)		
CDSW=TEMP(4)		
AVBMSW=TEMP(5)		
READ (10) ZZZ		
REWIND 10		
GOTO 10		

C 402	BLOCK 4 OPTION 2 REMOVED.	NO APENDAGES
	CONTINUE	
	GOTO 10	

C 500	STERNSEAL	
	CONTINUE	
	XSSI=TEMP(1)	
	ZSSI=TEMP(2)	









```

800 CONTINUE
805 GO TO (805,810),IOPT
CONTINUE
XPO=TEMP(1)
YPO=TEMP(2)
ZPO=TEMP(3)
GO TO 10
C BLOCK 8 OPTION 2 REMOVED. ENGINE OUT INPUT IN BLOCK 16
810 CONTINUE
GOTO 10

C RUDDER
900 CONTINUE
905 GO TO (905,910,915),IOPT
XRO = TEMP(1)
YR=TEMP(2)
ZRO = TEMP(3)
RSPAN=TEMP(4)
RASPR=TEMP(5)
RAREA=TEMP(6)
RCLB=2.*PI*RASPR/(RASPR+3.)
RTC=TEMP(7)
GO TO 10
C 910 NOT USED
910 CONTINUE
915 GO TO 10
GOTO 10

C AERODYNAMICS
1000 CONTINUE
XLAERO=TEMP(1)
BEAM=TEMP(2)
RHOA=.5*RHOINF*XLAERO*BEAM
GOTO 10

C WAVES
1100 CONTINUE
IWAWSW=IOPT
IF(IWAWSW.GT.4) GO TO 70
NWAWE=TEMP(1)
IF(NWAWE.EQ. 0) GOTO 10
IF(NWAWE.GT. 10) GOTO 70
BETAD=TEMP(2)
BETA=BETAD/RAD
COSBET=COS(BETA)
SINBET=SIN(BETA)
TC = 1.0

```

```

INC 2890
INC 2900
INC 2910
INC 2920
INC 2930
INC 2940
INC 2950
INC 2960
INC 2970
INC 2980
INC 2990
INC 3000
INC 3010
INC 3020
INC 3030
INC 3040
INC 3050
INC 3060
INC 3070
INC 3080
INC 3090
INC 3100
INC 3110
INC 3120
INC 3130
INC 3140
INC 3150
INC 3160
INC 3170
INC 3180
INC 3190
INC 3200
INC 3210
INC 3220
INC 3230
INC 3240
INC 3250
INC 3260
INC 3270
INC 3280
INC 3290
INC 3300
INC 3310
INC 3320
INC 3330
INC 3340
INC 3350
INC 3360

```



```

1104 GO TO (1104,1106,1108,1108,1108),IWAVSW
1105 DO 1105 I=1,NWAVE
1105 READ(5,1190) OMEGA(I),AW(I)
1106 GO TO 10
1107 DO 1107 I=1,NWAVE
1107 READ (5,1190) WAVLEN(I) ,AW(I)
1108 GO TO 10
1108 SHTWV=TEMP(3)
1108 GIG=32.17
1108 G2=GIG*GIG
1108 G4=G2*G2
1110 GO TO(10,10,1110,1111),IWAVSW
1110 CONTINUE
1110 PERL=TEMP(4)
1110 PERH=TEMP(5)
1110 WVN=(2.0*3.141592)*(1.0/PERH)
1110 WWX=(2.0*3.141592)*(1.0/PERL)
1111 GO TO 1112
1111 CONTINUE
1111 WVN = TEMP(4)
1111 WWX = TEMP(5)
1112 CONTINUE
1112 UUU=SQRT(SHTWV/0.0185)*1.6878
1112 UU4=UUU**4
1112 CCC=(WWX/WVN)**(1./NWAVE)
1112 WWPO=WWVN
1112 DO 1113 I = 1,NWAVE
1112 WWPN = WWPO*CCC
1112 WW = (WWPN+WWPO)/2
1112 DDW = WWPN-WWPO
1112 WWPO = WWPN
1112 WW4= WW**4.0
1112 WW5 = WW**5.0
1112 SS = 0.0081*G2/(EXP(0.74*G4/(WW4*UU4))*WW5)
1112 OMEGA(I) =WW
1112 AW(I) = SQRT(2.*SS*DDW)
1113 CONTINUE
1113 GO TO 10

C INITIAL CONDITIONS
1200 CONTINUE
1200 UO = TEMP(1)
1200 THETO = TEMP(2)
1200 DSO = TEMP(3)
1200 DELPI=TEMP(4)
1200 DPHI = TEMP(5)
1200 GO TO 10

```

```

INC 3370
INC 3380
INC 3390
INC 3400
INC 3410
INC 3420
INC 3430
INC 3440
INC 3450
INC 3460
INC 3470
INC 3480
INC 3490
INC 3500
INC 3510
INC 3520
INC 3530
INC 3540
INC 3550
INC 3560
INC 3570
INC 3580
INC 3590
INC 3600
INC 3610
INC 3620
INC 3630
INC 3640
INC 3650
INC 3660
INC 3670
INC 3680
INC 3690
INC 3700
INC 3710
INC 3720
INC 3730
INC 3740
INC 3750
INC 3760
INC 3770
INC 3780
INC 3790
INC 3800
INC 3810
INC 3820
INC 3830
INC 3840

```



```

1300 CONTINUE
C INPUT COMPLETED. 1) PRINT ALL INPUT
WRITE(6,2004) TITLC
WRITE(6,2001) STIME,FTIME,DELO,TPRINO,DELPNT
WRITE(6,2002) IACCEL,IVEL,ITRAJ,ISIDWL,IBOWSL,ISTNSL,IWAVES,IRUD,
1 IPROP,IAEROD,IRHS
WRITE(6,2021) I3DOCF,ISRGE,ITRIM,IDIA
WRITE(6,2003) NEQS, (TOL(J),J=1,NEQS)
WRITE(6,219) WEIGHT,XS,ZS,AIXX,AIYY,AIZZ,AIXZ
WRITE(6,217)A,AIMAX
WRITE(6,2018) NSTA
WRITE(6,490) YSW,XLSW,CFSW,CDSW,VANGLE,VSPAN,VCHORD,VXO,VY,VZO,
1 AVBMSW,VTC
WRITE(6,491) NAL,DAL,SAL,NDS,UDS,SDS,NTH,DTH,STH,NBB,DBB,SBB
IF (IMM.GT.0) WRITE(6,1549) (XMO(J),J=1,IMNX)
WRITE(6,1519) IMM,IMNX,IMNY,IBMFIL,BTIME,IMT
IF (IMM.GT.0) WRITE(6,1559) (YMI(J),J=1,IMNY)
WRITE(6,2010) XLBW,XBBW
WRITE(6,2011) XL,WIDTH,XCPO,VOLNOM,BUBHGT
WRITE(6,2020) DELPI
WRITE(6,2009) FNCRIT,XLTOT
WRITE(6,2028) ENBFAN,BRPM,ENMFAN,EMRPM,ENSFAN,SRPM
WRITE(6,2013) XRO,YR,ZPO,RONO,RMAXO,RRATO,RREVO,DLRDO
1 ,RSPAN,RASPR,RAREA,RCLB,RTC
WRITE(6,2012) XLAERO,BEAM,XPO,YPO,ZPO
WRITE(6,2027) XBSI,CFBS,DPBS,ELMAXB
WRITE(6,2026) XSSI,ZSSI,ALAEK,CFSS,ELMAXS,DPSS,XLF
WRITE(6,2025) XSSI,ZSSI,ALAEK,CFSS,ELMAXS,DPSS,XLF
WRITE(6,2017) UO,THETO,DSO
AND 2) INITIALIZE VARIABLES FOR CALCS.
DO 1302 I=1,40
1302 VAL(I) = 0.0
U=UO*1.6889
XSS=- (XS-XSSI)
ZSS=ZS-ZSSI
THETA = THETO/RAD
PHI = DPHI/RAD
THEQL=THETA
DS = DSO/12.
Z=-ZS+DS
ZEQUIL=Z
PHIMAX=0.
TRGULL=0.
IRDS=0.
TL=0.0
WAVE PARAMETERS TABLE
IF(NWAVE.EQ.0) GOTO 1321

```



```

1310 AMPTC=1.30287
1311 GOTO(1310,1315),IWAWSW
1311 DO 1311 I=1,NWAVE
1311 WAVLEN(I)=2.*PI*G/(OMEGA(I)*OMEGA(I))
1315 GOTO 1317
1316 DO 1316 I=1,NWAVE
1317 OMEGA(I)=SQRT(2.*PI*G/WAVLEN(I))
1317 CONTINUE

C CALCULATE INITIAL FREQUENCIES OF ENCOUNTER
DO 1318 I=1,NWAVE
WAVSLP(I) = 360.0*AW(I)/WAVLEN(I)
OMEGAE(I) = 2.*PI*(SQRT(G*WAVLEN(I))/(2.*PI))-U*COSBET)/WAVLEN(I)
ENCPER(I) = 2.0*PI/OMEGAE(I)
1318 CONTINUE
WRITE (6,1191) NWAVE,BETAD,(OMEGA(I),OMEGAE(I),WAVLEN(I),AW(I),
1 WAVSLP(I),ENCPER(I),I=1,NWAVE)

DO 1320 I=1,NWAVE
1321 GOTO 1322
1321 WRITE (6,1192)
1322 CONTINUE
DO 1303 I=1,4
DO 1303 N=1,11
1303 ETA(I,N) = 0.0
DVCLW = 0.0
FXWAV = 0.0
FYWAV = 0.0
FZWAV = 0.0
FKWAV = 0.0
FNWAV = 0.0
FNBWAV = 0.0
ZBAR=Z
PHIBAR=PHI
THEBAR=THETA
TIME=STIME
DELT = DELO
TPRINT=TPRINO-DELPNT
PWVCCN=4.*WEIGHT/(RHO*G*XLBW)
FNCON=SQRT(XLBW*G)
VX=VX0-XS
VZ = ZS-VZO
XP=XPO-XS
XR = XRO-XS
YP=YPO
ZP=ZS-ZPO
ZR = ZS-ZRO
IF (IMM.EQ. 0) GO TO 1305
DO 1304 J=1,IMNX
1304 XMI(J) = XMO(J) - XS

```





```

1305 CONTINUE
    XCP = XCP0-XS
    ZCP = ZS-BUBHGT
    XBS=XBSI-XS
    N=NSTA(3)
    ZBS=ZS-ZBSI
    DO 1364 J=1,N
        DELYBS=XBBW/(N-1)
        XX(3,J)=XBS-XSSI
        YY(3,J)=-0.5*XBBW+(J-1)*DELYBS
1364 CONTINUE
    N=N-1
    DO 1367 J=1,N
        YAVGB(J)=(YY(3,J+1)+YY(3,J))/2.
1367 CONTINUE
    N=NSTA(4)
    DELYSS=XBBW/(N-1)
    DO 1365 J=1,N
        XX(4,J)=-XS
        YY(4,J)=-.5*XBBW+(J-1)*DELYSS
1365 CONTINUE
    N=N-1
    DO 1368 J=1,N
        YAVGS(J)=(YY(4,J+1)+YY(4,J))/2.
1368 CONTINUE
    XBOH=XLTOT-XS
    N=NSTA(1)
    DELX=XBSI/(N-1)
    DO 1309 J=1,2
        DO 1309 I=1,N
            XX(J,I)=(I-1)*DELX-XS
            YY(J,I)=YSW*(2*J-3)
1309 WRITE(6,1366) ((XX(J,N),N=1,11),(YY(J,N),N=1,11),J=1,4)
1366 FORMAT(10H STBD. SIDEWALL /2(11F10.2/),
1366 10H STERN SEAL /2(11F10.2/),
1366 20H STERN SEAL /2(11F10.2/))
    N=NSTA(1)-1
    DO 1308 I=1,N
        XAVG(I)=DELX*(2*I-1)/2.-XS
1308 CALL WAVES(TIME)

C INITIALIZE BUBBLE PRESSURE, ABSOLUTE (PSF)
PB=PINF+DELP1
PBBAR=DELP1
PBAR=DELP1
PSS=PB+DPSS
PBS=PB+DPBS
AB=ABW-(ABW-AB)*(ZS+Z/BUBHGT)

```

```

INC 4810
INC 4820
INC 4830
INC 4840
INC 4850
INC 4860
INC 4870
INC 4880
INC 4890
INC 4900
INC 4910
INC 4920
INC 4930
INC 4940
INC 4950
INC 4960
INC 4970
INC 4980
INC 4990
INC 5000
INC 5010
INC 5020
INC 5030
INC 5040
INC 5050
INC 5060
INC 5070
INC 5080
INC 5090
INC 5100
INC 5110
INC 5120
INC 5130
INC 5140
INC 5150
INC 5160
INC 5170
INC 5180
INC 5190
INC 5200
INC 5210
INC 5220
INC 5230
INC 5240
INC 5250
INC 5260
INC 5270
INC 5280

```



```

CDBUB=.37/((U/FNCON)**1.5655981)
WATSLP=PWVCON*CDBUB/AB
IF (IDIA.EQ.1) GO TO 6
VOL=VOLNOM-.5*(AB+ABW)*(Z+ZS)-OVOLW
1+PWVHT*PWVCON*CDBUB
GO TO 7
6
VOL=VOLNOM-.5*(AB+ABW)*(Z+ZS)-DVOLW+PBAR*.3175333
CONTINUE
BMASS=(PB/PINF)**(1./GAM)*VOL*RHGINF
WRITE (6,2023)
RETURN
C
RUN TERMINATOR
1400 WRITE(6,98)
STOP
C
BENDING MOMENT
1500 GO TO (1510,1520,1530,1540), IOPT
1510 IMM = TEMP(1)
IF (IMM.GT.3) GO TO 70
IMNX = TEMP(2)
IF (IMNX.GT.10) GO TO 70
IMNY = TEMP(3)
IF (IMNY.GT.7) GO TO 70
IBMFIL = TEMP(4)
BTIME = TEMP(5)
IF (IMM.EQ.3) IMT = TEMP(6)
GO TO 10
1520 DO 1521 J=1,7
1521 XMO(J) = TEMP(J) GO TO 10
IF (IMNX.LE.7) GO TO 10
READ 1522, (XMO(J),J=8,IMNX)
GO TO 10
1530 DO 1531 J=1,IMNY
1531 YMI(J) = TEMP(J)
GO TO 10
1540 CONTINUE
GO TO 10
1600 CONTINUE
GO TO(1605,1610,1615),IOPT
1605 CONTINUE
C VALUES INPUT FOR STBD SCREW
THSTI=TEMP(1)
NPS=TEMP(2)
STHS=TEMP(3)
IF(NPS.EQ.0.0) GO TO 1609
READ(5,1950)(TIS(J),J=1,NPS)

```

```

INC 5290
INC 5300
INC 5310
INC 5320
INC 5330
INC 5340
INC 5350
INC 5360
INC 5370
INC 5380
INC 5390
INC 5400
INC 5410
INC 5420
INC 5430
INC 5440
INC 5450
INC 5460
INC 5470
INC 5480
INC 5490
INC 5500
INC 5510
INC 5520
INC 5530
INC 5540
INC 5550
INC 5560
INC 5570
INC 5580
INC 5590
INC 5600
INC 5610
INC 5620
INC 5630
INC 5640
INC 5650
INC 5660
INC 5670
INC 5680
INC 5690
INC 5700
INC 5710
INC 5720
INC 5730
INC 5740
INC 5750
INC 5760

```



```

READ(5,1950)(THSTS(J),J=1,NPS)
GO TO 10
1609 THSTS(1)=THST1
1610 CONTINUE
C VALUES INPUT FOR PORT SCREW
THST2=TEMP(1)
NPP=TEMP(2)
STHP=TEMP(3)
IF(NPP.EQ.0.0) GO TO 1614
READ(5,1950)(TIP(J),J=1,NPP)
READ(5,1950)(THSTP(J),J=1,NPP)
GO TO 10
1614 THSTP(1)=THST2
1615 CONTINUE
C VALUES INPUT FOR RUDDER
DELR=TEMP(1)
NPR=TEMP(2)
IF(NPR.EQ.0.0) GO TO 1616
READ(5,1950)(TIR(J),J=1,NPR)
READ(5,1950)(DELRUD(J),J=1,NPR)
GO TO 10
1616 DELRUD(1)=DELR
GO TO 10

1700 GO TO (1705,1710),IOPT
1705 NB=TEMP(1)
READ(5,1950)(TMEB(I),I=1,NB)
READ(5,1950)(DELB(I),I=1,NB)
GO TO 10
1710 NS=TEMP(1)
READ(5,1950)(TMES(I),I=1,NS)
READ(5,1950)(DETS(I),I=1,NS)
GOTO 10

C TITLE CARD (ALL 80 COLUMNS )
1800 READ (5,2022) TITLC
GO TO 10

C FAN MAPS
1900 CONTINUE
1905 GO TO (1905,1910,1915),IOPT
CONTINUE
ENBFAN=TEMP(1)
BRPM=TEMP(2)
NPTS8=TEMP(3)
READIN=TEMP(4)
IF (READIN.EQ. 0.0) GO TO 10
READ (5,1950) (PBFAN(J),J=1,NPTS8)

```



```

1910 READ (5,1950) (QBFAN(J),J=1,NPTSB)
      GO TO 10
      CONTINUE
      ENMFAN=TEMP(1)
      EMRPM=TEMP(2)
      NPTSM=TEMP(3)
      READIN=TEMP(4)
      IF (READIN.EQ. 0.0) GO TO 10
      READ (5,1950) (PMFAN(J),J=1,NPTSM)
      READ (5,1950) (QMFAN(J),J=1,NPTSM)
      GO TO 10
1915 CONTINUE
      ENSFAN=TEMP(1)
      SFPM=TEMP(2)
      NPTSS=TEMP(3)
      READIN=TEMP(4)
      IF (READIN.EQ. 0.0) GO TO 10
      READ (5,1950) (PSFAN(J),J=1,NPTSS)
      READ (5,1950) (QSFAN(J),J=1,NPTSS)
      GO TO 10
1950 FORMAT(8F10.0)
C      ERROR IN INPUT
      CONTINUE
      WRITE (6,79) ISYS
      STOP
79      FORMAT(34H INPUT ERROR - -- STOP -- ISYS=,I3)
98      FORMAT(1H1,20(/),50X,19H COMPLETED ALL RUNS )
99      FORMAT(13,I2,7F10.0)
191      FORMAT(16I5)
192      FORMAT(5F10.0)
195      FORMAT(//10X,65HERROR IN INPUT --- DELT AND/OR DELPNT EQUALS ZERO
1      --- JOB ABORTED )
175      FORMAT(2I2/(8F10.0))
216      FORMAT(//10X,82HERROR IN INPUT --- INPUT INERTIA ELEMENTS LEAD TO
1      ZERO DETERMINANT --- JOB ABORTED )
217      FORMAT(22H INERTIA MATRIX, A1MAX 6E15.4/(22X,6E15.4))
219      FORMAT(30H WEIGHT, C.G., INERTIA MOMENTS 7F12.3)
305      FORMAT(11F7.0)
490      FORMAT(15H SIDEWALL INPUT 12(F8.3,1X))
491      FORMAT(26H SIDEWALL TABLE PARAMETERS 4(I4,F7.3,F7.3))
1190      FORMAT(2F10.0)
1191      FORMAT(//12HONO OF WAVES 12,10H BETA(DEG)F5.0/15H OMEGA(RAD/SEC)
15X,16H OMEGAE(RAD/SEC) 5X,16H WAVE LENGTH(FT) 5X,14H AMPLITUDE(FT)
- 5X,16H MAX SLOPE (DEG)5X,13HPERIOD,E(SEC)/(F8.4,12X,F8.4,4F20.3))
1192      FORMAT(//11HOCALM WATER)
1519      FORMAT(32HONMOMENT CALC. CONTROL PARAMETERS 4I5, F8.3, I5 )
1522      FORMAT(5X,7F10.0)
1549      FORMAT(22H MOMENT CALCS. AT X OF 11F10.3)

```





```

1559 FORMAT(22H MOMENT CALCS. AT Y OF 11F10.3)
2004 FORMAT(33H1SES MOTIONS AND LOADS PROGRAM - 20A4,/)
2001 FORMAT(23H START AND FINISH TIMES 2F10.2/
-22H INITIAL TIME INTERVAL F12.4/
-18H START PRINTING AT F8.2,17H IN INCREMENTS OF F8.2)
2002 FORMAT(24H INTERMEDIATE PRINT TAGS 16I5)
2003 FORMAT(39H NO. OF STATE EQUATIONS, AND TOLERANCES 15/(10X,10E12.2))
2009 FORMAT(23H0CRITICAL FROUDE NUMBER F15.4,5X,19H TOTAL CRAFT LENGTH
1 F15.4)
2010 FORMAT(34H0PLENUM, LENGTH AND WIDTH AT WATER 2F12.4/
2011 FORMAT(34H PLENUM, LENGTH AND WIDTH AT HULL 2F12.4/
35H PLENUM, CENTER OF PRESSURE AT HULL F12.4/
-23H PLENUM, NOMINAL VOLUME F12.1,10X,6H HEIGHT F12.4)
2012 FORMAT(/33H PROPULSION, X, Y, Z COORDINATES 3F12.4/)
2013 FORMAT(/28H0RUDDER, X, Y, Z COORDINATES 3F12.4/
41H RUDDER, ON, MAX, RATE, REVERSE, INITIAL 5F12.4/
35H RUDDER, SPAN, ASPECT, AREA, CLB, T/C 5F12.4)
2017 FORMAT(/39H0INITIAL CONDITIONS, VELOCITY (KNOTS) = F7.2, 5X,
13HPITCH (DEG) = F8.3,5X,12HDRAFT (IN) = F8.2)
2018 FORMAT( 49H NUMBER OF STATIONS, SIDEWALLS (P+S), SEALS (B+S) ,4I5)
2020 FORMAT( 38H PLENUM, INITIAL PRESSURE, GAGE (PSF) F8.2)
2021 FORMAT(79H PROGRAM, OPTION SWITCH SETTINGS (LATERAL PLANE, CONSTANT
-SPEED, TRIM, MEMBRANE) 4I5)
2022 FORMAT (20A4 )
2023 FORMAT ( 1H1 ) STERNSEAL INPUT 7F12.4 )
2025 FORMAT( 16H BOWSEAL INPUT 7F12.4 )
2026 FORMAT( 16H BOWSEAL INPUT 7F12.4 )
2027 FORMAT( 19H0AERODYNAMICS INPUT 7F12.4 )
2028 FORMAT( 33H0FANS, NO. + RPM, BOW, MAIN, STERN 3(F10.0,F10.1))
END

```

```

INC 6730
INC 6740
INC 6750
INC 6760
INC 6770
INC 6780
INC 6790
INC 6800
INC 6810
INC 6820
INC 6830
INC 6840
INC 6850
INC 6860
INC 6870
INC 6880
INC 6890
INC 6900
INC 6910
INC 6920
INC 6930
INC 6940
INC 6950
INC 6960
INC 6970
INC 6980
INC 6990
INC 7000
INC 7010
INC 7020

```



## BIBLIOGRAPHY

1. Robert L. Trillo, Marine Hovercraft Technology, Leonard Hill, 1971.
2. Oceanics Incorporated, Report No. 71-84, August 1971, Technical Industrial Park, Plainview, N.Y. 11803.
3. Leo, D.G. and Boncal, R., XR-3 Surface Effects Ships Test Craft: A Mathematical Model and Simulation Program with Verification, Master's Thesis, Naval Postgraduate School, Monterey, 1973.
4. Mayer, R.D., Fan Laws Simplify Performance Calculations, Power, p. 77-80, August 1946.
5. Forbes, G.T., Validation of the Six Degree of Freedom Mathematical Model of the XR-3 in Calm Water, Master's Thesis, Naval Postgraduate School, Monterey, 1974.
6. Wener, N.L. and Burke, F.P., Surface Effect Ship Research with XR-1 Testcraft, AIAA Paper 74-313 presented at the AIAA/SNAME Advanced Marine Vehicles Conference, San Diego, Californai, February 25-27, 1974.



INITIAL DISTRIBUTION LIST

	No. Copies
1. Defense Documentation Center Cameron Station Alexandria, Virginia 22314	2
2. Library, Code 0212 Naval Postgraduate School Monterey, California 93940	2
3. Assoc. Professor Alex Gerba, Jr., Code 52GZ Department of Electrical Engineering Naval Postgraduate School Monterey, California 93940	5
4. Professor George J. Thaler, Code 52TR Department of Electrical Engineering Naval Postgraduate School Monterey, California 93940	1
5. Assoc. Professor Donald M. Layton, Code 57LN Department of Aeronautical Engineering Naval Postgraduate School Monterey, California 93940	1
6. CDR Donald Hay, USN Surface Effect Ships Project Office, Navy Dept. P.O. Box 34401 Bethesda, Maryland 20034	1
7. Mr. Sydney Davis, Code PMS-304-31A Department of the Navy Surface Effect Ships Project Office P.O. Box 34401 Bethesda, Maryland 20034	1
8. Mr. James E. Blalock, Code 1607 Department of the Navy Naval Ship Research and Development Center Carderock Laboratory Bethesda, Maryland 20034	1
9. Mr. Arnold W. Anderson, Code PMS-304-31A.1 Department of the Navy Surface Effect Ships Project Office, PM-17 Bethesda, Maryland 20034 (P.O. Box 34401)	1



- |     |   |   |
|-----|---|---|
| 10. | LCDR Robert A. Finley<br>USS W. V. PRATT (DLG-13)<br>FPO, New York, New York 09501  | 2 |
| 11. | LCDR Michael N. Hayes, NAVSEC 6110.10<br>Naval Ship Engineering Center<br>Center Building, Prince Georges Center<br>Hyattsville, Maryland 20782   | 1 |
| 12. | Mr. Reilly Conrad, Code 6136<br>Naval Ship Engineering Center<br>Center Building, Prince Georges Center<br>Hyattsville, Maryland 20782            | 1 |
| 13. | Mr. Al Ford, Code 163<br>Department of the Navy<br>Naval Ship Research and Development Center<br>Carderock Laboratory<br>Bethesda, Maryland 20034 | 1 |





20 FEB 79

25210

Thesis  
F4435  
c.1

Finley

156908

Refinements of the  
seal subroutines and  
fan air flow maps for  
the XR-3 loads and  
motion program.

20 FEB 79

25210

Thesis  
F4435  
c.1

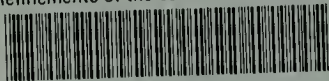
Finley

156908

Refinements of the  
seal subroutines and  
fan air flow maps for  
the XR-3 loads and  
motion programs.

thesF4435

Refinements of the seal subroutines and



3 2768 001 00369 2

DUDLEY KNOX LIBRARY